NASA Technical Paper 1176

Direct Measurements and Analysis of Skin Friction and Cooling Downstream of Multiple Flush-Slot Injection Into a Turbulent Mach 6 Boundary Layer

Floyd G. Howard and Andrew J. Srokowski

OCTOBER 1978

NASA

NASA Technical Paper 1176

Direct Measurements and Analysis of Skin Friction and Cooling Downstream of Multiple Flush-Slot Injection Into a Turbulent Mach 6 Boundary Layer

Floyd G. Howard and Andrew J. Srokowski
Langley Research Center
Hampton, Virginia

NASA
National Aeronautics
and Space Administration

**Scientific and Technical
Information Office**

1978

SUMMARY

Experiments have been conducted to determine the reduction in surface skin friction and the effectiveness of surface cooling downstream of one to four successive flush slots injecting cold air at an angle of 10° into a turbulent Mach 6 boundary layer. Data were obtained by direct measurements of surface shear and equilibrium temperatures, respectively. Increasing the number of slots decreased the skin friction, but the incremental improvement in skin-friction reduction decreased as the number of slots was increased. Cooling effectiveness was found to improve, for a given total mass injection, as the number of slots was increased from one to four. Comparison with previously reported step-slot data, however, indicates that step slots with tangential injection are more effective for both reducing skin friction and cooling than the present flush-slot configuration. Finite-difference predictions are in reasonable agreement with skin-friction data and with boundary-layer profile data.

INTRODUCTION

Injection of a layer of cold gas, through slots or holes (i.e., slot injection), into the air flowing over a surface is an active-cooling concept that has been applied primarily to the problems of cooling turbine blades (refs. 1 and 2), combustor liners (refs. 3 and 4), and rocket nozzles (ref. 5). System studies of hypersonic aircraft (ref. 6) have shown that weight and cost advantages may occur if operational surface temperatures can be reduced below normal radiation equilibrium temperatures by active-cooling methods. Slot injection is one such cooling method. Slot injection has also been shown to significantly reduce skin friction (refs. 7 to 10). Therefore, the potential for significant reduction in energy consumption of high-speed aircraft through reduced weight and drag makes slot injection an even more attractive research area. Counteracting these advantages would be any weight and cost penalties involved in collecting and cooling air and distributing it to injection slots.

Generally, slot injection research has focused on the film-cooling problem (refs. 11 to 31). However, some investigations have not determined the cooling effectiveness directly from measurements of equilibrium surface temperatures. The value of cooling effectiveness has been inferred indirectly from heat-transfer measurements and estimated heat-transfer coefficients downstream of one or more slots. The experimental cooling data shown in this report were determined from direct measurements of the surface temperature at equilibrium conditions.

The results of other studies (refs. 23 to 29) indicate that, when a number of successive slots were used, the film-cooling performance downstream of each slot is enhanced because of the "multiple slot effect." One purpose of our research was to examine the multiple slot effect on cooling.

Although some direct skin-friction measurements have been reported (refs. 9, 10, and 32), most skin-friction data currently available in the literature have been obtained by indirect means (from momentum thickness or heat-transfer measurements, for example). Since the downstream flow field near the slot is nonsimilar, the accuracy of indirect methods in this region is questionable; therefore, direct skin-friction measurements, as obtained in this investigation, are desirable.

Two basic slot configurations, the step slot and the flush slot, are shown in figure 1. Step slots may be undesirable on surfaces such as turbine blades or aircraft fuselages; therefore, the slot configurations of this investigation were flush, with an injection angle of 10°.

In this report, cooling and skin-friction data from direct measurements downstream of flush slots are compared with results previously reported for step slots. The multiple slot effect on skin friction is also examined. Predictions from a compressible, turbulent-boundary-layer computer program have been shown to agree reasonably well with experimental skin-friction data and boundary-layer profile data for step slots (refs. 10 and 33). This program was modified to deal with the flush-slot configuration by relaxing the no-slip condition of the wall boundary layer at the slot exit to provide predictions for comparison with the present experimental skin-friction data and boundary-layer profiles.

SYMBOLS

A	area, m^2
C_f	local skin friction, $\tau/(0.5\rho_\infty u_\infty^2)$
C_{fo}	local skin friction without slots
h	surface heat-transfer coefficient, $W/(m^2 \cdot K)$
L	axial distance from nozzle throat, m
M	Mach number
$\dot{m}$	mass-flow rate, kg/sec
N	number of slots
p	pressure, Pa
$p_{\infty,j}$	free-stream pressure in slot, Pa
Q	volume flow rate through slot, m^3/sec
q	heat-transfer rate, W/m^2
R	gas constant (air), 286.96 $m^2/sec^2 \cdot K$

R_∞ free-stream Reynolds number, $\rho_\infty u_\infty L/\mu_\infty$

r radius, m

s slot height (see figs. 1 and 3), m

T temperature, K

T_{eq} wall equilibrium temperature, K

T_o total temperature, free stream, K

$T_{r,j}$ recovery temperature of air in slot flow, K

T_w wall temperature, K

u velocity, m/sec

x downstream distance measured from upstream lip of last slot (see fig. 3), m

x' downstream distance measured from downstream lip of last slot; used only in cooling data (see fig. 6), m

y distance measured normal from tunnel wall, m

y_j distance measured normal from slot upper surface, m

γ heat capacity ratio, 1.4

δ boundary-layer thickness, m

ϵ cooling effectiveness (see eq. (2))

θ flow deflection behind shock, deg

λ mass-flow ratio, $\left(\frac{\dot{m}}{A}\right)_{slot} \Big/ (\rho u)_\infty = (\rho u)_j / (\rho u)_\infty$

(Note: λ is calculated separately for each slot in multiple slot configurations)

λ_{eff} $= \Sigma\, \lambda_1 + \lambda_2 + \ldots + \lambda_n$

λ_{nom} nominal value of λ

μ viscosity, kg/m·sec

ρ density, kg/m^3

τ shear stress at wall, $\left(\frac{\mu\, \partial u}{\partial y}\right)_w$, $kg/m \cdot sec^2$

Subscripts:

1,2,3,4	slot number
aw	adiabatic wall
∞	free-stream conditions ahead of slots
F	integrated skin friction
j	slot conditions
l	local conditions
m	measured
o	settling chamber conditions; no slots, stream stagnation conditions
r	recovery
t	local total conditions in boundary layers, total conditions in slot
w	at wall

DESCRIPTION OF INVESTIGATION

Experimental Investigation

Facility and model.- Tests were conducted in the Mach 6 high Reynolds number tunnel at the NASA Langley Research Center. The tunnel is a conventional blowdown type with an axisymmetric contoured nozzle followed by a 30.48-cm (inside diameter) pipe section into which instrumented segments can be installed at various axial stations. (See ref. 32.) Details of the tunnel are presented in reference 34. A schematic of the typical tunnel arrangement with slots is shown in figure 2. For these tests, the nominal operating conditions were: $p_o \approx 3.55$ MPa; $T_o \approx 505$ K; $M_\infty = 5.96$. For the skin-friction part of the tests, the Reynolds number R_∞ based on axial distance from the nozzle throat was varied from 70×10^6 to 100×10^6 and from 240×10^6 to 290×10^6. For the cooling-effectiveness measurements, R_∞ varied from 60×10^6 to 110×10^6. At the location of the first slot, the boundary-layer thickness δ for the no-slot configuration was about 4.32 cm for $R_\infty \approx 85 \times 10^6$.

An example of the multiple flush-slot arrangement is shown for two slots in figure 3, with a single skin-friction balance located downstream of the last slot. The slots are flush with the wind-tunnel wall and have an injection angle of 10^o, relative to the wall. Each slot is formed by two contoured rings with a spacer that determines the slot height. Although slot heights of 0.127 cm and 0.0635 cm were investigated for the single-slot configuration, the basic slot height for this investigation was 0.254 cm, and all references to slots will be to the basic slot (s = 0.254 cm) unless otherwise noted. Multiple

slots were assembled in series, with the distance between the slots held constant and equal to 67.5 slot heights.

Surface and pitot pressures were measured by multirange capacitance-type pressure transducers with accuracy rated at better than 1 percent of full scale on each range.

Skin friction was measured directly, using two commercial floating-element balances (ref. 35). Wall pressures and wall temperatures downstream of the slots were also measured. Oil flow distributions and circumferential pressure distributions measured at the wall indicate that the slot flow was uniform.

Cooling effectiveness for the basic slot height was determined directly from measured equilibrium surface temperatures downstream of one to four slots. ANSI Type K thermocouples were mounted on the back surface of the thin-wall liner (0.159 cm thick) and located immediately downstream of the most downstream slot. Thermocouples were positioned between the liner supports to minimize undesirable conduction effects. Details of the liner are shown in figure 4.

Surface measurements.- The floating-element skin-friction balances were of the null type with ranges of 0.100, 1.00, and 10.0 gm/cm^2. The friction loads during this investigation were always between 0.100 and 1.00 gm/cm^2; therefore, only the 1.00-gm/cm^2 range was required for these tests. Volume flow rates and pressures at each slot were controlled separately, with the mass-flow parameter λ ranging from approximately 0.0035 to 1.00 for the skin-friction data and from 0.05 to 0.28 for the cooling data. The slot mass-flow ratio was determined as follows:

$$\lambda = \frac{(\rho u)_j}{(\rho u)_\infty} = \left(\frac{Q}{A_j} \cdot \rho_{\infty,j}\right) \Bigg/ \left(\rho_\infty M_\infty \sqrt{\gamma R T_\infty}\right)$$

$$\lambda = \left(\frac{Q p_{\infty,j}}{A_j R T_{\infty,j}}\right) \Bigg/ \left(\frac{p_\infty M_\infty}{R T_\infty} \sqrt{\gamma R T_\infty}\right) \tag{1}$$

where values were determined from direct measurements or derived from measurements. The flush surfaces and sensitive elements of the balance housing were contoured to match the 15.24-cm tunnel radius. Water-cooled jackets around the balances were used to minimize errors due to temperature sensitivity. For purposes of normalization, reference values of C_{fo} were obtained by installing the balances in the tunnel without the slots and taking data over an appropriate Reynolds number range. The results are tabulated in table I and plotted in figure 5, where C_{fo} is shown as a function of free-stream Reynolds number R_∞. A curve was faired through the C_{fo} data for each of the two balances, and subsequent C_f data were normalized by using the appropriate C_{fo} curve. The data consistently fall about a gentle curve as indicated in the figure. Also shown for comparison is the variation in C_{fo} for a flat plate predicted by the theory of Spalding and Chi (ref. 36) with L used as the reference length.

The slight difference in slope between the theoretical curves and the faired data curves may be due to the effects of a small streamwise pressure gradient present in the test section of the tunnel (ref. 34) and the upstream history of the tunnel-wall boundary layer.

Slot-cooling effectiveness for high-speed flow is usually defined as:

$$\varepsilon = \frac{T_o - T_{aw}}{T_o - T_{r,j}} \tag{2}$$

where, for this experiment, T_{aw} was assumed to be equal to $T_{eq,m}$. The recovery temperature of the coolant $T_{r,j}$ was established by extrapolation of measured surface equilibrium temperatures back to the downstream lip of the slot ($x' = 0$) as illustrated in figure 6. The downstream lip was chosen for $x' = 0$ in the cooling effectiveness data, instead of the upstream lip ($x = 0$) as in the skin-friction data, to avoid extrapolation over a longer distance.

Equilibrium temperatures measured at the surface $T_{eq,m}$ were obtained by allowing the tunnel to run as much as 6.5 to 7.5 minutes; by that time the temperatures had leveled off at some constant values which were taken as $T_{eq,m}$. Ideally, measurements of this type would be made with a true adiabatic condition. However, this is virtually impossible with the tunnel run time available. The measured equilibrium temperature $T_{eq,m}$ for the most extreme test condition (no slots) was 3.74 percent below the theoretical adiabatic wall temperature T_{aw}. This is due to heat loss across the air gap and across the points of contact to the thick wall of the tunnel. (See fig. 4.) It should be noted that all values of ε shown in this report are based on the measured equilibrium temperature (i.e., $T_{aw} = T_{eq,m}$ in eq. (2)). However, estimates were made to establish the true, adiabatic wall temperature T_{aw} with no heat loss. (See fig. 7.) The thick-wall-heating computer program of reference 37 was used to make these estimates. The assumptions in these estimates are: (1) the recovery factor for no slot and turbulent flow was 0.89; and (2) the heat-transfer coefficient did not change with slot injection. (See ref. 11.) Although the uncorrected values of ε shown in this report are useful in showing trends and effects, care must be exercised before using the actual values.

Static pressures were measured on the surface in the region of the slot exit and downstream of the slot.

Probe measurements.- Pitot-pressure profiles and total-temperature profiles were measured in the undisturbed boundary layer just upstream of the slot and also at several stations downstream of the slot. Probe details are shown in figures 8(a) to (c), and dimensions of the probe tips are given in figure 9.

Numerical Investigation

A numerical method was formulated to solve the partial differential equations for the mean motion of a compressible turbulent boundary layer with tan-

gential slot injection. This method has been shown to give good agreement with experimental data. (See refs. 10 and 33.) Use of the method requires the input of an assumed or measured profile of the slot flow beneath an external boundary layer. The starting point for the calculation is normally just downstream of the most upstream slot lip ($x > 0$). The main assumption of the method is that the static-pressure field normal to the wall is constant. This assumption is erroneous to some extent in most slot-injection experiments. However, it was shown that satisfactory predictions could be obtained if the normal pressure gradients were not too severe (refs. 10 and 33). Also, it should be noted that the experimentally observed streamwise static-pressure variation (to be discussed later) was not included in the numerical prediction.

The slot and downstream-wall pressure data and the boundary-layer surveys of this investigation indicate that a shock due to injection attenuates very rapidly for the range of λ considered. Thus for values of x/s greater than about 20, neither normal nor streamwise pressure gradients would be severe enough to significantly affect the numerical predictions.

The computer program was modified to accommodate the flush-slot configuration in the following manner. An internal slot profile which gives the desired value of λ is assumed. At the slot exit (upstream lip), this profile is resolved into components normal to and parallel to the mainstream, as indicated in figure 10. The starting point for the calculation is upstream of the slot, with the measured profile of the tunnel-wall boundary layer used as input. When the upstream lip of the slot is reached, the wall boundary conditions are changed. Mass is transferred normal to the wall, and a slip boundary condition is imposed. When the downstream lip is reached, the zero-slip wall condition is reimposed. This method was chosen because the small size of the slot and the large normal pressure gradients near the slot precluded obtaining and using accurate slot-exit profiles, which is the usual starting procedure.

Adaptation of the step-slot injection program (ref. 33) to accommodate the flush-slot configuration required not only changes in boundary conditions (as discussed above) but also some modifications of the original mixing-length distributions. In the region of the slot exit (fig. 10), the Prandtl wall-mixing-length constant and the Van Driest damping function were not used. In addition, the mixing length at $y/s = 0$ was not set to zero in the region between the upstream and downstream slot lips. When the downstream slot lip is reached, the standard mixing-length relations are used, with the exception that the ratio of the mixing length in the free-mixing layer to the width of the mixing layer is assigned a value of 0.06. (See ref. 33 for details of the standard mixing-length relations.)

RESULTS AND DISCUSSION

Flow Structure and Surface-Pressure Distribution

The axisymmetric-slot configuration used in these tests did not permit any real-time flow-visualization studies. However, an examination of the behavior of the wall static pressures at the slot exit and downstream, as a function of the mass-flow parameter λ, yields some insight into the gross behavior of the

flow. The ratios of these pressures to free-stream stagnation pressure are shown in figure 11 and table II. Also shown in figure 11 are levels of slot-exit pressure at which sonic flow should occur at the slot exit based on measured slot plenum pressures. Sonic exit conditions were first achieved at a value of λ slightly below 0.15, as indicated by a comparison of the measured pressures at the first static-pressure orifice with sonic pressures computed from the measured plenum pressures. All pressures were higher than the wall static pressure with no slots. The highest overpressures occurred in the slot-exit region. A very rapid expansion of the slot flow, probably to supersonic velocities for the higher values of λ, occurred within the first 10 slot heights downstream. By 20 slot heights, the wall pressure was very close to the level of the undisturbed, wall static pressure.

The measured pressures indicate that even at the small mass flows some deflection of the external flow will occur and a shock will form in the vicinity of the slot exit. Thus, the so-called step-slot "matched pressure" condition, where the slot-exit pressure is equal to the free-stream static pressure, is not possible with the flush-slot configuration. However, it may be possible to match the slot-exit pressure to the pressure behind the shock. This would tend to minimize normal pressure gradients downstream of the shock.

The wall-pressure data, along with pitot-pressure surveys of the boundary layer (the pitot surveys will be discussed later), allow the location and strength of the shock to be determined. The solid curve of figure 12 shows the location of the shock as determined by the following method: The shock is assumed to begin at the upstream slot lip, and the slot flow is assumed to behave as an impermeable layer of constant thickness (0.254 cm in this case). This layer is turned 10° at the downstream lip until it is parallel to the mainstream flow direction as indicated in figure 12. The shock, which initially produces a 10° deflection in the external flow, is then assumed to be attenuated by a 10° Prandtl-Meyer expansion centered at the downstream lip. The first and last right-running expansion waves are indicated in figure 12 by dashed lines. The local shock-wave and expansion-wave angles were computed from profiles of the local Mach number which were based on the measured pitot pressures and wall static pressures for $\lambda = 0.05$. This method indicates that the shock has been attenuated until it produces a flow deflection of only 5° at slightly more than 30 slot heights downstream.

Also shown in figure 12 are the shock locations inferred from the pitot-pressure data (to be discussed later) which are in surprisingly good agreement with the simplified analysis of the flow. It can be concluded that the slot flow is rapidly turned parallel to the wall as it exits from the slot and that this expansion rapidly attenuates the shock. At downstream distances greater than 30 slot heights, the normal pressure gradients across the boundary layer would therefore be very weak, and they would have little effect on boundary-layer development.

Pitot-pressure and total-temperature profiles measured in the undisturbed boundary layer immediately upstream of the slot location are tabulated in table III. Pitot-pressure and total-temperature profiles measured downstream of a single slot are tabulated in table IV for $x/s = 5.8$, 17.12, 37.12, 67.12, and 107.12. Pitot-pressure profiles downstream of a single slot for $x/s = 5.8$,

17.12, and 67.12 are presented in figures 13(a) to (c), respectively. Also shown for reference is a fairing of the profile measured just upstream of the slot. The theoretical profiles calculated by the boundary-layer program are shown in these figures, are tabulated in table V, and will be discussed later. It should be noted that there is very little difference between the computed results for the two values of λ. At $x/s = 5.8$, the influence of the slot flow near the wall (at $y/s < 1.5$) is evident upon comparison of the data with the reference profile. The effect of increasing λ is noticeable only at $y/s < 0.7$ where the pitot pressures for $\lambda = 0.2$ are somewhat higher than for $\lambda = 0.1$ or 0.15. Pressure profiles at $x/s = 5.8$ indicate that the outer part of the boundary layer ($y/s > 5.0$) is unaffected by the slot flow. The profile shapes in the near-wall region ($y/s < 1.0$) at $x/s = 67.12$ (fig. 13(c)) appear to have nearly returned to the undisturbed reference-profile shape, an indication of the loss of slot-flow identity in this region. The discontinuity in the data for $x/s = 5.8$ from $y/s = 3.0$ to $y/s = 5.0$ indicates the presence of a shock due to injection. The propagation of this shock through the boundary layer is apparent from a comparison of the location of the discontinuity in figures 13(a) to (c). At $x/s = 67.12$ (fig. 13(c)), the shock is beyond the edge of the boundary layer.

Pitot-pressure and total-temperature profiles measured downstream of two and three slots are tabulated in tables VI and VII, respectively, for $x/s = 17.12$ and 67.12. Profile measurements of pitot pressure downstream of one, two, and three successive slots, for $\lambda_{nom} = 0.15$ at $x/s = 17.12$ and 67.12, are shown in figures 14(a) and (b), respectively. (Note, x is always the distance from the last slot.) The insert in figure 14(a) indicates the approximate location of the shock for each slot. Even as far downstream as the fourth slot, the shock from the first slot does not reach the tunnel centerline. Thus, the external inviscid flow in the region of measurement is affected only by a series of simple shocks. Also shown for reference in figure 14 is a fairing of the profiles measured just upstream of the first slot.

At $x/s = 17.12$ (fig. 14(a)), the experimental pitot-pressure levels for one slot at $y/s < 4.0$ are lower than the reference profiles. As the number of slots is increased from one to three, the pitot-pressure levels become even lower, but at a decreasing rate. The location of the shock is indicated by the discontinuity in the pitot-pressure profiles. The shock due to each succeeding slot appears to move farther from the wall than the shock from the previous slot. As the number of slots is increased, the increasing angles of the shock are probably caused by decreases in the average Mach number ahead of the succeeding slots. These decreases are due to the upstream shocks and the increasing boundary-layer thickness. The shock due to the first slot affects succeeding slot profiles by thickening the local boundary layer and by increasing the pitot-pressure levels at values of $y/s > 20.0$ for two and three slots.

At $x/s = 67.12$ (fig. 14(b)), the slope of the injection profiles for $y/s < 0.50$ approaches the reference-profile slope due to mixing of the slot and external flows. The shock for one slot moved from the wall to values of y/s between 18.0 and 22.0. The kink in the faired data curves for two slots (beginning at $y/s = 7.0$) and for three slots (beginning at $y/s = 9.0$) may indicate the presence of weak secondary shocks or expansion waves induced by previous slots.

Total-temperature profiles measured downstream of a single slot with x/s = 17.12, 37.12, 67.12, and 107.12 are presented in figures 15(a) to (d), respectively, for λ_{nom} = 0.1 and 0.2. The faired, undisturbed profile measured just upstream of the slot is also shown in figure 15 for comparison. These temperature profiles were used in conjunction with the experimental pitot-pressure profiles to establish the velocity profiles. The static pressure in the boundary layer out to the shock was assumed to be equal to the value measured at the surface. Tabulated in table VIII are the experimentally derived profiles of static temperature and velocity just upstream of the slot location. The experimentally derived profiles of static temperature and velocity downstream of one, two, and three slots are shown in table IX. Velocity profiles downstream of a single slot are presented in figures 16(a) to (d) for x/s = 17.12, 37.12, 67.12, and 107.12. The faired profile of undisturbed velocity just upstream of the slot is also shown for comparison. The velocity profiles for all four stations are shown on a single plot in figure 17(a) for λ_{nom} = 0.10 and in figure 17(b) for λ_{nom} = 0.20. For comparison, velocity profiles downstream of one, two, and three slots are shown in figure 18(a) for x/s = 17.12 and in figure 18(b) for x/s = 67.12. As shown in figures 16 to 18, the velocity profile downstream of slot injection returns to the undisturbed profile as the number of slots is decreased, as λ_{nom} decreases from 0.2 to 0.1, or as the distance downstream is increased.

Skin Friction

All of the skin-friction data presented have been normalized by C_{fo}, the coefficient of skin friction with no slots. Balances were used to directly measure C_{fo} over a range of free-stream Reynolds numbers. (See fig. 5.) Skin friction measured downstream of one, two, three, and four slots is tabulated in tables X, XI, XII, and XIII, respectively.

Slot injection of low momentum air reduces skin friction by reducing the velocity gradient at the wall. The lower the slot-flow momentum the faster the mixing with the external flow and the faster the slot flow loses its identity. In addition, the interaction effects caused by injecting at an angle to the mainstream will influence the magnitude and extent of skin-friction reduction. Thus, for a given value of x/s, there should be an injection rate λ which gives a minimum value of C_f/C_{fo} determined by the rate of mixing of the low-momentum slot flow with the boundary-layer flow and by the effects of viscous-inviscid interactions.

Single slot.- The effects noted above are illustrated in figure 19 where C_f/C_{fo} for one slot is plotted against λ. The curves all show a minimum value of C_f/C_{fo} which increases as x/s increases. The value of λ at which the minimum value of C_f/C_{fo} occurs also increases slightly with increasing x/s. At the smaller values of x/s, increasing λ past the minimum point results in a rapid rise in C_f/C_{fo}. This rapid rise is probably due to two effects: (1) an increase in the local wall velocity gradients due to increased injection rates; and (2) large overpressures at the slot exit (see fig. 11) for high values of λ and the associated strong interactions of the slot flow with the external flow. As x/s increases, the variation of C_f/C_{fo} with λ becomes less pronounced because of the longer mixing distances. For values of λ

smaller than approximately 0.01, the skin-friction reduction is consistently 4 to 5 percent for $x/s = 17.12$ and 27.12. Skin-friction measurements for $x/s < 17.12$ could not be obtained with the apparatus used. All of the previous data were taken over a Reynolds number range of 70×10^6 to 100×10^6 with a slot height s of 0.254 cm. In order to show the effect of slot height, data were also taken with slot heights of 0.1270 cm and 0.0635 cm, as tabulated in table XIV. These data are shown for three mass-flow ratios in figure 20. The results in this figure indicate that the larger slot opening (0.254 cm in this case) is slightly more effective in reducing skin friction. Skin-friction data were also taken for $R_\infty = 240 \times 10^6$ to 290×10^6 ($s = 0.254$ cm), as tabulated in table XV, in order to show the effect of significant change in Reynolds number. These data indicate that the skin friction is reduced slightly more in the higher Reynolds number range, as shown in figure 21.

Multiple slots.- All multiple-slot data were taken with the slot height(s) equal to 0.254 cm and are shown in figures 22(a) to (d) where C_f/C_{fo} is plotted against x/s downstream of one, two, three, and four slots, respectively (x is always the distance downstream from the last slot). All slots were operated at the same nominal value of λ, and data for each nominal value of λ were obtained from separate runs. Figure 22(a) is essentially a cross plot of the data from figure 19. As λ_{nom} increases from 0.05 to 0.15. C_f/C_{fo} decreases rapidly; as λ_{nom} increases further, there is little additional decrease in C_f/C_{fo}, since the lowest values on the curves of figure 19 are near $\lambda_{nom} = 0.25$. Also shown in figure 22(a) are data from reference 10 for a step slot operating at $\lambda_{nom} = 0.064$, which corresponds to the step-slot matched-pressure condition. The free-stream conditions of reference 10 were nominally the same as those of the present investigation, with $\delta/s = 11$. It appears that on a mass-flow basis, the step slot is more effective in reducing skin friction than the flush slot. The lower effectiveness of the flush slot is probably due to the increased mixing rates caused, at least partly, by the slot-flow injection angle and consequent interactions with the external flow.

By comparing figures 22(a) to (d), it can be seen that an improvement in effectiveness of succeeding slots occurs mainly for the lower mass-flow rates at small values of x/s and for the higher mass-flow rates at larger values of x/s. These results are shown in figures 23(a) to (c) where C_f/C_{fo} is plotted against λ_{nom} for $x/s = 17.12$, 47.12, and 100.12, respectively. The observed trends may be explained by the fact that, at small values of x/s and large values of λ, the local wall shear is almost completely dominated by the slot flow and its interactions with the external boundary layer. Thus, for this condition, little improvement and even some degradation is observed as the number of slots increases. However, at large values of x/s where the slot flow has mixed with the external flow, the larger mass-flow rates cause larger increases in the boundary-layer thickness and a larger reduction in skin friction as the number of slots increases.

Based on cooling-effectiveness data, multiple slots are more effective than a single slot (refs. 21 to 27). However, the improvement in the local effectiveness for each succeeding slot diminishes as the number of slots increases. This is also true for skin-friction reduction. However, it is important to note at this point that the goal in cooling effectiveness and the goal in skin-friction-reduction effectiveness are quite different. The

integrated cooling effectiveness is generally of little or no importance; it is the local absolute maximum temperature that is important. The opposite is true for the reduction of skin friction. The local reduction is of little or no importance; it is primarily the integrated reduction that is important.

The effect of diminishing returns may be seen more clearly in the behavior of the average integrated skin-friction ratio which was obtained from the data of figures 22(a) to (d) (extrapolated where necessary). The ratio was obtained by integrating the local skin-friction coefficient over a distance of 270 slot heights from the first slot for each of the one, two, three, and four slot configurations. A schematic of the curves is shown in figure 24 for illustration only. The integrated skin-friction ratio C_F/C_{Fo} is shown in figure 25 as a function of the number of slots N. Initially, there is a rapid decrease in C_F/C_{Fo} as the number of slots is increased. However, the effect of diminishing returns is clearly evident as the number of successive slots is increased from two to four.

Increasing the mass-flow parameter λ_{nom} from 0.10 to 0.20 lowers the level of the faired plot of C_F/C_{Fo} against N. As λ_{nom} is increased to 0.25, the slope of the faired curve becomes less negative with increasing N so that integrated skin friction for four slots is higher at $\lambda_{nom} = 0.25$ than at $\lambda_{nom} = 0.20$. This increase is probably due to the cumulative effect of upstream-slot free-stream interaction on succeeding slots for the larger mass-flow rates. Thus for angled injection, it cannot be assumed that the λ which gives the lowest C_F/C_{Fo} for one slot will also give the lowest C_F/C_{Fo} for N slots.

Multiple-Slot Cooling Effectiveness

Slot injection reduces equilibrium surface temperature by modifying the boundary-layer temperature profile near the wall; mixing between the coolant and the external boundary-layer flow begins immediately at the point of injection and continues downstream. Mixing between the slot flow and the external boundary layer is most rapid for lower slot mass-flow rates, hence the extent of downstream cooling effectiveness is significantly reduced with the lower slot-flow rates.

Cooling effectiveness was determined from thermocouple measurements of wall temperatures, as tabulated in table XVI, downstream of one to four slots. Temperatures of the thin-wall liner reached equilibrium after 6.5 to 7.5 minutes of tunnel operation. Thermocouples were located midway between liner supports (see fig. 4) to minimize lateral conduction effects. Temperatures near the upstream end of the liner were found to be low for the no-slot configuration, probably because of longitudinal conduction. This is shown in figure 26 where equilibrium temperatures are plotted against axial distance. (See temperatures for no-slot configuration.) This effect may exist to a lesser degree for the slot-injection configurations. However, if this influence does exist for the slot-injection configuration, ϵ (as determined from eq. (2)) downstream of the slot would be low with a low $T_{r,j}$, since $T_{r,j}$ is determined from an extrapolation of the measured wall temperatures.

Examples of how experimental values of ϵ vary with λ_{nom} downstream of one, two, three, and four slots are shown in table XVII and figure 27. A cross plot of the data shown in figure 27 is shown in figure 28 in the form of ϵ plotted against the number of slots N. The general indications from figures 27 and 28 are that, at higher values of λ, increasing the number of slots and/or increasing the level of λ increases the level of ϵ. Cooling effectiveness ϵ for one to four slots plotted against distance from the most downstream slot lip x' is shown in figure 29 for $\lambda_{nom} = 0.10$. Based on the data shown, there is a slight reversal in improvement in ϵ as the number of slots N increases for values of x'/s less than 60. However, at greater distances from the slot, there are significant increases in ϵ as the number of slots is increased. Also shown in figure 29 for comparison is ϵ for $T_{eq} = 0.89(T_o - T_\infty) + T_\infty$. (See solid symbols.) Indications are that significant cooling is being achieved, at least to values of $x'/s > 200$. Some of the cooling data obtained for one to four slots are shown plotted against the parameter $(x'/s)\lambda^{-0.8}$ in figure 30. Also shown are two curves from references 9, 10, and 14. Most of the current data fall between the two curves. The upper curve, however, is the most appropriate for comparison, since it is for $T_{t,j}/T_o = 0.63$ and $T_{r,j}/T_o$ for the current data ranges from 0.54 to 0.68. As shown in both previous and current investigations, the data indicate that a flush slot is not as effective as a step slot for cooling. The lower curve in figure 30 is for $T_{t,j}/T_o = 0.43$.

Shown in figure 31 are experimental values of ϵ downstream of single and multiple slots (one to four slots). The total mass injection (total mass = sum of flow rates from each slot) was the same for each configuration. As the number of slots is increased from one to four, the surface area maintained above a required value of ϵ increases. For example, if operating conditions required $\epsilon \geq 0.5$, the single slot with $\lambda_{eff} = 0.24$ (fig. 31(a)) would protect the surface to about 140 slot heights (x'/s). Two, three, or four slots with the same total mass injection would protect the surface for a distance of more than 280, 340, and 400 slot heights, respectively. If an ϵ of 0.75 or 0.80 were required, the slot spacing would have to be closer than the present arrangement. With $\lambda_{eff} = 0.06$, a second slot would be required at approximately $x'/s = 17$ to maintain $\epsilon \geq 0.80$. (See fig. 31(a).) As illustrated by numerical studies, the slot spacing can be increased with each additional slot (see ref. 29) because of the "multiple slot effect." However, it should be obvious that the slot spacing will reach some asymptotic value (not shown in this report).

This study shows that, for a given coolant mass-flow rate, thermal protection over the maximum surface area can best be accomplished by injecting the coolant flow through multiple slots. Note that numerical studies (refs. 38 and 39) indicate that skin-friction reduction by slot injection is most effective when the total available mass is injected from one slot as far upstream as possible. Of course, this is only true if the increase in mass through a single slot is obtained by increased slot opening and not by increased slot velocity.

Finite Difference Predictions

Profiles of velocity ratios u_j/u_∞ and total-temperature ratios $T_{t,j}/T_{t,\infty}$ were assumed in the slot for input to the numerical predictions. These values

are shown in table XVIII. Predictions of skin friction by the numerical method previously discussed are shown for $\lambda = 0.15$ and $\lambda = 0.20$ in figure 22(a). The difference in numerical results obtained when the slot-velocity profile shown in table XVIII was changed to a parabolic profile (with same mass flow) was insignificant. In the near-slot region ($x/s < 30$), the calculation predicts lower values of C_f/C_{fo} than indicated by the data for either value of λ; however, at larger values of x/s the present agreement is quite good. Since predictions of C_f/C_{fo} in the near-slot region were in agreement with data for a step slot (refs. 10 and 33), the present disagreement is probably caused by the shock/boundary-layer interactions and large, normal and streamwise pressure gradients for flush-slot injection. These effects are negligible for step-slot injection and are not accounted for in current theory. (If the large streamwise pressure gradients observed in the near-slot region were used as inputs for the present boundary-layer theory, the predictions could probably be improved significantly.) The predicted value of C_f/C_{fo} for $\lambda_{nom} = 0.15$ is below that for $\lambda = 0.20$ at $x/s < 20$ and above at $x/s > 20$. This result may be accounted for by the higher slot-flow velocity gradient for $\lambda = 0.20$, which results in a higher shear in the near-slot region. As x/s increases, mixing is more rapid for $\lambda = 0.15$ than for $\lambda = 0.20$, and the corresponding values of C_f/C_{fo} for $\lambda = 0.15$ rise above those predicted for $\lambda = 0.20$.

A comparison of the predicted pitot-pressure profiles with data obtained at $\lambda = 0.15$ and 0.20 is presented in figures 13(a), (b), and (c) for $x/s = 5.8$, 17.12, and 67.12, respectively. The pitot pressures calculated for $\lambda = 0.15$ and 0.20 are nearly identical, except for $y/s < 1.0$ where the pitot pressures for $\lambda = 0.15$ are somewhat lower. The pitot-pressure levels predicted for both values of λ at $y/s < 0.50$, for $x/s = 5.8$, are lower than the corresponding data. This difference in pitot-pressure levels near the wall may account, in part, for the lower skin-friction levels given by the predictions in the near-slot region. At $x/s = 67.12$ (fig. 13(c)), the data and theory show improved agreement for $y/s > 4.0$. At values of y/s between 1.0 and 4.0, predicted pitot-pressure levels are above the data for $x/s \geq 17.12$ (figs. 13(b) to (c)). A similar result of comparisons between theory and data for a single step slot has been noted in references 9 and 40.

CONCLUSIONS

Skin friction, wall pressures, wall temperatures, and profiles of boundary-layer pitot pressure and total temperature were measured downstream of one to four successive flush slots injecting at an angle of 10^o into a turbulent Mach 6 boundary layer. Cooling effectiveness was experimentally derived from temperatures of a thin-wall liner measured at steady-state conditions. A turbulent-boundary-layer computer program for tangential injection was modified to deal with the flush-slot configuration. The most important results of this investigation are as follows:

1. The "multiple slot effect," with a proportional increase in injected mass, was observed to increase the skin-friction reduction for flush-slot injection. This effect became less pronounced as the number of slots was increased and may even be reversed for high mass-flow rates in the slot.

2. Comparison of current results for a flush slot with previously reported data for a step slot indicates that the flush slot is less effective in reducing skin friction, probably due to the effects of more rapid mixing when the injectant enters the external stream at an angle.

3. Skin-friction values predicted by the numerical solutions are in good agreement with the data at downstream distances greater than 30 slot heights. At shorter distances, the theory underpredicts the skin friction, probably due to shock/boundary-layer interactions and associated pressure gradients not accounted for in the theory.

4. The data indicate that a slight improvement in skin-friction reduction was accomplished with increases in slot opening. A slight improvement is also indicated at the higher Reynolds number range.

5. For a given coolant mass-flow rate, thermal protection over the maximum surface area can best be accomplished by injecting the coolant flow through multiple slots rather than through a single slot.

6. The cooling data indicate that cooling downstream of flush slots, with an injection angle of 10°, is not as effective as the cooling downstream of step slots.

Langley Research Center
National Aeronautics and Space Administration
Hampton, VA 23665
June 28, 1978

REFERENCES

1. Metzger, D. E.; Biddle, J. R.; and Warren, J. M.: Evaluation of Film Cooling Performance on Gas Turbine Surfaces. High Temperature Turbines, AGARD-CP-73-71, Jan. 1971.

2. Liess, Christian: Film Cooling With Ejection From a Row of Inclined Circular Holes - An Experimental Study for the Application to Gas Turbine Blades. VKI-TN-97, Von Karman Inst. Fluid Dyn., Mar. 1973.

3. Metzger, D. E.; Baltzer, R. T.; Takeuchi, D. I.; and Kuenstler, P. A.: Heat Transfer to Film-Cooled Combustion Chamber Liners. Paper No. 72-WA/HT32, American Soc. Mech. Eng., Nov. 1972.

4. Ballal, D. R.; and Lefebvre, A. H.: A Proposed Method for Calculating Film-Cooled Wall Temperatures in Gas Turbine Combustion Chambers. Paper No. 72-WA/HT-24, American Soc. Mech. Eng., Nov. 1972.

5. Williams, J. J.; and Giedt, W. H.: The Effect of Gaseous Film Cooling on the Recovery Temperature Distribution in Rocket Nozzles. Space Systems and Thermal Technology for the 70's - Part II, American Soc. Mech. Eng., c.1970, Paper No. 70-HT/SpT-42.

6. Becker, John V.; and Kirkham, Frank S.: Hypersonic Transports. Vehicle Technology for Civil Aviation - The Seventies and Beyond, NASA SP-292, 1971, pp. 429-445.

7. Fischer, Michael C.; and Ash, Robert L.: A General Review of Concepts for Reducing Skin Friction, Including Recommendations for Future Studies. NASA TM X-2894, 1974.

8. Cary, Aubrey M., Jr.; and Hefner, Jerry N.: Film Cooling Effectiveness in Hypersonic Turbulent Flow. AIAA J., vol. 8, no. 11, Nov. 1970, pp. 2090-2091.

9. Hefner, Jerry N.; Cary, Aubrey M., Jr.; and Bushnell, Dennis M.: Downstream Influence of Swept Slot Injection in Hypersonic Turbulent Flow. NASA TN D-8506, 1977.

10. Cary, Aubrey M., Jr.; and Hefner, Jerry N.: Film-Cooling Effectiveness and Skin Friction in Hypersonic Turbulent Flow. AIAA J., vol. 10, no. 9, Sept. 1972, pp. 1188-1193.

11. Goldstein, Richard J.: Film Cooling. Advances in Heat Transfer, Vol. 7, Thomas F. Irvine, Jr., and James P. Hartnett, eds., Academic Press, Inc., 1971, pp. 321-379.

12. Eckert, E. R. G.; and Livingood, John N. B.: Comparison of Effectiveness of Convection-, Transpiration-, and Film-Cooling Methods With Air as Coolant. NACA Rep. 1182, 1954. (Supersedes NACA TN 3010.)

13. Laganelli, A. L.: A Comparison Between Film Cooling and Transpiration Cooling Systems in High Speed Flow. AIAA Paper No. 70-153, Jan. 1970.

14. Hefner, Jerry N.; and Cary, Aubrey M., Jr.: Swept-Slot Film-Cooling Effectiveness in Hypersonic Turbulent Flow. J. Spacecr. & Rockets, vol. 11, no. 5, May 1974, pp. 351-352.

15. Seban, R. A.: Heat Transfer and Effectiveness for a Turbulent Boundary Layer With Tangential Fluid Injection. Trans. ASME, Ser. C: J. Heat Transfer, vol. 82, no. 4, Nov. 1960, pp. 303-312.

16. Seban, R. A.; Chan, H. W.; and Scesa, S.: Heat Transfer to a Turbulent Boundary Layer Downstream of an Injection Slot. Paper No. 57-A-36, American Soc. Mech. Eng., 1957.

17. Chin, J. H.; Skirvin, S. C.; Hayes, L. E.; and Silver, A. H.: Adiabatic Wall Temperature Downstream of a Single, Tangential Injection Slot. Paper No. 58-A-107, American Soc. Mech. Eng., 1958.

18. Papell, S. Stephen; and Trout, Arthur M.: Experimental Investigation of Air Film Cooling Applied to an Adiabatic Wall by Means of an Axially Discharging Slot. NASA TN D-9, 1959.

19. Hartnett, J. P.; Birkebak, R. C.; and Eckert, E. R. G.: Velocity Distributions, Temperature Distributions, Effectiveness and Heat Transfer for Air Injected Through a Tangential Slot Into a Turbulent Boundary Layer. Trans. ASME, Ser. C: J. Heat Transfer, vol. 83, no. 3, Aug. 1961, pp. 293-306.

20. Goldstein, R. J.; Eckert, E. R. G.; Tsou, F. K.; and Haji-Sheikh, A.: Film Cooling With Air and Helium Injection Through a Rearward-Facing Slot Into a Supersonic Air Flow. AIAA J., vol. 4, no. 6, June 1966, pp. 981-985.

21. Parthasarathy, K.; and Zakkay, V.: Turbulent Slot Injection Studies at Mach 6. ARL 69-0066, U.S. Air Force, Apr. 1969. (Available from DDC as AD 692 503.)

22. Parthasarathy, K.; and Zakkay, V.: An Experimental Investigation of Turbulent Slot Injection at Mach 6. AIAA J., vol. 8, no. 7, July 1970, pp. 1302-1307.

23. Sherman, Arthur; Yeh, Hsuan; Reshotko, Eli; and McAssey, Edward, Jr.: Multiple Slot Laminar Film Cooling. AIAA Paper No. 72-290, Apr. 1972.

24. Chin, J. H.; Skirvin, S. C.; Hayes, L. E.; and Burggraf, F.: Film Cooling With Multiple Slots and Louvers. Trans. ASME, Ser. C: J. Heat Transfer, vol. 83, no. 3, Aug. 1961, pp. 281-292.
Part 1 - Multiple Continuous Slots.
Part 2 - Multiple Rows of Discrete Louvers.

25. Zakkay, Victor; and Wang, Chi Rong: Applications of Active Cooling to Nose Cones. ARL 73-0143, U.S. Air Force, Nov. 1973. (Available from DDC as AD-773178.)

26. Folayan, C. O.; and Whitelaw, J. H.: Multi-Slot Film Cooling. Lett. Heat & Mass Transfer, vol. 1, no. 1, 1974, pp. 31-36.

27. Mark, Andrew: Film Cooling With Injection Through Multiple Slots. DIT Rept. No. 69-20,139, Drexel Inst. Technol., 1969.

28. Sellers, John P., Jr.: Gaseous Film Cooling With Multiple Injection Stations. AIAA J., vol. 1, no. 9, Sept. 1963, pp. 2154-2156.

29. Bushnell, Dennis M.: Hypersonic Airplane Aerodynamic Technology. Vehicle Technology for Civil Aviation - The Seventies and Beyond, NASA SP-292, 1971, pp. 63-84.

30. Sivasegaram, S.; and Whitelaw, J. H.: Film Cooling Slots: The Importance of Lip Thickness and Injection Angle. J. Mech. Eng. Sci., vol. 11, no. 1, 1969, pp. 22-27.

31. Papell, S. Stephen: Effect of Gaseous Film Cooling of Coolant Injection Through Angled Slots and Normal Holes. NASA TN D-299, 1960.

32. Srokowski, A. J.; Howard, F. G.; and Feller, W. V.: Direct Measurements at Mach 6 of Turbulent Skin-Friction Reduction by Injection From Single and Multiple Flush Slots. AIAA Paper No. 76-178, Jan. 1976.

33. Beckwith, Ivan E.; and Bushnell, Dennis M.: Calculation by a Finite-Difference Method of Supersonic Turbulent Boundary Layers With Tangential Slot Injection. NASA TN D-6221, 1971.

34. Jones, Robert A.; and Feller, William V.: Preliminary Surveys of the Wall Boundary Layer in a Mach 6 Axisymmetric Tunnel. NASA TN D-5620, 1970.

35. Paros, Jerome M.: Application of the Force-Balance Principle to Pressure and Skin Friction Sensors. 16th Annual Technical Meeting Proceedings, Inst. Environ. Sci., 1970, pp. 363-368.

36. Spalding, D. B.; and Chi, S. W.: The Drag of a Compressible Turbulent Boundary Layer on a Smooth Flat Plate With and Without Heat Transfer. J. Fluid Mech., vol. 18, pt. 1, Jan. 1964, pp. 117-143.

37. Garrett, L. Bernard; and Pitts, Joan I.: A General Transient Heat-Transfer Computer Program for Thermally Thick Walls. NASA TM X-2058, 1970.

38. Howard, F. G.; Hefner, J. N.; and Srokowski, A. J.: Multiple Slot Skin Friction Reduction. J. Aircr., vol. 12, no. 9, Sept. 1975, pp. 753-754.

39. Marino, A.; Economos, C.; and Howard, F. G.: Evaluation of Viscous Drag Reduction Schemes for Subsonic Transports. NASA CR-132718, [1975].

40. Murray, Alvin L.; and Lewis, Clark H.: Supersonic Turbulent Boundary-Layer Flows With Mass Injection Through Slots and/or Porous Walls. NASA CR-2587, 1975.

TABLE I.- SKIN-FRICTION COEFFICIENTS MEASURED WITHOUT SLOTS AND CORRESPONDING FREE-STREAM REYNOLDS NUMBERS

[See fig. 5]

Skin-friction balance 221		Skin-friction balance 220	
R_∞	C_{fo}	R_∞	C_{fo}
(a) Low R_∞ range			
32.67×10^6	8.012×10^{-4}	33.28×10^6	7.704×10^{-4}
47.08	7.433	47.95	7.183
53.33	7.236	52.57	7.123
57.37	7.330	54.32	7.004
63.33	7.129	60.79	-----
64.68	6.908	63.19	-----
66.09	7.013	64.50	6.871
66.34	7.014	67.31	6.775
68.97	7.064	68.21	-----
72.57	6.918	68.22	-----
73.12	6.957	70.77	-----
73.54	6.754	73.91	6.673
74.44	6.897	75.17	6.390
74.45	7.002	85.45	-----
77.23	6.816	86.19	6.469
82.03	6.752	86.23	6.448
84.63	6.704	87.40	6.397
84.67	6.692	88.02	6.360
85.81	6.659	91.53	-----
86.43	6.612	92.74	6.360
91.05	6.604	92.84	6.418
91.15	6.589	100.16	6.224
93.25	6.562	101.21	6.210
98.34	6.468		
99.37	6.500		
99.89	6.533		
(b) High R_∞ range			
130.0×10^6	6.3×10^{-4}	120.0×10^6	6.1×10^{-4}
160.0	5.9	160.0	5.6
170.0	5.8	170.0	5.5
190.0	5.7	180.0	5.4
190.0	5.7	190.0	5.4
230.0	5.4	220.0	5.1
250.0	5.2	250.0	4.9

TABLE II.- WALL STATIC PRESSURE MEASURED IN REGION OF SLOT AND DOWNSTREAM OF SLOT

[s = 0.254 cm]

λ	p_w/p_o for x/s of -										
	0.7	2.7	4.7	10.12	16.12	25.12	37.12	97.12	167.12	247.12	327.12
	In slot (see fig. 11)				Downstream of slot						
0.0000	5.25×10^{-4}	6.03×10^{-4}	10.45×10^{-4}	7.31×10^{-4}	6.48×10^{-4}	6.88×10^{-4}	7.08×10^{-4}	6.99×10^{-4}	7.01×10^{-4}	7.05×10^{-4}	7.10×10^{-4}
.0000	5.24	6.02	10.43	7.30	6.48	6.87	7.07	6.99	7.01	7.05	7.09
.0000	5.24	6.00	10.47	7.30	6.47	6.87	7.07	6.98	7.01	7.05	7.09
.0000	5.24	6.02	10.43	7.31	6.48	6.88	7.08	6.99	7.01	7.06	7.09
.0000	5.19	5.97	10.44	7.26	6.41	6.83	7.03	----	6.95	----	----
.0000	5.19	5.97	10.42	7.27	6.42	6.83	7.04	----	6.95	----	----
.0000	5.19	5.97	10.43	7.27	6.42	6.84	7.04	----	6.95	----	----
0.0482	10.23×10^{-4}	10.48×10^{-4}	9.97×10^{-4}	7.48×10^{-4}	6.61×10^{-4}	7.07×10^{-4}	7.21×10^{-4}	7.07×10^{-4}	7.05×10^{-4}	7.10×10^{-4}	7.18×10^{-4}
.0482	10.23	10.49	9.96	7.49	6.61	7.07	7.21	7.07	7.05	7.11	7.18
.0496	10.23	10.49	9.98	7.49	6.61	7.07	7.21	7.07	7.05	7.11	7.18
.0514	10.24	10.49	9.99	7.49	6.61	7.07	7.21	7.08	7.05	7.11	7.18
.0497	10.22	10.52	9.99	7.50	6.58	7.07	7.21	----	7.02	----	----
.0498	10.21	10.51	9.97	7.50	6.59	7.07	7.21	----	7.03	----	----
.0499	10.21	10.51	9.99	7.49	6.58	7.07	7.21	----	7.03	----	----
0.1024	11.56×10^{-4}	12.83×10^{-4}	11.97×10^{-4}	7.91×10^{-4}	6.90×10^{-4}	7.29×10^{-4}	7.40×10^{-4}	7.17×10^{-4}	7.09×10^{-4}	7.13×10^{-4}	7.28×10^{-4}
.1025	11.56	12.83	11.98	7.92	6.90	7.29	7.40	7.17	7.09	7.14	7.28
.1056	11.51	12.78	11.95	7.91	6.90	7.29	7.40	7.17	7.09	7.14	7.28
.1056	11.56	12.83	11.96	7.92	6.90	7.30	7.40	7.17	7.09	7.15	7.28
.0993	11.61	12.70	11.82	7.90	6.85	7.29	7.40	----	7.09	----	----
.0993	11.62	12.67	11.83	7.90	6.85	7.29	7.40	----	7.08	----	----
.0994	11.60	12.68	11.79	7.91	6.85	7.29	7.40	----	7.09	----	----
0.1533	11.04×10^{-4}	13.56×10^{-4}	13.32×10^{-4}	8.19×10^{-4}	7.07×10^{-4}	7.43×10^{-4}	7.52×10^{-4}	7.25×10^{-4}	7.15×10^{-4}	7.22×10^{-4}	7.33×10^{-4}
.1534	11.03	13.57	13.36	8.20	7.08	7.44	7.53	7.25	7.15	7.24	7.34
.1519	11.02	13.54	13.33	8.21	7.08	7.45	7.53	7.25	7.15	7.24	7.34
.1519	10.98	13.47	13.33	8.20	7.07	7.45	7.53	7.25	7.15	7.24	7.34
.1483	11.05	13.50	13.19	8.19	7.04	7.44	7.52	----	7.13	----	----
.1483	11.06	13.58	13.28	8.19	7.05	7.44	7.53	----	7.13	----	----
.1484	11.09	13.58	13.27	8.19	7.04	7.44	7.53	----	7.13	----	----
0.2025	12.69×10^{-4}	13.10×10^{-4}	14.31×10^{-4}	8.41×10^{-4}	7.26×10^{-4}	7.55×10^{-4}	7.63×10^{-4}	7.29×10^{-4}	7.18×10^{-4}	7.24×10^{-4}	7.39×10^{-4}
.2026	12.72	13.17	14.33	8.41	7.26	7.55	7.63	7.29	7.18	7.25	7.39
.2027	12.71	13.01	14.24	8.42	7.25	7.55	7.64	7.29	7.18	7.26	7.39
.2028	12.70	13.09	14.27	8.41	7.25	7.55	7.63	7.29	7.18	7.26	7.39
.2070	13.13	13.02	14.41	8.48	7.27	7.59	7.67	----	7.17	----	----
.2072	13.13	12.89	14.38	8.49	7.27	7.59	7.67	----	7.17	----	----
.2072	13.13	13.02	14.36	8.49	7.27	7.59	7.67	----	7.17	----	----
0.2537	15.57×10^{-4}	12.48×10^{-4}	14.35×10^{-4}	8.57×10^{-4}	7.39×10^{-4}	7.65×10^{-4}	7.74×10^{-4}	7.35×10^{-4}	7.22×10^{-4}	7.30×10^{-4}	7.44×10^{-4}
.2537	15.57	12.41	14.38	8.57	7.38	7.65	7.74	7.36	7.22	7.30	7.44
.2539	15.54	12.50	14.43	8.57	7.38	7.65	7.74	7.36	7.22	7.30	7.44
.2536	15.69	12.33	14.40	8.58	7.36	7.65	7.73	----	7.19	----	----
.2524	15.69	12.43	14.33	8.58	7.35	7.64	7.73	----	7.19	----	----
.2527	15.66	12.48	14.40	8.58	7.35	7.64	7.73	----	7.19	----	----

TABLE III.- PROFILES OF PITOT PRESSURE AND TOTAL TEMPERATURE MEASURED THROUGH UNDISTURBED BOUNDARY LAYER JUST UPSTREAM OF SLOT LOCATION

[s = 0.254 cm]

Pitot pressure		Total temperature	
y/s	p_t/p_o	y/s	T_t/T_o
0.10	2.135×10^{-3}	0.34	0.796
.11	2.133	.35	.797
.15	2.013	.39	.802
.19	2.106	.43	.811
.29	3.201	.53	.820
.50	4.500	.74	.838
.89	5.270	1.13	.859
1.08	5.345	1.32	.869
1.23	5.931	1.47	.873
1.31	6.027	1.55	.878
1.52	6.319	1.76	.884
1.91	6.970	2.15	.891
2.09	7.337	2.33	.896
2.48	7.920	2.72	.900
3.69	9.763	3.93	.913
5.12	12.233	5.36	.929
7.09	15.261	7.33	.942
9.08	19.381	9.32	.955
10.59	21.845	10.83	.969
11.00	23.302	11.24	.970
12.10	25.108	12.34	.978
16.08	29.083	16.32	.985
22.16	28.941	22.40	.988
28.01	28.717	28.25	.991

Pitot pressure		Total temperature	
y/s	p_t/p_o	y/s	T_t/T_o
0.10	2.053×10^{-3}	0.34	0.825
.17	2.639	.41	.835
.27	3.610	.51	.851
.60	4.773	.84	.864
1.18	5.912	1.42	.886
1.59	6.702	1.83	.898
2.43	8.032	2.67	.909
2.89	8.756	3.13	.914
3.23	9.153	3.47	.919
4.04	10.725	4.28	.925
4.47	11.262	4.71	.933
5.56	12.912	5.80	.941
6.06	13.825	6.30	.944
8.04	17.708	8.28	.956
10.11	21.177	10.35	.971
13.17	26.136	13.41	.980
14.07	27.039	14.31	.985
14.76	27.657	15.00	.986
17.73	28.150	17.97	.986
20.14	28.084	20.38	.989
23.63	27.733	23.87	.987
26.56	27.587	26.80	.991

TABLE IV.- PROFILES OF PITOT PRESSURE AND TOTAL TEMPERATURE MEASURED DOWNSTREAM OF SINGLE SLOT

[s = 0.254 cm]

(a) x/s = 5.8

λ	Pitot pressure		Total temperature	
	y/s	P_t/P_o	y/s	T_t/T_o
0.0421	0.10	1.519×10^{-3}	0.23	0.730
.0424	.15	1.600	.28	.736
.0425	.20	1.703	.35	.741
.0425	.28	1.794	.41	.750
.0434	.33	1.888	.46	.757
.0427	.44	2.189	.57	.774
.0427	.58	2.657	.71	.795
.0428	.70	2.981	.83	.816
.0428	.84	3.829	.97	.833
.0452	.97	4.545	1.10	.855
.0429	1.12	5.157	1.25	.870
.0429	1.28	5.947	1.31	.881
.0434	1.43	6.384	1.55	.898
.0430	1.58	7.087	1.71	.907
.0429	1.74	7.962	1.87	.913
.0440	1.93	------	2.06	.922
.0450	2.14	8.722	2.27	.923
.0440	2.38	9.895	2.51	.926
.0427	2.74	10.254	2.87	.936
.0436	3.17	11.096	3.30	.943
.0432	3.77	11.222	3.90	.945
.0426	4.74	11.836	4.87	.958

λ	Pitot pressure		Total temperature	
	y/s	P_t/P_o	y/s	T_t/T_o
0.0497	0.10	1.500×10^{-3}	0.23	0.715
.0499	.18	1.634	.31	.723
.0506	.40	2.006	.53	.755
.0502	.63	2.667	.76	.791
.0526	.85	3.563	.98	.824
.0514	1.01	4.232	1.14	.843
.0512	1.27	5.462	1.40	.868
.0501	1.56	6.574	1.69	.896
.0509	1.79	7.261	1.92	.903
.0525	2.01	8.096	2.14	.910
.0499	2.77	10.099	2.90	.928
.0515	3.59	11.313	3.72	.935
.0503	4.98	12.221	5.11	.956
.0503	7.03	15.905	7.16	.971
.0506	9.06	20.206	9.19	.981
.0505	11.06	24.302	11.90	.988
.0507	13.05	28.143	13.18	.995
.0518	15.04	29.964	15.17	.997
.0507	17.04	30.739	17.17	.993
.0508	18.90	30.799	19.03	.992
.0508	21.02	30.630	21.15	.993
.0518	23.61	30.696	23.74	.994

λ	Pitot pressure		Total temperature	
	y/s	P_t/P_o	y/s	T_t/T_o
0.0445	0.10	1.472×10^{-3}	0.23	0.729
.0446	.17	1.666	.30	.740
.0445	.27	1.780	.40	.751
.0447	.50	2.425	.63	.789
.0447	.67	3.014	.80	.811
.0447	.91	4.085	1.04	.847
.0448	1.12	4.935	1.25	.873
.0468	1.38	6.265	1.51	.896
.0467	1.66	7.214	1.79	.912
.0451	1.99	8.180	2.12	.922
.0450	2.29	9.032	2.42	.934
.0452	3.21	11.029	3.34	.942
.0455	4.15	11.135	4.28	.958
.0453	6.03	13.636	6.16	.969
.0458	8.05	18.307	8.18	.982
.0451	10.15	22.682	10.28	.994
.0452	12.19	26.330	12.32	.998
.0456	14.16	29.780	14.29	.999
.0453	16.08	30.567	16.21	.996
.0458	18.16	30.786	18.29	.995
.0463	20.20	30.656	20.33	1.001
.0463	22.27	30.663	22.40	1.001

TABLE IV.- Continued

(a) Continued

λ	Pitot pressure		Total temperature	
	y/s	p_t/p_o	y/s	T_t/T_o
0.0964	0.10	1.543×10^{-3}	0.23	0.659
.0959	.14	1.571	.27	.659
.0967	.20	1.650	.33	.662
.0966	.26	1.710	.39	.667
.0977	.32	1.779	.45	.675
.0965	.42	1.896	.55	.689
.0975	.54	2.115	.67	.712
.1002	.70	2.539	.83	.737
.1000	.83	2.967	.96	.769
.0972	.97	3.510	1.10	.796
.0978	1.11	4.003	1.24	.823
.0982	1.26	4.504	1.39	.843
.0975	1.42	5.19	1.55	.861
.0982	1.57	6.008	1.70	.879
.0976	1.73	6.363	1.86	.896
.0975	1.92	7.351	2.05	.905
.1020	2.13	8.500	2.26	.920
.1020	2.37	9.126	2.50	.928
.0959	2.69	10.890	2.82	.932
.1004	3.22	12.66	3.35	.941
.0990	3.72	12.57	3.86	.947
.1027	4.65	11.98	4.78	.958
.1037	5.05	12.59	5.18	.958

λ	Pitot pressure		Total temperature	
	y/s	p_t/p_o	y/s	T_t/T_o
0.0986	0.10	1.603×10^{-3}	0.23	0.671
.0951	.29	1.785	.42	.683
.0989	.67	2.441	.80	.739
.0989	1.26	4.595	1.39	.830
.0986	2.02	7.531	2.15	.891
.0960	3.28	12.22	3.41	.921
.1017	4.88	12.08	5.01	.944
.0934	6.33	14.97	6.46	.954
.0989	7.87	17.75	8.00	.965
.1000	9.37	20.55	9.50	.976
.0945	11.05	24.75	11.18	.987
.0994	12.35	26.96	12.48	.986
.0992	13.91	28.54	14.04	.992
.1004	15.35	29.75	15.48	.987
.0937	16.81	30.56	16.94	.988
.0992	18.28	30.66	18.41	.990
.0993	20.38	30.55	20.51	.987
.0957	22.37	30.55	22.50	.986
.1048	24.29	30.45	24.42	.988
.1004	28.31	29.83	28.44	.997

λ	Pitot pressure		Total temperature	
	y/s	p_t/p_o	y/s	T_t/T_o
0.1416	0.10	1.814×10^{-3}	0.23	0.632
.1424	.15	1.831	.28	.631
.1388	.20	1.890	.33	.633
.1435	.30	1.969	.43	.639
.1425	.40	2.074	.53	.650
.1390	.51	2.215	.64	.664
.1442	.60	2.393	.73	.683
.1393	.70	2.652	.83	.708
.1445	.80	2.939	.93	.729
.1432	.90	3.174	1.03	.753
.1449	1.09	3.853	1.22	.796
.1433	1.30	4.793	1.43	.842
.1450	1.50	5.686	1.63	.866
.1446	1.69	6.678	1.82	.887
.1450	1.91	7.878	2.04	.903
.1413	2.10	8.489	2.23	.914
.1448	2.28	9.267	2.41	.918
.1452	2.70	11.082	2.83	.928
.1455	3.04	11.783	3.17	.936
.1409	3.73	12.251	3.86	.947
.1403	4.75	12.203	4.88	.957
.1411	7.36	17.059	7.49	.971

λ	Pitot pressure		Total temperature	
	y/s	p_t/p_o	y/s	T_t/T_o
0.1478	0.10	1.856×10^{-3}	0.23	0.639
.1487	.25	1.990	.38	.641
.1543	.61	2.469	.74	.684
.1550	1.21	4.351	1.34	.811
.1565	1.99	7.840	2.12	.895
.1570	3.29	------	3.42	.929
.1578	4.79	11.941	4.92	.949
.1581	6.29	13.569	6.42	.964
.1584	7.81	19.620	7.94	.969
.1584	9.27	20.422	9.40	.982
.1588	10.73	23.656	10.86	.989
.1590	12.28	25.814	12.41	.994
.1591	13.88	28.938	14.01	.995
.1591	15.56	30.308	15.69	.991
.1590	16.82	30.655	16.95	.991
.1595	18.22	30.722	18.35	.989
.1562	20.25	30.578	20.38	.993
.1597	22.33	30.574	22.46	.994
.1598	24.34	30.449	24.47	.994
.1547	27.31	29.986	27.44	.999

TABLE IV.- Continued

(a) Concluded

λ	Pitot pressure		Total temperature	
	y/s	p_t/p_o	y/s	T_t/T_o
0.2058	0.10	2.378×10^{-3}	0.23	0.619
.2070	.15	2.441	.28	.617
.2080	.19	2.526	.32	.616
.2087	.30	2.664	.43	.617
.2093	.41	2.788	.54	.623
.2098	.51	2.905	.64	.634
.2104	.60	3.025	.73	.646
.2107	.69	3.233	.82	.667
.2110	.80	3.398	.93	.692
.2111	.90	3.720	1.03	.722
.2117	1.09	4.307	1.22	.774
.2118	1.29	5.114	1.42	.823
.2123	1.49	5.705	1.62	.856
.2124	1.69	7.038	1.82	.883
.2127	1.91	7.728	2.04	.903
.2127	2.10	8.659	2.23	.910
.2131	2.28	9.075	2.41	.922
.2133	2.70	11.34	2.83	.936
.2134	3.13	12.40	3.26	.941
.2138	3.72	12.20	3.85	.952
.2138	4.77	12.14	4.90	.959
.2139	6.80	15.52	6.93	.974

λ	Pitot pressure		Total temperature	
	y/s	p_t/p_o	y/s	T_t/T_o
0.1925	0.10	2.295×10^{-3}	0.23	0.633
.1927	.15	2.488	.28	.634
.1927	.49	2.784	.62	.652
.1927	.66	3.006	.79	.678
.1930	1.16	4.458	1.29	.804
.1933	1.97	8.242	2.10	.897
.1932	3.28	12.92	3.41	.935
.1933	4.78	12.15	4.91	.957
.1940	6.32	14.98	6.45	.966
.1943	7.80	17.80	7.99	.973
.1948	9.32	20.55	9.45	.985
.1952	10.83	23.87	10.96	.992
.1954	12.28	26.81	12.41	1.001
.1955	13.84	29.60	13.97	.995
.1957	15.30	30.26	15.43	.997
.1958	16.81	30.66	16.94	.997
.1959	18.33	30.72	18.46	.996
.1959	20.36	30.59	20.49	.998
.1959	22.35	30.61	22.48	1.004
.1963	24.29	30.49	24.42	.997
.1962	26.29	30.12	26.42	1.006

TABLE IV.- Continued

(b) x/s = 17.12

λ	Pitot pressure		Total temperature	
	y/s	p_t/p_o	y/s	T_t/T_o
0.0483	0.10	1.511×10^{-3}	0.30	0.735
.0484	.09	1.424	.29	.736
.0481	.28	2.358	.48	.754
.0479	.68	3.253	.88	.785
.0485	1.13	4.084	1.33	.830
.0481	1.31	4.512	1.51	.843
.0483	1.70	5.769	1.90	.864
.0484	2.07	6.804	2.29	.881
.0489	2.47	7.310	2.67	.886
.0486	2.89	8.330	3.07	.893
.0486	4.30	10.605	4.50	.911
.0485	4.68	11.826	4.88	.916
.0483	5.10	12.867	5.30	.915
.0485	5.52	14.236	5.72	.922
.0486	5.80	16.139	6.00	.925
.0483	6.63	16.643	6.56	.932
.0486	6.71	18.113	6.91	.933
.0488	7.12	18.845	7.32	.940
.0486	7.51	18.922	7.71	.946
.0486	7.91	19.362	8.11	.944
.0484	8.31	19.657	8.51	.954
.0486	8.70	19.001	8.90	.953
.0485	9.05	20.670	9.25	.949
.0484	9.50	20.084	9.70	.959

λ	Pitot pressure		Total temperature	
	y/s	p_t/p_o	y/s	T_t/T_o
0.0505	0.10	1.384×10^{-3}	0.30	0.736
.0518	.45	2.759	.65	.763
.0518	.84	3.456	1.04	.795
.0517	1.47	4.858	1.67	.849
.0515	1.92	5.994	2.12	.870
.0521	2.69	7.814	2.89	.886
.0516	4.12	10.346	4.32	.905
.0517	10.01	22.606	10.21	.937
.0519	10.56	22.944	10.76	.957
.0520	11.45	24.407	11.65	.965
.0523	11.98	25.606	12.18	.971
.0524	12.57	26.978	12.77	.969
.0518	13.04	27.676	13.24	.977
.0524	13.54	28.522	13.74	.970
.0521	15.55	30.422	15.75	.970
.0524	16.02	30.540	16.22	.980
.0520	18.06	30.992	18.26	.980
.0522	19.10	31.023	19.30	.983
.0530	20.18	30.907	20.38	.981

λ	Pitot pressure		Total temperature	
	y/s	p_t/p_o	y/s	T_t/T_o
0.1029	0.10	1.288×10^{-3}	0.30	0.693
.1029	.16	1.449	.36	.696
.1022	.30	2.024	.50	.708
.1039	.62	2.614	.82	.738
.1033	.88	3.100	1.08	.769
.1037	.99	3.324	2.19	.783
.1023	1.26	3.778	1.46	.810
.1024	1.66	4.720	1.86	.853
.1027	2.44	6.638	2.64	.880
.1032	4.03	10.030	4.23	.905
.1036	4.48	10.807	4.68	.909
.1037	5.57	13.451	5.77	.917
.1036	6.06	14.627	6.26	.927
.1036	8.07	22.059	8.27	.949
.1049	10.11	21.577	10.31	.964
.1043	14.06	29.228	14.26	.979
.1035	17.99	30.898	18.19	.984
.1051	22.22	30.627	22.42	.992
.1050	28.01	30.323	28.21	.991

TABLE IV.- Continued

(b) Concluded

λ	Pitot pressure		Total temperature	
	y/s	p_t/p_o	y/s	T_t/T_o
0.1500	0.10	1.276×10^{-3}	0.30	0.665
.1499	.14	1.325	.34	.666
.1520	.30	2.009	.50	.679
.1520	.61	2.606	.81	.714
.1510	.91	3.108	1.11	.755
.1530	.98	3.312	1.18	.761
.1550	1.26	3.718	1.46	.800
.1530	1.63	4.502	1.73	.841
.1540	2.45	6.388	2.65	.883
.1540	4.05	9.480	4.25	.909
.1540	4.46	10.442	4.66	.915
.1540	5.57	13.521	5.77	.924
.1560	6.05	15.658	6.25	.927
.1540	8.04	22.736	8.24	.950
.1550	10.03	21.792	10.23	.961
.1560	10.60	23.482	10.80	.965
.1570	11.11	24.221	11.31	.970
.1570	11.62	25.285	11.82	.975
.1560	14.03	29.107	14.23	.981
.1550	18.06	31.018	18.26	.985
.1550	22.18	30.705	22.38	.988
.1550	28.02	30.422	28.22	.994

λ	Pitot pressure		Total temperature	
	y/s	p_t/p_o	y/s	T_t/T_o
0.1420	0.10	1.271×10^{-3}	0.30	0.671
.1420	.14	1.356	.34	.673
.1400	.21	1.731	.41	.678
.1420	.38	2.197	.58	.696
.1420	.77	2.862	.97	.742
.1430	1.03	3.244	1.23	.780
.1440	1.11	3.542	1.31	.787
.1430	1.20	3.744	1.41	.795
.1430	1.43	4.032	1.63	.827
.1430	1.84	5.148	2.04	.859
.1440	2.01	5.307	2.21	.869
.1440	2.41	6.609	2.61	.887
.1440	3.71	10.158	3.91	.908
.1440	5.01	12.371	5.21	.920
.1450	6.97	19.472	7.17	.939
.1440	8.97	21.275	9.17	.961
.1440	10.03	22.534	10.23	.964
.1450	11.04	24.579	11.24	.971
.1450	12.05	26.750	12.25	.977
.1450	16.04	30.665	16.24	.987
.1450	20.26	30.891	20.46	.994

λ	Pitot pressure		Total temperature	
	y/s	p_t/p_o	y/s	T_t/T_o
0.2030	0.10	1.271×10^{-3}	0.30	0.631
.2030	.14	1.273	.34	.633
.2040	.22	1.734	.42	.637
.2050	.41	2.403	.61	.655
.2050	.80	3.052	1.00	.706
.2050	1.03	3.387	1.23	.742
.2050	1.12	3.535	1.32	.755
.2060	1.23	3.620	1.43	.773
.2060	1.43	4.117	1.63	.797
.2060	1.84	4.714	2.04	.845
.2060	2.01	5.246	2.21	.859
.2070	2.42	6.191	2.62	.882
.2070	3.68	8.907	3.88	.910
.2070	5.03	11.624	5.23	.921
.2070	7.03	20.308	7.23	.937
.2070	8.99	21.089	9.19	.958
.2080	10.53	23.367	10.73	.964
.2070	11.15	24.655	11.35	.970
.2080	11.63	25.662	11.83	.971
.2080	12.11	26.517	12.31	.975
.2080	16.04	30.519	16.24	.983
.2080	20.05	------	20.25	.989

λ	Pitot pressure		Total temperature	
	y/s	p_t/p_o	y/s	T_t/T_o
0.2030	0.10	1.261×10^{-3}	0.30	0.634
.2040	.13	1.254	.33	.636
.2040	.29	2.062	.49	.646
.2050	.62	2.799	.82	.684
.2050	.92	3.232	1.12	.726
.2050	.97	3.277	1.17	.736
.2050	1.26	3.723	1.46	.777
.2050	1.64	4.448	1.84	.826
.2050	2.42	6.110	2.62	.880
.2060	4.05	9.519	4.25	.916
.2060	4.48	10.487	4.58	.916
.2060	5.56	13.952	5.66	.926
.2070	6.06	15.543	6.26	.930
.2070	8.02	23.199	8.22	.948
.2070	10.03	21.557	10.23	.963
.2070	10.61	23.409	10.81	.968
.2070	11.15	24.131	11.35	.971
.2080	14.06	29.506	14.26	.979
.2080	18.03	31.049	18.23	.985
.2080	22.22	30.833	22.42	.989
.2080	28.05	30.553	28.25	.997

TABLE IV.- Continued

(c) x/s = 37.12

λ	Pitot pressure		Total temperature	
	y/s	p_t/p_o	y/s	T_t/T_o
0.0515	0.10	1.365×10^{-3}	0.30	0.770
.0517	.15	1.674	.35	.773
.0521	.21	2.145	.41	.777
.0530	.30	2.757	.50	.783
.0535	.49	3.355	.69	.783
.0528	.88	3.783	1.08	.817
.0538	1.12	4.357	1.32	.831
.0547	1.23	4.402	1.43	.837
.0531	1.29	4.508	1.49	.848
.0532	1.53	4.961	1.73	.851
.0549	1.91	5.725	2.11	.868
.0540	2.09	6.115	2.29	.876
.0532	2.51	7.160	2.71	.883
.0551	3.71	9.305	3.91	.901
.0534	5.08	11.726	5.28	.915
.0538	7.07	14.993	7.27	.935
.0556	9.05	18.108	9.25	.950
.0551	10.33	21.864	10.53	.953
.0549	11.36	25.801	11.56	.962
.0543	12.24	30.870	12.44	.966
.0539	16.03	30.899	16.23	.978
.0562	20.22	30.905	20.42	.985

λ	Pitot pressure		Total temperature	
	y/s	p_t/p_o	y/s	T_t/T_o
0.0966	0.10	1.415×10^{-3}	0.30	0.734
.0974	.16	1.589	.36	.741
.0971	.22	1.969	.42	.746
.0975	.31	2.367	.51	.754
.0977	.51	2.907	.71	.765
.0970	.88	3.290	1.08	.790
.0969	1.10	3.674	1.30	.804
.0982	1.20	3.866	1.40	.816
.0985	1.31	4.056	1.51	.817
.0977	1.51	4.309	1.71	.831
.0980	1.93	5.280	2.13	.854
.0971	2.10	5.718	2.30	.866
.0979	2.50	6.521	2.70	.883
.0988	3.79	9.154	3.99	.911
.0978	5.36	11.379	5.56	.928
.0977	7.15	13.985	7.35	.942
.0983	9.16	18.405	9.36	.954
.0974	10.66	22.169	10.86	.965
.0986	11.19	24.500	11.39	.966
.0978	12.16	27.812	12.36	.974
.0974	16.13	28.923	16.33	.984

λ	Pitot pressure		Total temperature	
	y/s	p_t/p_o	y/s	T_t/T_o
0.1012	0.10	1.373×10^{-3}	0.30	0.736
.1017	.16	1.687	.36	.741
.1015	.33	2.453	.53	.752
.1022	.62	3.042	.82	.775
.1011	1.30	4.000	1.50	.817
.1027	1.64	4.614	1.84	.842
.1025	2.48	6.436	2.68	.879
.1029	2.91	6.890	3.11	.893
.1035	3.29	7.582	3.49	.902
.1016	4.09	9.348	4.29	.914
.1038	4.51	10.379	4.71	.919
.1042	5.59	12.036	5.79	.924
.1036	6.09	12.594	6.29	.932
.1037	8.10	15.858	8.30	.947
.1038	10.21	20.829	10.41	.959
.1016	13.26	31.880	13.46	.979
.1031	14.12	30.285	14.32	.978
.1045	14.83	29.165	15.03	.981
.1029	17.77	29.454	17.97	.986
.1036	20.25	29.386	20.45	.987
.1041	22.25	29.198	22.45	.995
.1040	28.04	29.409	28.24	.993

TABLE IV.- Continued

(c) Concluded

λ	Pitot pressure		Total temperature	
	y/s	p_t/p_o	y/s	T_t/T_o
0.1525	0.10	1.335×10^{-3}	0.30	0.699
.1547	.15	1.406	.35	.700
.1566	.22	1.811	.42	.706
.1576	.30	2.513	.50	.710
.1577	.48	2.573	.68	.721
.1600	.87	3.133	1.07	.745
.1592	1.00	3.386	1.29	.764
.1599	1.23	3.602	1.43	.776
.1583	1.50	4.069	1.70	.796
.1572	1.90	4.873	2.10	.829
.1608	2.10	4.896	2.30	.845
.1613	2.37	5.460	2.57	.857
.1613	3.61	8.260	3.81	.895
.1597	5.12	10.860	5.32	.915
.1616	7.09	14.220	7.29	.931
.1585	9.07	17.52	9.27	.948
.1626	10.66	22.19	10.86	.959
.1585	12.15	28.16	12.35	.970
.1611	16.12	29.67	16.32	.984

λ	Pitot pressure		Total temperature	
	y/s	p_t/p_o	y/s	T_t/T_o
0.1549	0.10	1.375×10^{-3}	0.30	0.703
.1553	.14	1.498	.34	.705
.1567	.32	2.306	.52	.716
.1555	.63	2.873	.83	.735
.1577	1.26	3.566	1.46	.779
.1577	1.66	4.804	1.86	.809
.1599	2.45	5.758	2.65	.860
.1600	2.88	6.678	3.08	.878
.1585	3.28	7.199	3.48	.893
.1577	4.06	9.036	4.26	.903
.1607	4.49	9.988	4.69	.911
.1614	5.58	11.65	5.78	.923
.1586	6.07	12.44	6.27	.928
.1577	8.08	15.51	8.28	.943
.1609	10.13	19.92	10.33	.954
.1616	13.20	32.92	13.40	.972
.1581	14.09	32.10	14.29	.975
.1624	14.84	30.14	15.06	.979
.1622	17.67	29.80	17.87	.984
.1610	20.19	29.81	20.39	.987
.1622	22.15	29.65	22.35	.986
.1626	28.01	29.08	28.21	.992

λ	Pitot pressure		Total temperature	
	y/s	p_t/p_o	y/s	T_t/T_o
0.1993	0.10	1.384×10^{-3}	0.30	0.676
.1994	.15	1.420	.35	.679
.1997	.21	1.778	.41	.682
.1996	.30	2.211	.50	.688
.1999	.48	2.613	.68	.702
.1999	.86	3.140	1.06	.728
.2000	1.08	3.442	1.28	.749
.2003	1.22	3.634	1.42	.762
.2006	1.30	3.825	1.50	.777
.2006	1.52	4.262	1.72	.794
.2006	1.90	4.641	2.10	.830
.2009	2.08	4.944	2.28	.842
.2007	2.49	5.687	2.69	.866
.2011	3.72	8.890	3.92	.910
.2009	5.10	10.73	5.30	.924
.2013	7.13	13.68	7.33	.940
.2011	9.17	17.58	9.37	.953
.2013	10.60	22.05	10.80	.962
.2013	11.07	23.38	11.27	.964
.2013	12.10	27.97	12.30	.968
.2018	16.07	29.15	16.27	.986

TABLE IV.- Continued

(d) x/s = 67.12

λ	Pitot pressure		Total temperature	
	y/s	p_t/p_o	y/s	T_t/T_o
0.1024	0.10	1.451×10^{-3}	0.30	0.755
.1027	.18	1.936	.38	.762
.1041	.34	2.848	.54	.773
.1051	.45	3.154	.65	.781
.1046	.57	3.419	.77	.785
.1047	.69	3.819	.89	.793
.1047	.85	3.692	1.05	.796
.1054	1.24	4.173	1.44	.820
.1049	1.47	4.391	1.67	.828
.1061	1.66	4.670	1.86	.837
.1057	1.89	5.205	2.09	.844
.1075	2.30	5.801	2.50	.856
.1071	2.50	6.011	2.70	.865
.1072	2.85	6.567	3.05	.873
.1055	4.06	9.041	4.26	.902
.1077	5.44	11.38	5.64	.917
.1083	6.64	13.15	6.84	.926
.1055	7.75	14.95	7.95	.938
.1066	8.80	16.91	9.00	.943
.1090	10.10	19.48	10.30	.953
.1093	11.12	21.76	11.32	.957
.1074	11.69	22.99	11.89	.963
.1083	13.94	25.70	14.14	.975
.1092	15.20	27.89	15.40	.979
.1087	16.33	30.27	16.53	.978
.1087	17.65	32.63	17.85	.982

λ	Pitot pressure		Total temperature	
	y/s	p_t/p_o	y/s	T_t/T_o
0.0976	0.10	1.446×10^{-3}	0.30	0.768
.0981	.14	1.743	.34	.774
.0974	.32	2.955	.52	.787
.0980	.64	3.553	.84	.806
.0986	1.25	4.211	1.45	.834
.0981	1.64	4.721	1.84	.849
.0987	2.45	5.908	2.65	.875
.0973	2.89	6.849	3.09	.890
.0986	3.29	7.508	3.49	.899
.0982	4.07	9.292	4.27	.909
.0971	4.51	9.863	4.71	.917
.0984	5.59	11.69	5.79	.930
.0983	6.05	11.90	6.25	.934
.0995	8.07	15.61	8.27	.945
.0989	10.14	19.11	10.34	.955
.0989	13.19	24.86	13.39	.974
.0996	14.07	26.19	14.27	.979
.0993	14.80	27.53	15.00	.978
.0975	17.71	32.83	17.91	.985
.0996	20.22	35.86	20.42	.983
.0987	22.29	29.43	22.49	.986
.0985	28.04	29.16	28.24	.993

λ	Pitot pressure		Total temperature	
	y/s	p_t/p_o	y/s	T_t/T_o
0.1401	0.10	1.441×10^{-3}	0.30	0.752
.1405	.12	1.476	.32	.755
.1423	.19	1.953	.39	.761
.1411	.28	2.480	.48	.768
.1436	.48	3.195	.68	.783
.1420	.82	3.529	1.02	.798
.1426	1.08	3.822	1.28	.815
.1435	1.19	4.064	1.39	.819
.1416	1.27	3.914	1.47	.824
.1425	1.50	4.251	1.70	.834
.1416	1.87	4.931	2.07	.849
.1437	2.07	5.315	2.27	.860
.1446	2.47	5.961	2.67	.875
.1400	3.68	8.007	3.88	.904
.1426	5.09	10.53	5.29	.926
.1450	7.07	13.32	7.27	.945
.1432	9.04	17.10	9.24	.954
.1418	10.55	19.86	10.75	.961
.1440	11.06	21.18	11.26	.971
.1440	12.08	22.81	12.28	.971
.1405	16.06	28.90	16.26	.982

λ	Pitot pressure		Total temperature	
	y/s	p_t/p_o	y/s	T_t/T_o
0.1489	0.10	1.448×10^{-3}	0.30	0.738
.1485	.14	1.565	.34	.742
.1482	.19	1.916	.39	.749
.1483	.28	2.518	.48	.752
.1491	.44	3.042	.64	.761
.1460	.63	3.384	.83	.772
.1476	1.25	3.881	1.45	.806
.1470	1.64	4.472	1.84	.822
.1482	2.45	5.691	2.65	.856
.1474	2.89	6.293	3.09	.876
.1477	3.28	7.217	3.48	.882
.1503	4.05	8.380	4.25	.901
.1498	4.48	10.981	4.68	.911
.1492	5.58	11.136	5.78	.921
.1486	6.07	12.023	6.27	.927
.1492	8.18	15.948	8.38	.943
.1513	10.25	19.084	10.45	.956
.1493	13.20	24.680	13.40	.970
.1522	14.14	26.631	14.34	.978
.1527	14.70	27.614	14.90	.980
.1530	17.71	32.867	17.91	.983
.1532	20.19	37.736	20.39	.989
.1517	22.24	29.872	22.44	.986

TABLE IV.- Continued

(d) Concluded

λ	Pitot pressure		Total temperature	
	y/s	p_t/p_o	y/s	T_t/T_o
0.2094	0.10	1.413×10^{-3}	0.30	0.715
.2104	.14	1.433	.34	.717
.2108	.20	1.874	.40	.722
.2113	.29	2.366	.49	.728
.2117	.49	2.956	.69	.740
.2124	.85	3.497	1.05	.759
.2128	1.09	3.706	1.29	.772
.2132	1.22	3.839	1.42	.778
.2129	1.32	4.032	1.52	.786
.2135	1.52	4.196	1.72	.795
.2138	1.90	4.787	2.10	.816
.2139	2.09	4.950	2.29	.822
.2141	2.48	5.642	2.68	.849
.2149	3.86	7.978	4.06	.893
.2150	5.18	10.940	5.38	.918
.2152	7.13	12.884	7.33	.935
.2152	9.15	16.597	9.35	.949
.2154	10.67	19.919	10.87	.961
.2153	11.28	21.869	11.48	.961
.2155	12.16	22.598	12.36	.970
.2152	16.16	30.031	16.36	.982

λ	Pitot pressure		Total temperature	
	y/s	p_t/p_o	y/s	T_t/T_o
0.2025	0.10	1.413×10^{-3}	0.30	0.723
.2037	.15	1.488	.35	.724
.2046	.32	2.529	.52	.735
.2053	.64	3.211	.84	.753
.2056	1.28	3.834	1.48	.786
.2063	1.63	4.401	1.83	.804
.2064	2.47	5.432	2.67	.845
.2066	2.89	6.502	3.09	.867
.2069	3.29	7.037	3.49	.881
.2072	4.09	8.368	4.29	.901
.2073	4.50	9.484	4.70	.908
.2074	5.55	10.91	5.75	.927
.2079	6.09	12.10	6.29	.929
.2083	8.11	14.26	8.31	.947
.2085	10.16	19.56	10.36	.958
.2086	13.27	24.55	13.47	.977
.2089	14.09	26.43	14.29	.974
.2090	14.81	28.00	15.01	.980
.2094	17.74	33.11	17.94	.984
.2094	20.24	37.63	20.44	.989
.2096	24.41	29.54	24.61	.992
.2098	26.85	29.51	27.05	.994

TABLE IV.- Continued

(e) x/s = 107.12

λ	Pitot pressure		Total temperature	
	y/s	p_t/p_o	y/s	T_t/T_o
0.0485	0.10	1.502×10^{-3}	0.30	0.780
.0498	.15	1.510	.35	.783
.0487	.21	2.051	.41	.792
.0486	.30	2.804	.50	.800
.0485	.49	3.677	.69	.819
.0496	.87	4.311	1.07	.838
.0506	1.10	4.579	1.30	.850
.0494	1.21	4.754	1.41	.853
.0486	1.29	5.013	1.49	.857
.0488	1.51	5.230	1.71	.864
.0491	1.87	5.820	2.07	.876
.0493	2.12	6.228	2.32	.878
.0507	2.51	6.550	2.71	.890
.0491	3.65	8.544	3.85	.906
.0503	5.15	10.757	5.35	.925
.0488	7.07	13.460	7.27	.937
.0493	9.16	17.009	9.36	.955
.0496	10.63	19.531	10.83	.963
.0499	11.19	21.152	11.39	.965
.0492	12.15	23.061	12.35	.971
.0494	16.08	29.167	16.28	.982

λ	Pitot pressure		Total temperature	
	y/s	p_t/p_o	y/s	T_t/T_o
0.0485	0.10	1.489×10^{-3}	0.30	0.783
.0490	.15	1.477	.35	.789
.0490	.31	3.064	.51	.806
.0513	.64	4.077	.84	.828
.0504	1.26	4.826	1.46	.854
.0514	1.65	5.382	1.85	.863
.0508	2.47	6.720	2.67	.880
.0500	2.88	6.924	3.08	.893
.0502	3.27	7.888	3.47	.893
.0500	4.07	9.510	4.27	.906
.0499	4.47	10.714	4.67	.914
.0509	5.61	11.345	5.81	.925
.0516	6.67	11.95	6.27	.929
.0511	8.12	15.25	8.32	.944
.0498	10.20	18.73	10.40	.958
.0510	13.18	24.65	13.38	.972
.0509	14.14	25.66	14.34	.979
.0504	14.86	27.85	15.06	.979
.0509	17.68	29.92	17.88	.983
.0497	20.24	29.99	20.44	.985
.0515	22.18	30.16	22.38	.984
.0507	28.03	32.86	28.23	.988

λ	Pitot pressure		Total temperature	
	y/s	p_t/p_o	y/s	T_t/T_o
0.0973	0.10	1.478×10^{-3}	0.30	0.772
.0988	.15	1.744	.35	.776
.0977	.21	2.236	.41	.783
.1002	.30	2.869	.50	.789
.0985	.50	3.499	.70	.803
.0965	.87	4.099	1.07	.818
.0988	1.11	4.316	1.31	.833
.0995	1.21	4.258	1.41	.837
.0984	1.30	4.647	1.50	.840
.0970	1.53	4.708	1.73	.846
.1016	1.91	5.217	2.11	.856
.1018	2.10	5.534	2.30	.861
.0989	2.48	6.356	2.68	.871
.1012	3.71	7.761	3.91	.896
.0992	5.14	10.43	5.34	.917
.0991	7.16	13.27	7.36	.934
.0973	9.15	16.80	9.35	.949
.1029	10.65	19.17	10.85	.956
.1034	11.21	19.95	11.41	.964
.1040	12.33	22.49	12.53	.972
.0994	16.00	28.49	16.20	.982

λ	Pitot pressure		Total temperature	
	y/s	p_t/p_o	y/s	T_t/T_o
0.0961	0.10	1.461×10^{-3}	0.30	0.785
.1016	.15	1.799	.35	.785
.1008	.30	2.852	.50	.792
.1036	.65	3.712	.85	.814
.1046	1.28	4.409	1.48	.838
.1103	1.68	4.903	1.88	.850
.1075	2.48	5.799	2.68	.867
.1114	2.89	6.412	3.09	.874
.1106	3.30	7.002	3.50	.884
.1079	4.07	8.635	4.27	.898
.1121	4.50	9.054	4.70	.904
.1122	5.71	11.20	5.91	.922
.1133	8.13	14.48	8.33	.942
.1026	10.24	18.29	10.44	.954
.1089	12.89	23.72	13.09	.965
.1149	14.05	25.94	14.25	.976
.1138	15.01	26.72	15.21	.979
.1123	17.73	30.33	17.93	.984
.1094	20.29	30.70	20.49	.986
.1089	22.25	31.11	22.45	.988
.1136	28.06	36.34	28.26	.992

TABLE IV.- Concluded

(e) Concluded

λ	Pitot pressure		Total temperature	
	y/s	p_t/p_o	y/s	T_t/T_o
0.1496	0.10	1.425×10^{-3}	0.30	0.765
.1490	.12	1.425	.32	.766
.1485	.17	1.835	.37	.773
.1507	.26	2.569	.46	.779
.1504	.45	3.275	.65	.793
.1496	.83	3.694	1.03	.812
.1520	1.06	4.071	1.26	.824
.1512	1.17	4.103	1.37	.827
.1510	1.26	4.297	1.46	.830
.1525	1.47	4.559	1.67	.839
.1525	1.87	4.998	2.07	.849
.1522	2.06	5.263	2.26	.855
.1528	2.48	5.742	2.68	.866
.1536	3.63	7.662	3.83	.897
.1515	5.03	10.16	5.23	.918
.1544	7.03	12.47	7.23	.938
.1546	9.01	16.19	9.21	.949
.1547	10.53	19.41	10.73	.962
.1549	11.05	19.69	11.25	.962
.1549	12.05	21.71	12.25	.969
.1551	16.06	28.81	16.26	.981

λ	Pitot pressure		Total temperature	
	y/s	p_t/p_o	y/s	T_t/T_o
0.1462	0.10	1.414×10^{-3}	0.30	0.760
.1479	.12	1.420	.32	.763
.1463	.29	2.657	.49	.778
.1484	.60	3.491	.80	.799
.1479	1.23	4.191	1.43	.825
.1490	1.60	4.739	1.80	.837
.1492	2.42	5.517	2.62	.860
.1480	2.88	6.315	3.08	.872
.1491	3.27	7.367	3.47	.880
.1485	4.04	8.736	4.24	.897
.1474	4.46	8.937	4.66	.906
.1497	5.55	10.70	5.75	.921
.1475	6.04	11.94	6.24	.928
.1485	8.07	14.54	8.27	.943
.1472	10.13	18.25	10.33	.958
.1476	13.17	24.61	13.37	.968
.1476	14.06	25.70	14.26	.971
.1481	14.76	27.11	14.96	.975
.1478	17.65	30.06	17.85	.983
.1484	20.18	30.72	20.38	.986
.1482	22.13	30.87	22.33	.987
.1485	28.36	36.65	28.56	.991

λ	Pitot pressure		Total temperature	
	y/s	p_t/p_o	y/s	T_t/T_o
0.1964	0.10	1.433×10^{-3}	0.30	0.746
.1976	.12	1.467	.32	.749
.1986	.18	1.918	.38	.755
.1993	.27	2.545	.47	.761
.1999	.46	3.215	.66	.773
.2003	.84	3.754	1.04	.791
.2008	1.08	3.957	1.28	.802
.2011	1.19	4.095	1.39	.808
.2016	1.27	4.202	1.47	.807
.2017	1.48	4.471	1.68	.816
.2022	1.89	5.054	2.09	.829
.2023	2.06	5.101	2.26	.837
.2027	2.46	5.546	2.66	.850
.2030	3.69	7.209	3.89	.882
.2034	4.77	9.642	4.97	.904
.2038	5.06	10.337	5.26	.911
.2042	7.06	12.429	7.26	.932
.2044	9.04	15.004	9.24	.949
.2046	10.57	18.669	10.77	.961
.2048	10.65	19.694	10.85	.961
.2049	12.07	21.302	12.27	.967
.2051	16.04	28.486	16.24	.980

λ	Pitot pressure		Total temperature	
	y/s	p_t/p_o	y/s	T_t/T_o
0.2084	0.10	1.508×10^{-3}	0.30	0.735
.2088	.12	1.403	.32	.737
.2093	.28	2.502	.48	.751
.2101	.58	3.294	.78	.772
.2105	1.24	4.011	1.44	.798
.2111	1.62	4.489	1.82	.814
.2114	2.41	5.571	2.61	.841
.2117	2.85	6.222	3.05	.851
.2120	3.25	6.663	3.45	.863
.2123	4.04	7.721	4.24	.888
.2125	4.45	8.439	4.65	.885
.2127	5.54	10.607	5.74	.915
.2129	6.02	11.541	6.22	.920
.2130	8.03	14.319	8.23	.940
.2134	10.10	17.882	10.30	.954
.2137	13.15	23.753	13.35	.971
.2137	14.02	25.364	14.22	.971
.2140	14.75	26.816	14.95	.979
.2140	17.65	30.140	17.85	.983
.2143	20.14	31.190	20.34	.986
.2145	22.09	31.346	22.29	.987
.2146	27.92	23.895	28.12	.958

TABLE V.- THEORETICAL PROFILES OF PITOT PRESSURE WITH SINGLE SLOT

[s = 0.254 cm]

Upstream of slot		Downstream of slot											
		λ = 0.15						λ = 0.20					
x/s = -1.97		x/s = 5.8		x/s = 17.12		x/s = 67.12		x/s = 5.8		x/s = 17.12		x/s = 67.12	
y/s	p_t/p_o	y/s	p_t/p_o	y/s	p_t/p_o	y/s	p_t/p_o	y/s	p_t/p_o	y/s	p_t/p_o	y/s	p_t/p_o
0.0523	0.9854×10^{-3}	0.2025	1.018×10^{-3}	0.3235	1.416×10^{-3}	0.1305	1.558×10^{-3}	0.1969	1.282×10^{-3}	0.3126	1.548×10^{-3}	0.1297	1.538×10^{-3}
.1230	1.835	.3083	1.057	.4701	1.802	.2229	2.251	.2987	1.590	.4486	1.899	.2209	2.225
.2084	2.697	.4342	2.366	.6631	2.461	.3391	2.832	.4300	1.803	.6248	2.377	.3356	2.803
.3145	3.420	.5907	2.566	.9146	3.416	.4879	3.357	.6074	1.809	.8598	3.107	.4824	3.324
.4491	4.074	.8039	2.540	1.240	4.352	.6803	3.863	.8603	2.253	1.178	4.151	.6723	3.826
.6216	4.704	1.128	2.946	1.659	5.321	.9803	4.393	1.214	3.717	1.597	5.165	.9192	4.347
.8439	5.343	1.592	4.558	2.194	6.355	1.253	5.114	2.198	6.330	2.135	6.237	1.239	5.052
1.131	6.014	2.152	6.016	2.868	7.449	1.664	6.065	2.867	7.579	2.815	7.375	1.648	5.988
1.150	6.732	2.835	7.361	3.720	8.654	2.186	6.957	3.702	8.808	3.670	8.565	2.169	6.871
1.980	7.556	3.680	8.662	4.780	10.229	2.856	7.853	4.744	10.32	4.738	10.08	2.840	7.755
2.592	8.549	4.731	10.16	6.074	12.281	3.718	8.815	6.024	12.29	6.045	12.12	3.704	8.704
3.368	9.743	6.022	12.13	7.625	14.987	4.814	10.13	7.564	14.95	7.610	14.83	4.808	10.00
4.343	11.18	7.575	14.78	9.452	18.570	6.174	12.09	9.379	18.52	9.449	18.42	6.177	11.96
5.554	13.05	9.402	18.36	11.57	23.08	7.804	14.91	11.49	23.02	11.58	22.94	7.819	14.77
7.024	15.72	11.52	22.87	14.05	27.93	9.710	18.65	16.95	30.44	14.07	27.84	9.736	18.51
8.766	19.25	13.98	27.81	17.07	30.44	11.91	23.20	20.99	30.49	17.10	30.43	11.95	23.08
10.81	23.64	16.99	30.78	21.16	30.49	14.49	27.96			21.18	30.49	14.53	27.88
13.20	28.33	21.03	30.49			17.64	30.45					17.69	30.45
16.17	30.46					21.89	30.49					21.94	30.49
20.19	30.49												

TABLE VI.- PROFILES OF PITOT PRESSURE AND TOTAL TEMPERATURE MEASURED DOWNSTREAM OF TWO SLOTS

[s = 0.254 cm]

(a) x/s = 17.12

λ_1	λ_2	Pitot pressure		Total temperature	
		y/s	p_t/p_o	y/s	T_t/T_o
0.0518	0.0492	0.10	1.405×10^{-3}	0.30	0.725
.0523	.0500	.13	1.393	.33	.725
.0525	.0507	.18	1.677	.38	.730
.0526	.0503	.27	2.031	.47	.736
.0527	.0511	.46	2.463	.66	.751
.0528	.0512	.85	3.053	1.05	.781
.0529	.0500	1.08	3.471	1.28	.796
.0531	.0517	1.18	3.542	1.38	.808
.0531	.0502	1.27	3.682	1.47	.814
.0531	.0517	1.48	4.105	1.68	.829
.0533	.0519	1.89	4.961	2.09	.851
.0533	.0514	2.08	5.289	2.28	.864
.0535	.0509	2.45	5.884	2.65	.869
.0536	.0521	3.67	8.145	3.87	.892
.0536	.0526	5.07	10.554	5.27	.912
.0537	.0526	7.06	16.270	7.26	.928
.0536	.0520	9.02	18.113	9.22	.954
.0537	.0525	10.56	20.281	10.76	.962
.0538	.0527	11.04	21.300	11.24	.963
.0538	.0523	12.08	23.239	12.28	.972
.0539	.0531	16.01	28.811	16.21	.979

λ_1	λ_2	Pitot pressure		Total temperature	
		y/s	p_t/p_o	y/s	T_t/T_o
0.0486	0.0475	0.10	1.351×10^{-3}	0.30	0.732
.0490	.0475	.12	1.435	.32	.735
.0498	.0481	.26	2.077	.46	.747
.0502	.0481	.59	2.703	.79	.771
.0504	.0484	1.22	3.723	1.42	.818
.0507	.0495	1.60	4.318	1.80	.846
.0509	.0498	2.36	5.728	2.56	.876
.0507	.0492	2.83	6.608	3.03	.885
.0510	.0486	3.27	6.980	3.47	.893
.0512	.0496	4.14	8.926	4.34	.906
.0512	.0496	4.46	8.808	4.66	.914
.0512	.0500	5.50	11.276	5.70	.925
.0514	.0498	6.02	13.794	6.22	.927
.0515	.0499	8.07	17.806	8.27	.947
.0515	.0499	10.09	19.270	10.29	.959
.0515	.0494	13.12	25.312	13.32	.972
.0515	.0506	13.98	26.269	14.18	.977
.0516	.0505	14.70	27.076	14.90	.982
.0517	.0491	17.61	29.591	17.81	.984
.0517	.0502	20.03	32.033	20.33	.989
.0518	.0500	22.02	34.667	22.32	.986
.0519	.0505	27.80	39.522	28.10	.990

TABLE VI.- Continued

(a) Continued

λ_1	λ_2	Pitot pressure		Total temperature	
		y/s	p_t/p_o	y/s	T_t/T_o
0.0986	0.1007	0.10	1.272×10^{-3}	0.30	0.672
.0987	.1008	.12	1.256	.32	.674
.0992	.1018	.16	1.380	.36	.675
.0992	.1020	.25	1.752	.45	.683
.0995	.1013	.45	2.155	.65	.700
.0998	.1010	.82	2.511	1.02	.725
.0999	.1020	1.03	2.790	1.23	.753
.1000	.1014	1.17	3.042	1.37	.766
.1002	.1021	1.25	3.132	1.45	.776
.1001	.1019	1.45	3.425	1.65	.794
.1002	.1022	1.83	4.007	2.03	.820
.1003	.1022	2.02	4.338	2.22	.835
.1004	.1027	2.44	4.989	2.64	.855
.1005	.1036	3.64	6.880	3.84	.891
.1006	.1032	5.05	9.202	5.25	.913
.1007	.1024	6.98	13.848	7.18	.934
.1008	.1027	9.02	19.534	9.22	.953
.1009	.1051	10.51	20.052	10.71	.961
.1009	.1031	10.99	20.585	11.19	.965
.1009	.1023	12.04	22.228	12.24	.972
.1010	.1019	16.04	28.537	16.24	.979

λ_1	λ_2	Pitot pressure		Total temperature	
		y/s	p_t/p_o	y/s	T_t/T_o
0.1000	0.1039	0.10	1.274×10^{-3}	0.30	0.627
.1006	.1040	.11	1.274	.31	.659
.1009	.1035	.17	1.384	.37	.658
.1013	.1045	.26	1.718	.46	.667
.1015	.1030	.59	2.309	.79	.693
.1018	.1047	1.21	3.275	1.41	.754
.1018	.1047	1.57	3.645	1.77	.782
.1020	.1034	2.39	4.806	2.59	.832
.1023	.1045	2.85	5.661	3.05	.852
.1025	.1039	3.26	6.224	3.46	.864
.1028	.1050	4.02	7.374	4.22	.881
.1027	.1044	4.44	8.305	4.64	.887
.1029	.1053	5.55	10.569	5.75	.907
.1031	.1062	6.06	12.037	6.26	.910
.1032	.1067	8.01	19.757	8.21	.934
.1033	.1055	10.11	19.596	10.31	.954
.1034	.1056	13.16	24.634	13.36	.970
.1036	.1052	14.03	26.161	14.23	.973
.1035	.1050	14.79	27.190	14.99	.975
.1037	.1060	17.55	29.713	17.75	.979
.1038	.1057	20.14	32.638	20.34	.984

TABLE VI.- Continued

(a) Concluded

λ_1	λ_2	Pitot pressure		Total temperature	
		y/s	p_t/p_o	y/s	T_t/T_o
0.1457	0.1411	0.10	1.353×10^{-3}	0.30	0.631
.1468	.1432	.14	1.491	.34	.633
.1485	.1477	.20	1.757	.40	.635
.1490	.1490	.39	2.122	.59	.649
.1495	.1471	.75	2.603	.95	.680
.1504	.1492	1.01	2.817	1.21	.708
.1500	.1452	1.14	3.086	1.34	.720
.1510	.1457	1.22	3.187	1.42	.736
.1511	.1461	1.39	3.449	1.59	.747
.1509	.1458	1.81	4.103	2.01	.784
.1512	.1459	2.02	4.401	2.22	.799
.1513	.1462	2.40	4.803	2.60	.828
.1515	.1461	3.57	6.491	3.77	.868
.1513	.1467	4.01	7.198	4.21	.880
.1519	.1469	5.01	9.467	5.21	.902
.1518	.1467	6.97	14.839	7.17	.924
.1521	.1507	8.97	19.994	9.17	.935
.1527	.1471	10.47	19.609	10.67	.957
.1522	.1472	10.95	20.257	11.15	.959
.1527	.1474	12.00	22.585	12.20	.966
.1529	.1475	15.94	28.672	16.14	.977

λ_1	λ_2	Pitot pressure		Total temperature	
		y/s	p_t/p_o	y/s	T_t/T_o
0.1443	0.1413	0.10	1.301×10^{-3}	0.30	0.633
.1430	.1382	.15	1.525	.35	.637
.1422	.1376	.21	1.728	.41	.642
.1421	.1374	.52	2.267	.72	.669
.1422	.1424	1.16	3.027	1.36	.736
.1421	.1372	1.55	3.604	1.75	.772
.1422	.1423	2.34	4.971	2.54	.828
.1424	.1425	2.75	5.252	2.95	.849
.1425	.1426	3.20	6.395	3.40	.865
.1427	.1377	3.95	7.465	4.15	.885
.1427	.1378	4.40	8.249	4.60	.895
.1428	.1378	5.45	10.049	5.65	.910
.1429	.1429	5.94	11.661	6.14	.917
.1429	.1379	7.98	18.817	8.18	.940
.1430	.1418	10.04	19.026	10.24	.960
.1431	.1423	13.08	25.048	13.28	.969
.1432	.1424	13.95	25.560	14.15	.976
.1433	.1382	14.66	26.861	14.86	.979
.1432	.1433	17.59	29.344	17.79	.985
.1436	.1435	20.06	31.813	20.26	.987
.1434	.1424	22.27	34.424	22.47	.989
.1434	.1384	27.83	28.906	28.03	.995

TABLE VI.- Continued

(b) x/s = 67.12

λ_1	λ_2	Pitot pressure		Total temperature	
		y/s	p_t/p_o	y/s	T_t/T_o
0.0494	0.0507	0.10	1.409×10^{-3}	0.30	0.759
.0493	.0516	.16	1.822	.36	.766
.0494	.0509	.22	2.256	.42	.774
.0493	.0505	.41	2.973	.61	.787
.0494	.0512	.79	3.659	.99	.810
.0494	.0505	1.01	4.023	1.21	.821
.0494	.0514	1.12	3.927	1.32	.827
.0494	.0513	1.21	4.067	1.41	.831
.0495	.0514	1.40	4.418	1.60	.837
.0494	.0513	1.80	4.820	2.00	.850
.0496	.0513	2.05	5.095	2.25	.858
.0496	.0504	2.39	5.643	2.59	.867
.0496	.0521	3.60	7.222	3.80	.891
.0497	.0515	4.01	8.208	4.21	.898
.0496	.0519	4.97	9.894	5.17	.907
.0497	.0519	6.97	12.626	7.17	.933
.0498	.0511	9.02	15.676	9.22	.945
.0499	.0499	10.47	17.925	10.67	.959
.0500	.0506	10.92	19.931	11.12	.955
.0500	.0512	12.04	21.264	12.24	.965
.0500	.0505	15.97	27.871	16.17	.979

λ_1	λ_2	Pitot pressure		Total temperature	
		y/s	p_t/p_o	y/s	T_t/T_o
0.0492	0.0501	0.10	1.415×10^{-3}	0.34	0.772
.0494	.0498	.15	1.804	.39	.778
.0495	.0500	.30	2.767	.54	.787
.0497	.0495	.53	3.524	.77	.803
.0497	.0502	1.19	4.238	1.43	.827
.0499	.0509	1.56	4.599	1.80	.840
.0499	.0507	2.38	5.927	2.62	.861
.0499	.0507	2.82	6.466	3.06	.871
.0500	.0514	3.20	7.233	3.44	.882
.0500	.0513	3.98	8.118	4.22	.894
.0502	.0511	4.41	9.599	4.65	.899
.0501	.0511	5.51	11.170	5.75	.913
.0501	.0508	6.00	11.290	6.24	.920
.0502	.0509	7.96	14.743	8.20	.933
.0503	.0512	10.05	18.319	10.29	.949
.0504	.0525	13.13	23.507	13.37	.965
.0505	.0516	14.01	24.648	14.25	.973
.0504	.0513	14.70	26.015	14.94	.975
.0505	.0510	17.59	30.880	17.83	.980
.0505	.0517	20.09	33.490	20.33	.978
.0505	.0515	22.10	29.548	22.34	.985
.0506	.0508	27.92	30.448	28.26	.994

TABLE VI.- Continued

(b) Continued

λ_1	λ_2	Pitot pressure		Total temperature	
		y/s	p_t/p_o	y/s	T_t/T_o
0.0987	0.0988	0.10	1.359×10^{-3}	0.34	0.743
.0985	.0985	.13	1.366	.37	.746
.0988	.0993	.24	2.100	.48	.755
.0990	.0985	.44	2.913	.68	.768
.0991	.0972	.75	3.267	1.03	.783
.0994	.1035	1.09	3.599	1.33	.796
.0994	.0993	1.18	3.650	1.42	.803
.0995	.1025	1.26	3.797	1.50	.800
.0995	.1012	1.43	3.909	1.77	.811
.0996	.0990	1.87	4.347	2.11	.829
.0998	.0980	2.03	4.670	2.27	.838
.0999	.1010	2.40	5.101	2.64	.848
.0999	.0993	3.63	6.577	3.88	.878
.0998	.0950	5.01	8.731	5.25	.905
.0998	.0992	7.04	11.490	7.28	.930
.0999	.1010	9.00	15.155	9.24	.964
.1000	.1007	10.53	17.209	10.73	.954
.1000	.0993	11.04	18.468	11.28	.956
.1001	.1007	12.02	20.475	12.26	.975
.1001	.0993	16.00	26.865	16.24	.980
.1001	.1010	27.87	30.437	28.11	.991

λ_1	λ_2	Pitot pressure		Total temperature	
		y/s	p_t/p_o	y/s	T_t/T_o
0.1072	0.1042	0.10	1.312×10^{-3}	0.34	0.755
.1095	.1081	.14	1.548	.38	.756
.1111	.1109	.24	2.178	.48	.759
.1121	.1149	.56	2.938	.80	.774
.1130	.1149	1.26	3.673	1.50	.797
.1134	.1099	1.58	3.840	1.82	.811
.1137	.1147	2.37	4.946	2.61	.839
.1140	.1123	2.81	5.261	3.05	.851
.1141	.1141	3.21	5.583	3.45	.861
.1144	.1170	4.01	6.669	4.25	.879
.1145	.1152	4.45	7.436	4.69	.889
.1148	.1140	5.52	9.105	5.76	.910
.1149	.1105	6.00	10.262	6.24	.913
.1148	.1144	7.98	12.892	8.22	.934
.1147	.1166	10.09	17.982	10.33	.947
.1149	.1158	13.11	22.602	13.35	.963
.1151	.1142	14.02	23.637	14.26	.972
.1152	.1128	14.71	25.607	14.95	.969
.1152	.1177	17.60	31.234	17.84	.987
.1154	.1170	20.11	35.691	20.35	.989
.1156	.1185	22.23	33.698	22.47	.981

TABLE VI.- Concluded

(b) Concluded

λ_1	λ_2	Pitot pressure		Total temperature	
		y/s	p_t/p_o	y/s	T_t/T_o
0.1475	0.1449	0.10	1.356×10^{-3}	0.34	0.732
.1481	.1442	.15	1.493	.39	.733
.1483	.1442	.24	2.099	.48	.738
.1483	.1451	.40	2.649	.64	.748
.1484	.1437	.79	3.198	1.03	.765
.1488	.1440	1.02	3.511	1.26	.776
.1491	.1445	1.15	3.541	1.39	.777
.1492	.1457	1.23	3.536	1.47	.783
.1495	.1440	1.44	3.911	1.68	.790
.1496	.1455	1.84	4.121	2.08	.813
.1496	.1460	2.02	4.356	2.26	.816
.1498	.1446	2.41	4.877	2.65	.829
.1497	.1445	3.63	6.289	3.87	.868
.1499	.1451	5.01	8.342	5.25	.900
.1500	.1466	6.98	11.919	7.22	.929
.1498	.1450	9.00	14.004	9.24	.946
.1502	.1459	10.49	17.798	10.73	.952
.1501	.1465	11.04	18.152	11.28	.957
.1505	.1454	11.97	19.925	12.21	.962
.1505	.1463	15.99	27.161	16.23	.976

λ_1	λ_2	Pitot pressure		Total temperature	
		y/s	p_t/p_o	y/s	T_t/T_o
0.1526	0.1472	0.10	1.354×10^{-3}	0.34	0.723
.1531	.1494	.15	1.347	.39	.727
.1535	.1481	.25	2.003	.49	.733
.1536	.1489	.56	2.898	.80	.749
.1540	.1487	1.19	3.609	1.43	.773
.1540	.1496	1.53	3.735	1.77	.791
.1541	.1491	2.37	4.813	2.61	.826
.1542	.1500	2.82	5.382	3.06	.846
.1548	.1505	3.20	5.651	3.44	.856
.1546	.1508	3.99	6.905	4.23	.877
.1549	.1507	4.43	7.399	4.67	.891
.1549	.1506	5.50	9.332	5.74	.910
.1553	.1508	6.03	10.546	6.27	.921
.1552	.1510	7.98	12.383	8.22	.939
.1555	.1506	10.08	16.331	10.32	.953
.1555	.1508	13.12	22.096	13.36	.966
.1555	.1519	14.06	23.991	14.30	.972
.1557	.1524	14.71	24.993	14.95	.973
.1558	.1516	17.63	30.173	17.87	.979
.1559	.1527	20.19	35.686	20.43	.984

TABLE VII.- PROFILES OF PITOT PRESSURE AND TOTAL TEMPERATURE MEASURED DOWNSTREAM OF THREE SLOTS

[s = 0.254 cm]

(a) x/s = 17.12

λ_1	λ_2	λ_3	Pitot pressure		Total temperature	
			y/s	p_t/p_o	y/s	T_t/T_o
0.0525	0.0497	0.0510	0.10	1.319×10^{-3}	0.34	0.719
.0534	.0501	.0517	.14	1.301	.38	.722
.0535	.0504	.0507	.21	1.462	.45	.728
.0537	.0505	.0512	.34	2.036	.58	.736
.0538	.0506	.0526	.42	2.183	.66	.742
.0540	.0508	.0515	.78	2.743	1.02	.774
.0541	.0509	.0506	1.04	3.250	1.28	.789
.0542	.0509	.0520	1.13	3.133	1.37	.797
.0542	.0509	.0503	1.23	3.459	1.47	.801
.0542	.0509	.0522	1.24	3.453	1.48	.801
.0544	.0510	.0514	1.45	3.785	1.69	.810
.0544	.0511	.0532	1.82	4.510	2.06	.837
.0545	.0511	.0523	2.02	4.671	2.26	.849
.0546	.0511	.0533	2.40	5.281	2.64	.855
.0547	.0512	.0534	3.64	6.825	3.88	.880
.0548	.0514	.0521	4.99	9.433	5.23	.900
.0548	.0514	.0515	7.02	15.309	7.26	.921
.0550	.0513	.0534	8.93	17.431	9.27	.942
.0550	.0514	.0532	10.52	18.099	10.76	.958
.0551	.0514	.0540	11.03	19.814	11.27	.957
.0551	.0514	.0538	12.08	21.288	12.22	.962
.0552	.0516	.0541	15.98	28.176	16.22	.979
.0553	.0516	.0514	22.08	33.892	22.32	.986
.0553	.0517	.0514	28.11	29.801	28.35	.990

λ_1	λ_2	λ_3	Pitot pressure		Total temperature	
			y/s	p_t/p_o	y/s	T_t/T_o
0.0512	0.0478	0.0487	0.10	1.309×10^{-3}	0.34	0.737
.0515	.0480	.0486	.16	1.348	.40	.743
.0516	.0482	.0493	.24	1.781	.48	.750
.0517	.0484	.0483	.57	2.444	.81	.771
.0519	.0484	.0494	1.21	3.371	1.45	.819
.0519	.0484	.0493	1.58	3.939	1.82	.841
.0521	.0485	.0488	2.38	5.455	2.62	.870
.0521	.0486	.0487	2.84	5.721	3.08	.878
.0523	.0487	.0501	3.21	6.732	3.45	.884
.0524	.0488	.0505	4.00	7.525	4.24	.897
.0525	.0488	.0501	4.44	8.335	4.68	.903
.0526	.0490	.0509	5.51	10.560	5.75	.915
.0526	.0490	.0510	6.01	12.036	6.25	.920
.0527	.0490	.0493	7.99	16.999	8.23	.944
.0527	.0491	.0490	10.07	18.469	10.31	.955
.0528	.0491	.0497	13.14	23.152	13.38	.973
.0528	.0492	.0510	13.99	25.662	14.23	.975
.0528	.0491	.0517	14.74	25.823	14.98	.976
.0530	.0493	.0516	17.60	29.047	17.84	.985
.0530	.0493	.0510	20.10	31.200	20.34	.987
.0531	.0493	.0498	21.98	32.123	22.22	.985

TABLE VII.- Continued

(a) Continued

λ_1	λ_2	λ_3	Pitot pressure		Total temperature	
			y/s	p_t/p_o	y/s	T_t/T_o
0.1200	0.1090	0.1077	0.10	1.468×10^{-3}	0.34	0.665
.1205	.1096	.1087	.15	1.269	.39	.660
.1166	.1060	.1068	.21	1.437	.45	.668
.1136	.1030	.1035	.28	1.706	.52	.674
.1123	.1019	.1008	.41	1.953	.65	.686
.1120	.1015	.1006	.79	2.426	1.03	.718
.1119	.1016	.1014	1.02	2.748	1.26	.740
.1121	.1016	.1001	1.13	2.921	1.37	.751
.1123	.1018	.1016	1.22	2.979	1.46	.808
.1124	.1019	.1021	1.42	3.185	1.66	.773
.1128	.1022	.1009	1.85	3.832	2.09	.803
.1130	.1023	.1020	2.01	4.073	2.25	.807
.1131	.1025	.1016	2.40	4.531	2.64	.833
.1134	.1027	.1016	3.68	6.107	3.92	.870
.1135	.1027	.1015	4.67	7.366	4.91	.888
.1137	.1030	.1011	6.99	12.144	7.23	.921
.1140	.1030	.1026	9.00	18.123	9.24	.931
.1141	.1032	.1014	10.54	17.913	10.78	.956
.1141	.1033	.1028	11.00	18.620	11.24	.960
.1143	.1033	.1021	11.99	20.331	12.23	.959
.1143	.1034	.1020	16.03	26.274	16.27	.978
.1147	.1036	.1017	22.06	33.182	22.30	.987
.1148	.1037	.1024	27.96	29.886	28.20	.994

λ_1	λ_2	λ_3	Pitot pressure		Total temperature	
			y/s	p_t/p_o	y/s	T_t/T_o
0.1097	0.0990	0.0993	0.10	1.275×10^{-3}	0.34	0.669
.1100	.0994	.0980	.14	1.259	.38	.672
.1102	.0996	.0986	.19	1.477	.43	.675
.1103	.0998	.0987	.51	2.117	.75	.699
.1105	.0999	.0985	1.12	2.789	1.36	.750
.1106	.1001	.0991	1.52	3.319	1.76	.784
.1113	.1006	.1001	2.39	4.717	2.63	.815
.1114	.1006	.0993	2.69	5.049	2.93	.844
.1117	.1007	.0981	3.14	5.531	3.38	.855
.1116	.1010	.0997	3.90	6.269	4.14	.872
.1118	.1011	.1003	4.37	7.137	4.61	.880
.1122	.1012	.0993	5.48	8.743	5.72	.899
.1122	.1013	.0988	6.05	10.167	6.29	.908
.1123	.1015	.0982	7.94	15.965	8.18	.928
.1124	.1015	.0996	10.02	18.578	10.26	.951
.1126	.1016	.0999	13.05	21.775	13.29	.966
.1128	.1017	.1013	13.92	23.848	14.16	.970
.1128	.1019	.1012	14.69	25.515	14.93	.972
.1131	.1020	.0986	17.57	29.029	17.81	.978
.1131	.1020	.0983	19.88	30.987	20.12	.984

TABLE VII.- Continued

(a) Concluded

λ_1	λ_2	λ_3	Pitot pressure		Total temperature	
			y/s	p_t/p_o	y/s	T_t/T_o
0.1581	0.1514	0.1468	0.10	1.274×10^{-3}	0.34	0.639
.1587	.1518	.1471	.15	1.279	.39	.641
.1589	.1520	.1463	.18	1.388	.42	.643
.1590	.1522	.1459	.26	1.709	.50	.647
.1594	.1525	.1467	.41	1.999	.65	.657
.1598	.1528	.1467	.78	2.532	1.02	.687
.1599	.1528	.1480	1.00	2.791	1.24	.707
.1601	.1530	.1458	1.11	2.858	1.35	.720
.1602	.1532	.1470	1.21	3.032	1.45	.729
.1603	.1531	.1474	1.41	3.228	1.65	.747
.1605	.1533	.1471	1.79	3.667	2.03	.773
.1607	.1535	.1462	1.96	3.824	2.20	.785
.1608	.1537	.1478	2.39	4.548	2.63	.811
.1612	.1538	.1484	3.58	5.427	3.82	.852
.1613	.1540	.1478	4.99	7.743	5.23	.880
.1615	.1542	.1484	7.02	11.090	7.26	.917
.1618	.1546	.1488	9.00	17.960	9.24	.940
.1619	.1545	.1477	10.49	18.755	10.73	.954
.1621	.1548	.1478	10.98	18.466	11.22	.959
.1620	.1548	.1485	12.01	19.094	12.25	.964
.1624	.1550	.1501	16.02	26.503	16.26	.977
.1626	.1551	.1492	21.82	33.394	22.06	.989
.1630	.1555	.1480	28.15	30.471	28.39	.991

λ_1	λ_2	λ_3	Pitot pressure		Total temperature	
			y/s	p_t/p_o	y/s	T_t/T_o
0.1553	0.1487	0.1418	0.10	1.258×10^{-3}	0.34	0.643
.1557	.1488	.1422	.16	1.358	.40	.644
.1559	.1490	.1431	.19	1.518	.43	.644
.1565	.1492	.1440	.50	2.124	.74	.665
.1566	.1495	.1428	1.13	2.848	1.37	.721
.1568	.1494	.1436	1.51	3.314	1.75	.757
.1568	.1496	.1420	2.34	4.262	2.58	.807
.1570	.1497	.1445	2.79	5.046	3.03	.824
.1571	.1498	.1435	3.18	5.174	3.42	.843
.1573	.1499	.1449	3.93	6.482	4.17	.859
.1574	.1501	.1436	4.37	6.977	4.61	.875
.1579	.1503	.1433	5.44	7.917	5.68	.889
.1579	.1505	.1445	5.99	9.124	6.23	.904
.1582	.1508	.1445	7.93	14.961	8.17	-----
.1584	.1509	.1441	10.00	19.079	10.24	.952
.1586	.1511	.1460	13.03	21.717	13.27	.965
.1590	.1515	.1446	13.97	23.004	14.11	.969
.1590	.1514	.1467	14.61	24.357	14.85	.976
.1592	.1516	.1459	17.58	28.939	18.82	.978
.1594	.1518	.1474	20.07	31.034	20.31	.986
.1595	.1519	.1476	22.10	33.243	22.34	.987
.1597	.1520	.1478	27.33	30.554	27.57	.992

TABLE VII.- Continued

(b) x/s = 67.12

λ_1	λ_2	λ_3	Pitot pressure		Total temperature	
			y/s	p_t/p_o	y/s	T_t/T_o
0.0499	0.0481	0.0476	0.10	1.407×10^{-3}	0.34	0.776
.0501	.0483	.0493	.14	1.528	.38	.780
.0501	.0483	.0490	.18	1.950	.42	.785
.0504	.0485	.0489	.24	2.352	.48	.788
.0505	.0486	.0490	.39	2.916	.63	.800
.0506	.0487	.0498	.74	3.567	.98	.815
.0507	.0487	.0488	.99	3.847	1.23	.828
.0508	.0488	.0496	1.10	3.880	1.34	.834
.0508	.0489	.0490	1.09	4.118	1.43	.836
.0509	.0490	.0494	1.30	4.288	1.64	.842
.0510	.0492	.0496	1.70	4.595	2.04	.852
.0511	.0491	.0504	1.89	4.914	2.23	.860
.0511	.0491	.0497	2.26	5.421	2.60	.869
.5012	.0491	.0495	3.47	6.914	3.81	.889
.0513	.0492	.0498	4.87	9.089	5.21	.909
.0513	.0493	.0499	6.85	11.903	7.19	.919
.0514	.0493	.0498	8.83	15.751	9.17	.946
.0515	.0494	.0499	10.36	17.116	10.70	.954
.0515	.0493	.0493	10.87	18.406	11.21	.957
.0515	.0494	.0496	11.87	20.757	12.21	.966
.0515	.0494	.0503	15.91	26.882	16.25	.977
.0516	.0495	.0508	21.98	30.174	22.32	.985
.0516	.0495	.0506	27.93	30.764	28.27	.992

λ_1	λ_2	λ_3	Pitot pressure		Total temperature	
			y/s	p_t/p_o	y/s	T_t/T_o
0.0510	0.0491	0.0488	0.10	1.375×10^{-3}	0.34	0.785
.0511	.0492	.0510	.15	1.628	.39	.789
.0514	.0493	.0505	.20	1.992	.44	.792
.0515	.0495	.0508	.51	3.175	.75	.814
.0515	.0496	.0497	1.16	3.988	1.40	.838
.0516	.0495	.0510	1.53	4.422	1.77	.849
.0517	.0496	.0497	2.35	5.411	2.59	.868
.0517	.0497	.0510	2.81	5.798	3.05	.875
.0518	.0498	.0497	3.19	6.273	3.43	.885
.0519	.0498	.0495	3.95	7.035	4.19	.902
.0520	.0499	.0508	4.39	8.276	4.63	.899
.0521	.0500	.0504	5.48	10.031	5.72	.906
.0522	.0499	.0502	5.95	10.906	6.19	.921
.0522	.0500	.0506	8.00	13.108	8.24	.934
.0523	.0502	.0506	10.01	16.868	10.25	.952
.0523	.0502	.0507	13.10	22.160	13.34	.964
.0524	.0502	.0511	13.95	23.733	14.19	.971
.0524	.0503	.0503	14.69	25.097	14.93	.972
.0525	.0504	.0508	17.59	30.021	17.83	.980
.0524	.0504	.0503	20.12	34.396	20.36	.985
.0525	.0503	.0503	22.10	30.249	22.34	.987
.0526	.0504	.0512	27.89	30.599	28.13	.992

TABLE VII.- Continued

(b) Continued

λ_1	λ_2	λ_3	Pitot pressure		Total temperature	
			y/s	p_t/p_o	y/s	T_t/T_o
0.1015	0.0973	0.1017	0.10	1.392×10^{-3}	0.34	0.745
.1020	.0978	.0970	.15	1.606	.39	.747
.1025	.0979	.0999	.22	2.027	.46	.752
.1026	.0982	.1011	.28	2.325	.52	.757
.1027	.0983	.0978	.35	2.636	.59	.763
.1030	.0985	.1030	.73	3.155	.97	.778
.1031	.0987	.1021	.97	3.528	1.21	.790
.1033	.0987	.0999	1.08	3.480	1.32	.792
.1033	.0988	.1032	1.16	3.633	1.40	.796
.1034	.0988	.0996	1.36	3.650	1.60	.804
.1035	.0989	.0989	1.75	4.203	1.99	.816
.1036	.0990	.1010	1.95	4.220	2.19	.820
.1037	.0992	.0985	2.35	4.695	2.59	.832
.1039	.0992	.0989	3.58	5.877	3.82	.864
.1040	.0992	.1038	4.98	8.167	5.22	.891
.1040	.0994	.0986	6.96	10.735	7.20	.922
.1041	.0995	.1017	8.90	13.129	9.14	.939
.1042	.0996	.0997	10.48	16.033	10.72	.951
.1043	.0996	.0992	10.90	16.100	11.14	.954
.1044	.0997	.1027	11.96	18.929	12.20	.961
.1044	.0997	.0997	15.92	25.545	16.16	.973
.1046	.0999	.1029	22.05	35.889	22.29	.987
.1046	.1000	.0991	27.95	30.884	28.19	.992

λ_1	λ_2	λ_3	Pitot pressure		Total temperature	
			y/s	p_t/p_o	y/s	T_t/T_o
0.1024	0.0983	0.0987	0.10	1.373×10^{-3}	0.34	0.726
.1027	.0985	.1009	.14	1.372	.38	.743
.1030	.0987	.1031	.18	1.574	.42	.746
.1033	.0990	.0993	.51	2.879	.75	.765
.1036	.0991	.0996	1.11	3.526	1.35	.787
.1036	.0992	.1033	1.48	3.804	1.72	.798
.1039	.0994	.0993	2.33	4.657	2.57	.826
.1041	.0995	.0989	2.79	5.281	3.03	.842
.1043	.0997	.0989	3.17	5.455	3.41	.850
.1045	.0999	.0993	3.93	6.121	4.27	.867
.1047	.1002	.0993	4.37	6.932	4.61	.879
.1049	.1002	.1014	5.44	8.357	5.68	.895
.1050	.1005	.1028	5.98	9.801	6.22	.902
.1052	.1006	.1051	7.96	11.610	8.20	.928
.1054	.1008	.0998	10.00	15.248	10.24	.939
.1055	.1010	.1054	13.09	20.746	13.31	.962
.1057	.1011	.1000	13.96	21.677	14.10	.964
.1057	.1011	.1001	14.07	23.186	14.91	.969
.1059	.1013	.1003	17.58	28.032	17.82	.976
.1061	.1014	.1005	20.07	33.672	20.31	.982
.1063	.1016	.1057	22.03	36.116	22.27	.983
.1064	.1017	.1033	27.83	30.457	28.07	.988

TABLE VII.- Concluded

(b) Concluded

λ_1	λ_2	λ_3	Pitot pressure		Total temperature	
			y/s	p_t/p_o	y/s	T_t/T_o
0.1462	0.1510	0.1445	0.10	1.415×10^{-3}	0.34	0.706
.1469	.1516	.1463	.13	1.395	.37	.710
.1485	.1528	.1477	.16	1.455	.40	.713
.1493	.1536	.1466	.24	2.026	.48	.720
.1503	.1544	.1500	.36	2.555	.60	.725
.1510	.1540	.1492	.74	3.123	.98	.738
.1513	.1552	.1493	.98	3.417	1.22	.751
.1517	.1555	.1496	1.07	3.377	1.31	.757
.1519	.1556	.1519	1.17	3.557	1.41	.757
.1521	.1556	.1515	1.38	3.698	1.62	.765
.1524	.1560	.1513	1.77	3.992	2.01	.779
.1528	.1561	.1517	1.96	4.313	2.20	.788
.1531	.1561	.1515	2.37	4.435	2.61	.803
.1534	.1563	.1533	3.53	5.557	3.77	.834
.1540	.1568	.1529	4.66	7.139	4.90	.869
.1543	.1572	.1510	6.94	10.336	7.18	.908
.1546	.1572	.1536	8.96	12.546	9.10	.929
.1549	.1575	.1524	10.44	15.125	10.68	.940
.1551	.1576	.1549	11.03	16.302	11.27	.945
.1554	.1578	.1553	11.96	17.718	12.20	.954

λ_1	λ_2	λ_3	Pitot pressure		Total temperature	
			y/s	p_t/p_o	y/s	T_t/T_o
0.1596	0.1624	0.1603	0.10	1.381×10^{-3}	0.34	0.703
.1612	.1639	.1617	.15	1.530	.39	.704
.1620	.1645	.1626	.22	1.990	.46	.707
.1628	.1652	.1626	.30	2.335	.54	.712
.1637	.1659	.1641	.50	2.746	.74	.722
.1642	.1663	.1636	1.17	3.366	1.41	.749
.1644	.1663	.1636	1.53	3.701	1.77	.762
.1645	.1665	.1627	2.33	4.427	2.57	.789
.1645	.1664	.1639	2.76	4.880	3.00	.809
.1647	.1664	.1635	3.18	5.251	3.42	.819
.1649	.1666	.1640	3.96	6.068	4.20	.844
.1652	.1669	.1642	4.37	6.337	4.61	.853
.1655	.1671	.1641	5.43	8.026	5.67	.879
.1657	.1674	.1637	5.93	8.601	6.17	.888
.1659	.1676	.1652	7.92	11.453	8.16	.916
.1663	.1678	.1639	10.03	13.505	10.27	.939
.1666	.1679	.1654	13.05	19.409	13.29	.960
.1667	.1682	.1642	13.93	21.463	14.17	.959
.1670	.1686	.1641	14.65	22.424	14.89	.966
.1671	.1686	.1659	17.79	28.097	18.03	.973
.1675	.1688	.1664	20.15	33.814	20.39	.979
.1678	.1693	.1662	22.02	38.550	22.26	.986
.1679	.1693	.1654	27.86	31.520	28.10	.992

TABLE VIII.- EXPERIMENTALLY DERIVED PROFILES OF STATIC TEMPERATURE AND VELOCITY THROUGH UNDISTURBED BOUNDARY LAYER JUST UPSTREAM OF SLOT

[s = 0.254 cm]

y/s	T_1, K	u_1, m/sec	u_∞, m/sec	u_1/u_∞
0.29	259.9	542.2	952.8	0.569
.5	244.1	595.0	↓	.624
.89	242.0	624.5		.655
1.08	243.9	629.7		.661
1.23	240.4	643.4		.675
1.31	239.8	648.9		.681
1.52	238.1	655.6		.688
1.91	234.5	670.0		.703
2.09	232.1	676.0		.710
2.48	228.9	686.1		.720
3.69	218.8	710.5		.746
5.12	207.5	734.0		.770
7.09	198.4	758.3		.796

y/s	T_1, K	u_1, m/sec	u_∞, m/sec	u_1/u_∞
0.60	248.7	613.0	949.2	0.646
1.18	242.2	647.7	↓	.682
1.59	237.8	665.1		.701
2.43	228.9	689.2		.726
2.89	225.7	698.3		.736
3.23	223.3	705.3		.743
4.04	214.5	721.2		.760
4.47	212.2	726.9		.766
5.56	206.4	742.2		.782
6.06	203.2	748.6		.789
8.04	194.6	768.1		.809

TABLE IX.- EXPERIMENTALLY DERIVED PROFILES OF TEMPERATURE AND VELOCITY DOWNSTREAM OF ONE, TWO, THREE, AND FOUR SLOTS

[s = 0.254 cm]

(a) Single slot

y/s	T_1, K	u_1, m/sec	u_∞, m/sec	u_1/u_∞
x/s = 17.12 and λ_{nom} = 0.1				
0.30	264.5	433.7	951.6	0.456
.62	255.6	484.0		.509
.88	251.0	516.9		.543
.99	250.6	531.3		.558
1.26	251.0	558.4		.587
1.66	248.6	607.5		.638
2.44	237.4	655.6		.689
4.03	218.3	706.8		.743
4.48	214.2	714.1		.750
5.57	203.1	734.9		.772
6.06	199.4	744.3		.782
8.07	181.7	782.7	↓	.823
x/s = 37.12 and λ_{nom} = 0.1				
0.31	266.7	456.2	943.1	0.484
.51	258.8	495.3		.525
.88	257.3	521.0		.552
1.10	253.7	540.9		.574
1.20	252.1	550.1		.583
1.31	251.4	559.2		.593
1.51	250.9	571.3		.606
1.93	245.7	606.7		.643
2.10	244.4	621.5		.659
2.50	239.0	640.6		.679
3.79	225.2	687.8		.728
5.36	215.2	712.5		.755
7.15	206.1	735.5	↓	.780

y/s	T_1, K	u_1, m/sec	u_∞, m/sec	u_1/u_∞
x/s = 17.12 and λ_{nom} = 0.2				
0.41	237.3	438.0	956.2	0.458
.80	235.6	487.1		.509
1.03	239.6	513.3		.537
1.12	241.3	524.0		.548
1.23	245.7	533.7		.558
1.43	246.8	561.1		.587
1.84	252.5	596.2		.623
2.01	250.6	615.7		.644
2.42	246.6	644.3		.674
3.68	228.7	691.0		.722
5.03	217.2	723.6		.757
7.03	188.2	773.0	↓	.808
x/s = 37.12 and λ_{nom} = 0.2				
0.30	260.8	427.5	952.3	0.449
.48	252.3	458.6		.482
.86	249.0	495.4		.520
1.08	246.7	512.7		.538
1.22	248.1	525.5		.552
1.30	246.5	534.9		.562
1.52	247.7	558.8		.587
1.90	251.8	580.9		.610
2.08	251.8	594.0		.624
2.49	250.0	520.4		.652
3.72	230.9	683.6		.718
5.10	224.5	710.0		.746
7.13	212.6	736.5	↓	.773

TABLE IX.- Continued

(a) Concluded

y/s	T_1, K	u_1, m/sec	u_∞, m/sec	u_1/u_∞
x/s = 67.12 and λ_{nom} = 0.1				
0.34	269.2	501.0	956.6	0.524
.45	263.8	518.2		.542
.57	261.1	532.6		.557
.69	253.4	549.3		.574
.85	259.7	548.0		.573
1.24	257.2	571.3		.597
1.47	255.7	580.2		.607
1.66	254.4	591.6		.618
1.89	250.8	610.2		.638
2.30	246.6	627.1		.656
2.50	245.9	632.8		.662
2.85	244.1	648.6		.678
4.06	229.9	691.6		.723
5.44	217.9	717.0		.750
6.64	212.3	735.0		.768
7.75	206.9	749.9		.784
x/s = 107.12 and λ_{nom} = 0.1				
0.30	266.6	499.9	947.3	0.530
.50	257.7	534.9		.567
.87	253.3	564.1		.598
1.11	252.7	573.7		.606
1.21	255.9	574.4		.606
1.30	252.0	588.2		.621
1.53	252.8	592.0		.625
1.91	248.7	608.0		.642
2.10	246.4	617.1		.651
2.48	239.5	635.4		.671
3.71	233.1	666.7		.704
5.14	219.6	703.1		.742
7.16	209.5	731.1		.772

y/s	T_1, K	u_1, m/sec	u_∞, m/sec	u_1/u_∞
x/s = 67.12 and λ_{nom} = 0.2				
0.29	268.9	450.2	950.8	0.473
.49	257.0	489.9		.515
.85	251.6	520.9		.548
1.09	251.0	533.0		.561
1.22	250.8	540.1		.568
1.32	249.2	548.8		.577
1.52	249.5	557.0		.586
1.90	246.4	580.6		.611
2.09	246.8	587.7		.618
2.48	243.7	611.5		.643
3.86	235.4	668.9		.704
5.18	221.2	708.9		.746
7.13	215.5	730.0		.768
x/s = 107.12 and λ_{nom} = 0.2				
0.27	264.8	464.0	944.7	0.491
.46	254.9	506.4		.536
.84	251.4	536.3		.568
1.08	250.1	545.7		.578
1.19	250.7	553.6		.586
1.27	254.1	551.7		.584
1.48	247.7	568.3		.602
1.89	243.6	588.5		.623
2.06	244.6	592.3		.627
2.46	251.7	617.7		.654
3.69	234.6	647.9		.686
4.77	221.6	685.2		.725
5.06	219.1	694.3		.735
7.06	213.2	719.4		.762

TABLE IX.- Concluded

(b) Two slots

y/s	T_1, K	u_1, m/sec	u_∞, m/sec	u_1/u_∞
x/s = 17.12 and λ_{nom} = 0.1				
0.25	266.1	399.4	949.5	0.421
.45	254.6	440.3		.464
.82	252.7	472.7		.498
1.03	250.3	484.7		.507
1.17	249.9	481.1		.539
1.25	252.4	520.5		.548
1.45	252.9	539.8		.569
1.83	250.8	570.3		.601
2.02	243.9	591.8		.623
2.44	247.6	611.6		.644
3.64	236.3	661.4		.697
5.05	223.4	698.1		.735
6.98	203.5	741.5		.781
x/s = 67.12 and λ_{nom} = 0.1				
0.24	287.5	444.4	955.2	0.465
.44	266.7	503.6		.527
.79	265.7	527.2		.552
1.09	262.6	545.8		.571
1.18	262.8	549.2		.575
1.26	259.9	554.6		.581
1.43	261.1	562.1		.588
1.87	257.4	580.6		.608
2.03	254.3	591.8		.620
2.40	253.0	608.8		.637
3.63	243.7	648.5		.679
5.01	231.8	687.3		.720
7.04	221.1	724.0		.758

(c) Three slots

y/s	T_1, K	u_1, m/sec	u_∞, m/sec	u_1/u_∞
x/s = 17.12 and λ_{nom} = 0.1				
0.28	268.4	395.3	953.4	0.415
.41	258.7	420.6		.441
.79	251.4	463.9		.486
1.02	250.4	490.2		.514
1.13	248.3	501.1		.526
1.22	249.8	507.1		.532
1.42	251.1	522.6		.548
1.85	249.4	559.4		.587
2.01	248.9	571.6		.600
2.40	246.2	590.4		.619
3.68	239.6	642.1		.674
4.67	232.8	669.6		.702
6.99	209.1	727.3		.763
x/s = 67.12 and λ_{nom} = 0.1				
0.28	286.3	468.2	948.8	0.493
.35	266.8	481.2		.507
.73	261.4	516.1		.544
.97	256.3	535.1		.564
1.08	259.0	535.0		.564
1.16	257.6	541.3		.571
1.36	258.6	544.9		.574
1.75	252.8	568.1		.599
1.95	255.0	571.5		.602
2.35	249.8	587.8		.620
3.58	236.0	615.9		.649
4.98	228.7	670.2		.706
6.96	219.1	706.2		.744

TABLE X.- SKIN FRICTION MEASURED DOWNSTREAM OF SINGLE SLOT

[s = 0.254 cm; skin-friction balance 221]

x/s	λ	R_∞	C_f	C_f/C_{fo}
17.12	0.0035	85.86 × 10^6	6.45 × 10^{-4}	0.962
	.0056	78.87	6.51	.954
	.0078	86.02	6.42	.958
	.0078	78.94	6.63	.971
	.0108	82.26	6.42	.947
	.0117	79.01	6.48	.950
	.0187	78.57	6.33	.928
	.0403	79.83	5.68	.833
	.0811	79.30	4.94	.724
	.1166	81.00	3.82	.563
	.1859	81.27	3.25	.479
↓	.2341	90.54	3.07	.465
27.12	0.0039	86.34 × 10^6	6.44 × 10^{-4}	0.962
	.0061	80.25	6.48	.953
	.0087	80.76	6.46	.951
	.0119	84.25	6.36	.946
	.0180	83.21	6.30	.933
	.0402	84.21	5.82	.865
	.0795	80.35	5.45	.801
	.1166	81.53	4.72	.696
	.1869	79.83	4.39	.644
	.2569	77.67	4.17	.609
	.3732	81.10	4.36	.642
	.5055	80.73	4.95	.729
↓	.7527	80.01	5.89	.865

x/s	λ	R_∞	C_f	C_f/C_{fo}
47.12	0.0058	81.78 × 10^6	6.68 × 10^{-4}	0.985
	.0117	83.26	6.44	.955
	.0185	84.24	6.31	.938
	.0389	83.51	6.15	.913
	.0819	81.76	5.80	.856
	.1164	83.18	5.38	.797
	.1893	80.16	5.25	.771
	.2619	79.79	5.20	.762
	.3734	80.74	5.12	.753
	.4379	81.65	5.27	.778
	.4635	83.55	5.12	.759
	.5962	83.76	5.46	.810
↓	.7272	84.76	5.60	.833
67.12	0.0000	85.34 × 10^6	6.60 × 10^{-4}	0.983
	.0039	83.48	6.65	.990
	.0081	86.37	6.44	.969
	.0184	82.10	6.52	.963
	.0359	84.85	6.30	.937
	.0799	82.47	5.94	.879
	.1851	84.85	5.54	.824
	.2535	86.45	5.43	.811
	.3831	79.67	5.43	.796
	.4743	81.59	5.49	.810
	.5943	81.75	5.53	.815
↓	.9321	83.17	5.68	.842

TABLE XI.- SKIN FRICTION MEASURED DOWNSTREAM OF TWO SLOTS

[s = 0.254 cm]

λ_1	λ_2	Balance 221				Balance 220			
		x/s	R_∞	C_f	C_f/C_{fo}	x/s	R_∞	C_f	C_f/C_{fo}
0.1039	0.0041	17.12	83.63×10^6	5.83×10^{-4}	0.864	37.12	85.12×10^6	5.70×10^{-4}	0.884
.1036	.0117	↓	83.43	5.65	.837	↓	84.91	5.58	.864
.1035	.0304		83.73	5.26	.781		85.22	5.37	.830
.0952	.0818		80.09	4.55	.668		81.52	5.07	.776
.0945	.1180		84.83	3.58	.532		86.33	4.63	.718
.1022	.1898		85.05	3.32	.494		86.56	4.44	.690
.1018	.1930		82.42	3.38	.500		83.88	4.47	.690
.1018	.2783		84.75	3.39	.505		86.26	4.40	.684
.1023	.3583		83.83	3.95	.586		85.33	4.44	.668
.0986	.4301		87.54	4.24	.635		89.10	4.66	.729
.1011	.7065		85.05	5.86	.871		86.56	5.41	.841
0.0000	0.0000	27.12	87.96×10^6	6.09×10^{-4}	0.914	57.12	90.29×10^6	6.10×10^{-4}	0.957
.0987	.0016	↓	90.32	5.57	.842	↓	92.71	5.76	.910
.1006	.0048		85.51	5.54	.826		87.77	5.75	.897
.1014	.0141		84.99	5.46	.813		87.24	5.70	.888
.1006	.0583		86.80	4.90	.733		89.09	5.32	.833
.0986	.0860		85.57	4.70	.701		87.83	5.26	.820
.1020	.1140		81.61	4.51	.665		83.76	5.16	.797
.0990	.1874		84.71	3.91	.581		86.95	4.83	.753
.0998	.2629		85.13	3.88	.578		87.38	4.79	.747
.1004	.3583		84.12	4.27	.634		86.34	4.74	.737
0.0957	0.0020	87.12	95.96×10^6	5.96×10^{-4}	0.915	127.12	99.17×10^6	5.87×10^{-4}	0.943
.1010	.0035	↓	92.50	5.92	.901	↓	95.60	6.00	.955
.0974	.0133		94.36	5.88	.898		97.52	5.93	.949
.1050	.0187		87.41	5.95	.892		90.33	6.04	.949
.0991	.0838		93.63	5.47	.833		96.77	5.62	.897
.0967	.2492		93.88	5.04	.769		97.02	5.23	.836
.0969	.4021		93.90	4.88	.744		97.04	4.96	.792
0.1041	0.0207	107.12	94.74×10^6	5.91×10^{-4}	0.904	87.12	93.18×10^6	5.71×10^{-4}	0.903
.1044	.0350	↓	92.10	5.93	.900	↓	90.59	5.66	.890
.1037	.0601		93.40	5.66	.863		91.86	5.39	.850
.1068	.0843		91.27	5.68	.861		89.77	5.42	.849
.1024	.0885		89.27	5.57	.839		87.80	5.45	.850
.1031	.0977		90.93	5.65	.852		88.55	5.34	.835
.1014	.1063		93.85	5.52	.842		92.31	5.16	.815
.1014	.1182		95.12	5.45	.835		93.55	5.16	.817
.1016	.1566		95.86	5.37	.824		94.29	5.09	.808
.1003	.2096		97.06	5.17	.796		95.46	4.87	.775
0.1024	0.0304	147.12	98.48×10^6	6.00×10^{-4}	0.927	127.12	96.91×10^6	5.73×10^{-4}	0.916
.1002	.0695	↓	100.27	5.79	.899	↓	98.67	5.55	.891
.1002	.0823		98.41	5.76	.890		96.84	5.49	.877
.0997	.0844		99.44	5.69	.881		97.86	5.53	.886
.1045	.0953		94.88	5.78	.885		93.37	5.52	.873
.1102	.1009		91.58	5.83	.884		90.12	5.55	.872
.1027	.1083		95.30	5.73	.877		93.79	5.45	.863
.1047	.1235		95.73	5.65	.866		94.20	5.36	.850
.1009	.1295		97.62	5.70	.879		96.06	5.38	.858
.1025	.2498		96.23	5.47	.840		94.70	5.15	.819

TABLE XI.- Concluded

λ_1	λ_2	Balance 221				Balance 220			
		x/s	R_∞	C_f	C_f/C_{fo}	x/s	R_∞	C_f	C_f/C_{fo}
0.0495	0.0508	37.12	94.36×10^6	5.57×10^{-4}	0.851	17.12	92.71×10^6	5.07×10^{-4}	0.801
.1370	.1332	↓	99.17	4.23	.654	↓	97.44	2.93	.470
.1543	.1499		94.15	4.14	.632		92.50	2.87	.453
.1973	.2017		97.61	3.91	.602		95.90	2.91	.463
.2053	.2103		88.34	4.39	.659		86.80	3.39	.528
.2382	.2451		96.72	3.81	.585		95.03	3.07	.487
0.0471	0.0483	57.12	100.00×10^6	5.35×10^{-4}	0.829	27.12	97.42×10^6	4.75×10^{-4}	0.760
.1369	.1426	↓	95.71	4.58	.703	↓	93.25	3.63	.574
.1912	.1987		95.20	4.26	.653		92.75	3.36	.531
.2426	.2489		96.63	4.06	.623		94.15	3.38	.536
0.0515	0.0460	107.12	98.08×10^6	5.89×10^{-4}	0.908	87.12	96.47×10^6	5.67×10^{-4}	0.905
.0511	.0485	↓	92.69	6.12	.930	↓	91.16	5.93	.933
.0482	.0487		91.97	6.11	.927		90.45	5.99	.942
.0528	.0497		91.40	6.01	.914		91.17	5.76	.907
.1542	.1481		93.57	5.27	.804		92.03	4.94	.780
.1933	.2019		94.93	5.03	.770		93.36	4.70	.744
.2520	.2506		93.80	4.78	.730		92.26	4.45	.703
0.0506	0.0462	147.12	108.37×10^6	6.13×10^{-4}	0.974	127.12	106.64×10^6	5.94×10^{-4}	0.974
.0509	.0506	↓	103.35	6.00	.940	↓	101.71	5.74	.929
.1558	.1472		100.45	5.46	.848		98.85	5.15	.828
.1981	.1980		96.54	5.30	.814		95.00	4.98	.792
.2044	.2042		95.50	5.49	.841		93.98	5.29	.839
.2503	.2411		100.50	5.12	.796		98.90	4.78	.767
.2731	.2470		95.94	5.12	.785		94.41	4.79	.761

TABLE XII.- SKIN FRICTION MEASURED DOWNSTREAM OF THREE SLOTS

[s = 0.254 cm]

λ_1	λ_2	λ_3	Balance 221				Balance 220			
			x/s	R_∞	C_f	C_f/C_{fo}	x/s	R_∞	C_f	C_f/C_{fo}
0.1027	0.1034	0.0078	37.12	94.59×10^6	5.35×10^{-4}	0.817	17.12	93.03×10^6	5.12×10^{-4}	0.811
.0990	.1002	.0229	↓	95.82	5.26	.806	↓	94.24	4.96	.787
.1002	.1012	.0417		95.50	4.96	.759		93.92	4.45	.706
.0930	.0909	.0778		94.72	----	-----		93.15	3.78	.598
.1018	.1023	.0881		92.63	4.67	.710		91.10	3.79	.597
.1030	.1032	.1007		92.86	4.58	.697		91.33	3.59	.565
.1028	.1029	.1087		93.16	4.46	.679		91.62	3.45	.544
.1003	.1010	.1145		95.52	4.41	.675		93.94	3.33	.527
.1019	.1021	.1626		94.53	4.27	.652		92.97	3.21	.508
0.1017	0.1018	0.0598	57.12	94.59×10^6	5.00×10^{-4}	0.764	27.12	92.29×10^6	4.36×10^{-4}	0.688
.1031	.1049	.0900	↓	92.56	4.92	.748	↓	90.31	4.18	.657
.1031	.1032	.0988		94.57	4.87	.744		92.27	4.07	.642
.1000	.1002	.1050		98.12	4.74	.731		95.74	3.92	.625
.0985	.0983	.1147		100.60	4.75	.738		98.15	3.91	.626
.1036	.1043	.1204		93.23	4.90	.746		90.96	4.05	.637
.1032	.1025	.1343		96.17	4.73	.726		93.82	3.81	.604
.1002	.1004	.1486		96.29	4.68	.719		93.95	3.74	.593
.1013	.1014	.1767		95.86	4.58	.703		93.52	3.67	.582
.0972	.0978	.2475		98.92	4.47	.691		96.51	3.90	.622
0.0973	0.1020	0.0038	72.12	97.66×10^6	5.64×10^{-4}	0.869	47.12	96.09×10^6	5.27×10^{-4}	0.840
.0966	.1016	.0074	↓	96.79	5.55	.854	↓	95.24	5.19	.826
.1022	.0985	.0233		95.54	5.44	.834		94.01	5.06	.802
.1104	.1090	.0455		91.65	5.39	.818		90.17	5.00	.786
.0976	.1017	.0693		96.79	5.23	.804		95.23	4.75	.756
.0929	.0965	.0856		109.82	4.46	.712		108.05	4.11	.676
.0972	.0923	.0906		103.18	5.12	.802		101.51	4.63	.748
.0908	.1022	.0908		95.93	5.02	.770		94.39	4.57	.725
.0975	.1016	.0944		99.56	4.98	.772		97.96	4.58	.734
.1109	.1208	.0958		91.70	5.07	.769		90.22	4.79	.752
.1058	.1058	.1098		94.15	5.07	.775		92.63	4.63	.732
.0983	.1028	.1354		96.08	5.15	.791		94.54	4.69	.745
.0980	.1021	.1598		98.39	4.80	.741		96.81	4.26	.680
.0993	.1030	.1608		96.61	5.02	.771		95.06	4.57	.726
.0991	.1038	.1810		99.75	4.90	.760		98.15	4.49	.719
.1008	.1006	.2255		94.91	4.81	.736		93.38	4.34	.687
.0983	.1030	.3142		96.57	4.67	.718		95.02	4.24	.674
.1006	.1043	.4445		92.80	4.75	.723		91.31	4.50	.708
.0961	.1000	.5658	↓	97.16	4.87	.750	↓	95.60	4.69	.747

TABLE XII.- Concluded

λ_1	λ_2	λ_3	Balance 221				Balance 220			
			x/s	R_∞	C_f	C_f/C_{fo}	x/s	R_∞	C_f	C_f/C_{fo}
0.1007	0.1006	0.0074	87.12	99.79×10^6	5.59×10^{-4}	0.866	67.12	98.21×10^6	5.29×10^{-4}	0.848
.1043	.1043	.0212	↓	95.29	5.64	.864	↓	93.78	5.30	.840
.1039	.1028	.0436		97.50	5.47	.843		95.95	5.12	.817
.0995	.0987	.0635		99.66	5.40	.837		98.08	5.02	.805
.0962	.1021	.0864		100.45	5.19	.806		98.86	5.02	.806
.0994	.0994	.0952		100.20	5.20	.808		98.61	4.82	.777
.1016	.1032	.0973		99.64	5.20	.807		98.06	4.82	.773
.1020	.1025	.1181		98.93	5.17	.799		97.37	4.77	.763
.1050	.1043	.1423		96.31	5.07	.779		94.79	4.69	.745
.1017	.1011	.1787		98.53	4.95	.765		96.97	4.55	.727
.1022	.1022	.3232	↓	98.27	4.61	.743	↓	96.72	4.42	.706
0.0556	0.0485	0.0467	37.12	90.29×10^6	5.41×10^{-4}	0.817	17.12	88.81×10^6	5.00×10^{-4}	0.782
.0493	.0475	.0497	↓	91.06	5.37	.813	↓	89.55	4.89	.767
.1536	.1526	.1351		91.32	4.04	.612		89.81	3.00	.471
.1545	.1496	.1414		89.90	4.31	.651		88.42	3.28	.513
.1525	.1488	.1510		93.65	4.06	.619		92.11	2.97	.469
.1503	.1472	.1589		94.38	4.01	.612		92.82	3.03	.479
.2040	.1968	.2030		94.15	3.77	.576		92.60	3.06	.484
.2419	.2394	.2464		96.76	3.79	.583		95.16	3.49	.555
.2613	.2636	.2567	↓	93.62	3.72	.568	↓	92.08	3.47	.548
0.0488	0.0480	0.0489	77.12	100.74×10^6	5.63×10^{-4}	0.876	57.12	99.13×10^6	5.26×10^{-4}	0.845
.1508	.1516	.1492	↓	99.40	4.69	.727	↓	97.81	4.25	.681
.1959	.1906	.2013		102.56	4.37	.683		100.92	3.93	.634
.2542	.2505	.2510	↓	98.38	4.37	.675	↓	96.81	4.04	.645
0.0492	0.0484	0.0508	97.12	101.34×10^6	5.76×10^{-4}	0.897	77.12	99.75×10^6	5.54×10^{-4}	0.892
.1552	.1577	.1535	↓	98.56	4.87	.753	↓	97.03	4.61	.737
.2008	.1982	.2031		100.81	4.51	.701		99.23	4.16	.668
.2448	.2499	.2519		100.54	4.27	.665		98.96	3.94	.633
.2578	.2554	.2612	↓	101.60	4.22	.658	↓	100.00	3.86	.622

TABLE XIII.- SKIN FRICTION MEASURED DOWNSTREAM OF FOUR SLOTS

[s = 0.254 cm]

λ_1	λ_2	λ_3	λ_4	Balance 221				Balance 220			
				x/s	R_∞	C_f	C_f/C_{fo}	x/s	R_∞	C_f	C_f/C_{fo}
0.0540	0.0535	0.0510	0.0514	47.12	103.65×10^6	5.51×10^{-4}	0.864	17.12	101.24×10^6	4.68×10^{-4}	0.755
.0503	.0535	.0515	.0523	↓	98.48	5.54	.856	↓	96.19	4.98	.794
.1062	.1031	.1035	.1048		102.99	4.79	.749		100.60	3.45	.556
.1095	.1047	.1055	.1065		101.05	4.77	.742		98.70	3.44	.552
.0986	.1041	.1050	.1086		99.40	4.71	.729		97.09	3.76	.601
.1503	.1540	.1532	.1532		106.00	4.37	.689		103.53	3.28	.533
.2141	.2107	.2100	.2121		104.97	3.91	.616		102.53	3.13	.507
.2645	.2673	.2679	.2794	↓	100.39	3.78	.588	↓	98.06	3.48	.558

TABLE XIV.- SKIN FRICTION MEASURED DOWNSTREAM OF SINGLE SLOT

[s = 0.1270 and 0.0635 cm]

s, cm	λ	Balance 221				Balance 220			
		x/s	R_∞	C_f	C_f/C_{fo}	x/s	R_∞	C_f	C_f/C_{fo}
0.1270	0.049	108.48	83.0×10^6	6.4×10^{-4}	0.951	28.48	80.0×10^6	5.8×10^{-4}	0.883
	.103		83.0	6.1	.906		80.0	5.4	.822
	.156		79.0	6.0	.882		76.0	4.7	.708
	.191		81.0	6.0	.886		78.0	4.1	.621
	.228		79.0	6.0	.882		76.0	3.6	.542
	.268		80.0	6.0	.884		77.0	3.4	.513
0.1270	0.051	78.48	76.0×10^6	6.5×10^{-4}	0.948	38.48	75.0×10^6	5.9×10^{-4}	0.886
	.101		78.0	6.1	.894		77.0	5.4	.814
	.157		78.0	6.0	.880		76.5	5.0	.754
	.200		75.5	6.0	.875		74.0	4.9	.734
	.227		76.0	6.0	.875		74.5	4.8	.720
	.243		78.5	5.8	.852		77.0	4.4	.665
	.280		73.5	5.9	.854		72.5	4.5	.671
0.1270	0.051	128.48	76.5×10^6	6.5×10^{-4}	0.948	48.48	74.0×10^6	6.0×10^{-4}	0.898
	.107		76.0	6.3	.918		73.0	5.6	.836
	.147		80.0	6.3	.929		77.0	5.3	.801
	.203		77.0	6.2	.908		74.0	5.4	.808
	.226		78.0	6.1	.894		75.0	5.2	.780
	.245		79.0	6.0	.882		76.0	5.0	.753
	.280		76.5	6.0	.875		74.0	4.9	.734
0.1270	0.050	108.48	78.0×10^6	6.5×10^{-4}	0.953	68.48	77.0×10^6	6.0×10^{-4}	0.905
	.102		79.0	6.2	.912		77.5	5.8	.863
	.156		79.5	6.1	.898		78.0	5.5	.833
	.200		76.5	6.0	.877		75.0	5.7	.855
	.224		78.0	6.0	.880		77.0	5.4	.814
	.243		79.0	5.8	.853		78.0	5.3	.803
	.270		78.0	6.1	.894		76.5	5.6	.844
0.0635	0.050	131.2	80.5×10^6	6.5×10^{-4}	0.960	51.20	78.5×10^6	6.2×10^{-4}	0.939
	.100		79.5	6.4	.943		78.5	6.0	.909
	.160		76.0	6.3	.918		75.0	5.9	.886
	.206		82.0	6.1	.904		80.5	5.5	.838
	.208		78.0	6.3	.924		77.0	5.3	.800
	.244		76.0	6.4	.933		75.0	5.4	.818
	.280		73.0	6.3	.912		72.0	5.4	.699
0.0635	0.054	151.2	75.5×10^6	6.6×10^{-4}	0.962	71.20	74.0×10^6	5.9×10^{-4}	0.883
	.104		75.5	6.4	.933		74.5	6.0	.900
	.154		80.0	6.3	.929		78.5	5.9	.894
	.196		85.0	6.3	.940		83.0	---	-----
	.226		71.0	6.4	.920		69.5	---	-----
	.240		79.5	6.2	.913		78.0	5.6	.847
	.240		83.0	6.3	.936		81.0	5.5	.840
	.290		72.0	6.2	.895		70.5	5.5	.711

TABLE XV.- SKIN FRICTION MEASURED DOWNSTREAM OF SINGLE SLOT

AT REYNOLDS NUMBER OF 240 × 10^6 AND HIGHER

[s = 0.254 cm]

λ_{nom}	Balance 221				Balance 220			
	x/s	R_∞	C_f	C_f/C_{fo}	x/s	R_∞	C_f	C_f/C_{fo}
0.053	37.12	270 × 10^6	4.3 × 10^{-4}	0.850	17.12	260 × 10^6	3.3 × 10^{-4}	0.682
.108	↓	260	3.8	.739	↓	260	2.6	.537
.162		260	3.5	.681		250	2.3	.469
.223		260	3.4	.661		250	2.3	.469
.269		260	3.3	.642		250	2.5	.510
0.054	47.12	260 × 10^6	4.6 × 10^{-4}	0.895	27.12	260 × 10^6	3.8 × 10^{-4}	0.739
.109	↓	260	4.1	.780	↓	250	3.2	.653
.164		250	3.8	.731		240	3.0	.604
.224		260	3.6	.700		250	2.9	.592
.269		260	3.6	.700		250	3.0	.612
0.053	87.12	290 × 10^6	4.8 × 10^{-4}	0.976	67.12	280 × 10^6	4.3 × 10^{-4}	0.915
.111	↓	260	4.6	.875	↓	260	4.1	.798
.161		280	4.2	.842		270	3.7	.776
.225		270	4.1	.810		270	3.7	.776
.274		260	4.1	.780		250	3.7	.755
0.054	127.12	290 × 10^6	4.9 × 10^{-4}	0.996	107.12	280 × 10^6	4.6 × 10^{-4}	0.980
.108	↓	280	4.7	.942	↓	275	4.2	.880
.163		285	4.4	.889		280	4.1	.872
.223		280	4.3	.862		280	3.9	.830
.270		270	4.4	.870		270	4.0	.839

TABLE XVI.- SLOT TEMPERATURE AND SURFACE EQUILIBRIUM TEMPERATURE MEASURED DOWNSTREAM OF ONE, TWO, THREE, AND FOUR SLOTS

[s = 0.254 cm]

No. of slots	λ_{nom}				T_o, K	$T_{r,j}$, K	$\frac{T_{r,j}}{T_o}$	$T_{eq,m}$, K, for x'/s of -											
	Slot 1	Slot 2	Slot 3	Slot 4				4.36	7.36	10.36	13.36	16.36	22.36	25.36	31.36	36.36	41.36	46.36	51.36
1	0.050	NA	NA	NA	506.4	343.9	0.679	349.3	355.6	361.6	370.5	376.3	385.6	389.2	395.1	399.2	402.8	405.4	-----
	.100	↓	↓	↓	503.3	317.8	.631	320.9	325.9	332.9	341.3	347.8	359.4	363.1	371.5	377.5	382.8	386.8	-----
	.147				504.0	305.6	.606	307.8	311.1	316.5	323.2	329.3	340.9	345.9	355.0	361.1	367.0	372.1	-----
	.202				508.0	297.2	.585	298.1	300.3	304.3	309.2	314.1	324.4	329.3	338.9	346.8	353.4	359.4	-----
	.267				505.8	290.6	.574	291.6	293.3	296.0	299.0	302.7	310.8	314.8	323.1	330.5	337.1	343.2	-----
2	0.050	0.051	NA	NA	507.8	313.9	0.618	317.1	321.8	328.6	336.7	342.9	353.7	358.0	364.5	370.2	374.8	378.7	-----
	.110	.108			516.5	293.9	.569	294.5	296.2	299.7	303.9	308.3	317.4	321.7	330.0	337.2	343.2	348.6	-----
	.157	.160			504.9	287.8	.570	288.5	289.8	292.6	295.6	298.9	306.3	309.9	317.1	323.5	329.1	334.4	-----
	.242	.231	↓	↓	514.3	280.0	.544	280.9	281.8	283.8	285.8	288.2	293.6	296.1	301.7	306.8	311.5	315.9	-----
	.280	.277			511.8	274.4	.536	274.6	275.2	276.9	278.5	280.7	284.8	286.9	291.1	295.2	298.5	302.6	-----
3	0.055	0.057	0.060	NA	507.1	326.7	0.644	330.3	335.1	-----	348.7	354.1	361.6	365.2	370.9	375.4	379.1	381.9	384.6
	.107	.110	.111		507.4	305.6	.602	307.3	310.1	-----	319.8	324.5	333.1	336.9	343.7	349.2	353.7	357.6	360.9
	.154	.155	.161		510.5	294.4	.577	295.1	296.7	-----	303.2	307.1	314.5	317.9	324.6	330.4	335.4	339.8	343.9
	.211	.202	.210		507.4	287.8	.567	288.3	289.2	-----	292.9	295.5	300.8	303.3	308.5	313.5	317.7	321.7	325.4
	.282	.280	.288	↓	502.9	275.0	.547	275.1	275.7	-----	278.1	279.7	283.2	284.6	288.3	291.8	294.9	298.1	301.2
4	0.050	0.050	0.053	0.058	506.3	339.4	0.670	342.6	346.8	351.8	357.6	-----	367.5	270.1	374.7	278.3	381.2	383.3	385.4
	.100	.100	.106	.116	507.7	315.6	.622	317.8	320.2	324.3	328.7	-----	340.1	343.2	348.9	353.6	357.5	360.3	362.2

TABLE XVI.- Concluded

No. of slots	λ_{nom}				T_o, K	$T_{r,j}$, K	$\frac{T_{r,j}}{T_o}$	$T_{eq,m}$, K, for x'/s of -										
	Slot 1	Slot 2	Slot 3	Slot 4				61.36	71.36	76.36	86.36	101.36	111.36	121.36	141.36	171.36	181.36	201.36	211.36
1	0.050	NA	NA	NA	506.4	343.9	0.679	411.8	414.9	416.4	419.3	421.1	422.5	423.4	425.2	425.9	426.1	426.9	427.0
	.100	↓	↓	↓	503.3	317.8	.631	396.8	401.6	403.7	407.5	411.1	413.4	414.9	418.0	419.8	420.2	421.6	421.6
	.147				504.0	305.6	.606	384.2	390.0	392.8	397.4	401.9	404.9	407.0	410.9	413.8	414.4	416.1	416.4
	.202				508.0	297.2	.585	373.1	380.3	383.5	389.1	395.1	398.9	401.9	406.8	411.1	412.2	414.5	415.0
	.267				505.8	290.6	.574	358.6	365.6	369.1	375.4	382.4	386.9	390.3	396.1	401.6	403.0	405.7	406.5
2	0.050	0.051	NA	NA	507.8	313.9	0.618	387.7	392.2	394.3	398.0	401.2	403.5	405.0	407.8	409.2	409.5	410.7	410.5
	.110	.108			516.5	293.9	.569	360.9	367.9	370.9	376.5	382.5	386.4	389.3	394.3	398.6	399.7	402.1	402.4
	.157	.160			504.9	287.8	.570	347.6	354.8	358.0	362.7	369.2	373.4	376.7	382.3	387.6	389.0	391.7	392.2
	.242	.231			514.3	280.0	.544	328.6	336.0	339.4	345.6	353.1	358.1	361.1	368.1	375.4	377.5	380.9	382.0
	.280	.277	↓	↓	511.8	274.4	.536	313.4	320.1	323.2	329.3	336.4	341.5	345.6	353.1	360.9	362.0	365.8	367.2
3	0.055	0.057	0.060	NA	507.1	326.7	0.644	388.9	392.3	393.9	-----	399.4	401.2	402.3	403.7	404.6	404.3	405.0	404.2
	.107	.110	.111		507.4	305.6	.602	366.1	370.9	373.0	376.9	381.5	384.3	386.3	389.6	392.5	392.9	394.8	394.6
	.154	.155	.161		510.5	294.4	.577	351.1	356.9	359.2	363.1	368.6	372.1	374.9	379.4	383.9	384.8	387.3	387.5
	.211	.202	.210		507.4	287.8	.567	332.5	338.5	341.2	290.7	352.5	356.3	359.5	363.6	369.4	370.6	373.6	374.4
	.282	.280	.288	↓	502.9	275.0	.547	307.4	313.1	315.7	320.9	327.6	332.0	335.9	342.5	350.2	352.1	356.1	357.4
4	0.050	0.050	0.053	0.058	506.3	339.4	0.670	388.4	390.1	390.9	392.9	395.3	396.8	397.2	397.1	396.0	395.9	396.8	396.0
	.100	.100	.106	.116	507.7	315.6	.622	367.0	370.4	371.9	375.0	378.7	381.1	382.4	384.2	385.4	385.9	387.8	387.7

TABLE XVII.- SLOT TEMPERATURE AND COOLING EFFECTIVENESS DOWNSTREAM OF ONE, TWO, THREE, AND FOUR SLOTS

[s = 0.254 cm]

No. of slots	λ_{nom}, each slot	T_o, K	$T_{r,j}$, K	$\frac{T_{r,j}}{T_o}$	Cooling effectiveness ϵ for x'/s of -						
					4.36	22.36	36.36	61.36	101.36	141.36	201.36
1	0.050	506.4	343.9	0.679	0.967	0.743	0.660	0.582	0.525	0.500	0.489
	.100	503.3	317.8	.631	.983	.776	.678	.574	.497	.460	.441
	.147	504.0	305.6	.606	.989	.822	.720	.604	.514	.469	.443
	.202	508.0	297.2	.585	.996	.871	.765	.640	.535	.480	.444
	.267	505.8	290.6	.574	.995	.906	.814	.684	.573	.510	.465
2	0.051	507.8	313.9	0.618	0.983	0.795	0.710	0.620	0.550	0.516	0.501
	.108	516.5	293.9	.569	.997	.894	.806	.699	.602	.549	.514
	.160	504.9	287.8	.570	.997	.914	.835	.724	.625	.565	.521
	.231	514.3	280.0	.544	.996	.942	.886	.793	.688	.624	.569
	.277	511.8	274.4	.536	.999	.956	.913	.836	.739	.668	.615
3	0.060	507.1	326.7	0.644	0.980	0.806	0.730	0.655	0.597	0.573	0.566
	.111	507.4	305.6	.602	.991	.863	.784	.700	.624	.584	.558
	.161	510.5	294.4	.577	.993	.907	.829	.738	.624	.607	.567
	.210	507.4	287.8	.567	.997	.941	.883	.796	.705	.655	.601
	.288	502.9	275.0	.547	.999	.964	.926	.858	.769	.704	.644
4	0.058	506.3	339.4	0.670	0.981	0.832	0.767	0.707	0.665	0.654	0.656
	.106	507.7	315.6	.622	.989	.872	.802	.732	.671	.643	.624

TABLE XVIII.- THEORETICAL PROFILES OF SLOT VELOCITY AND TOTAL TEMPERATURE USED IN NUMERICAL PREDICTIONS

[s = 0.254 cm]

y_j/s	$\lambda_{nom} = 0.15$		$\lambda_{nom} = 0.20$	
	u_j/u_∞	$T_{t,j}/T_{t,\infty}$	u_j/u_∞	$T_{t,j}/T_{t,\infty}$
*0.00	0.0000	0.7022	0.0000	0.7022
.02	.0563	.5934	.0654	.5934
.04	.1127	↓	.1307	↓
.06	.1690		.1961	
.08	.2253		.2615	
.10	.2817		.3268	
.12	.3380		.3922	
.14	.3943		.4575	
.16	.4225		.4902	
.18	↓		↓	
.20				
.40				
.60				
.80				
.82				
.84	↓		↓	
.86	.3943		.4575	
.88	.3380		.3922	
.90	.2817		.3268	
.92	.2253		.2615	
.94	.1690		.1961	
.96	.1127		.1307	
.98	.0563		.0654	
1.00	.0000	↓	.0000	↓

*Note: $y_j/s = y/s = 0.000$ at most upstream slot lip.

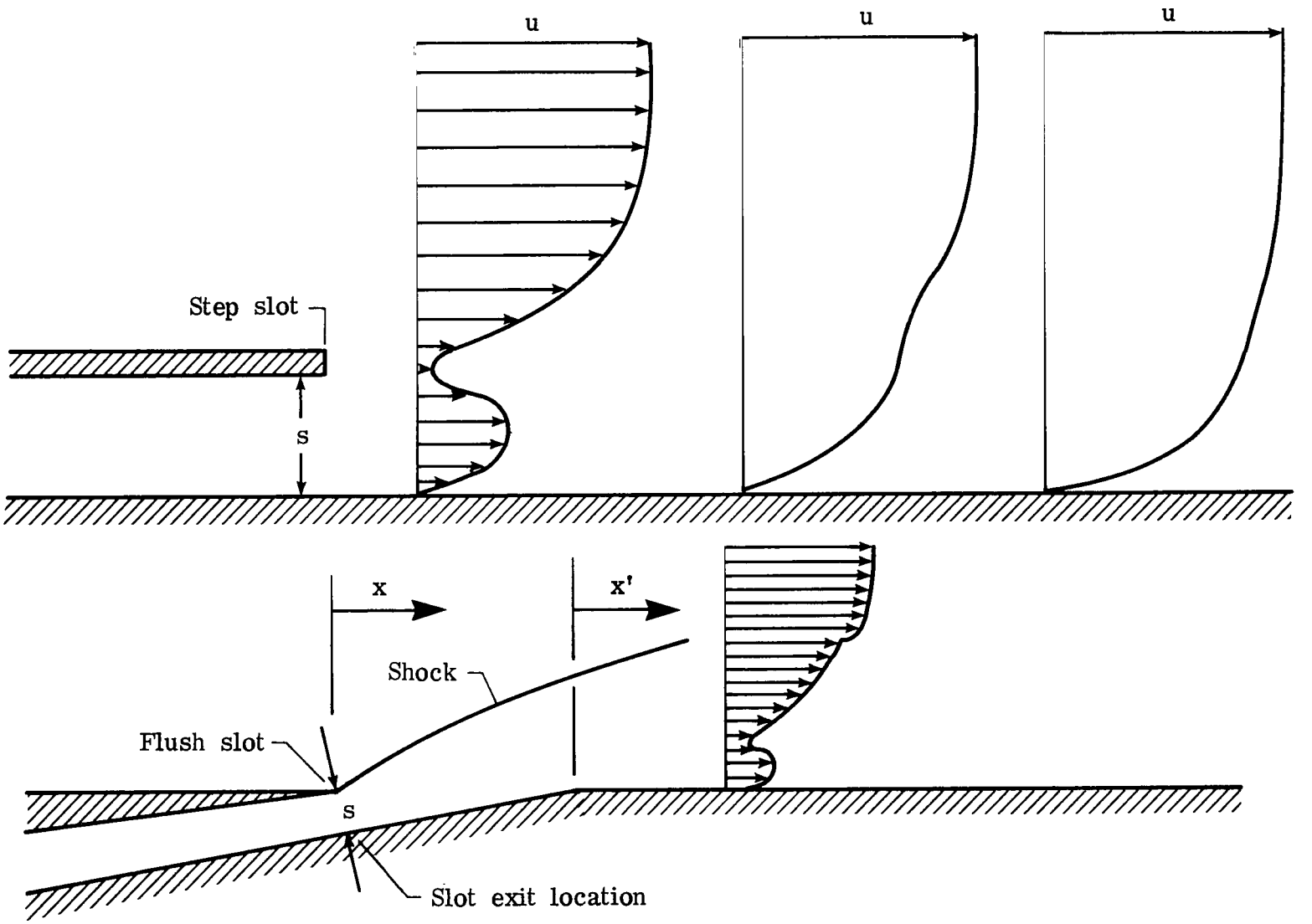

Figure 1.- Typical configurations for step and flush slots.

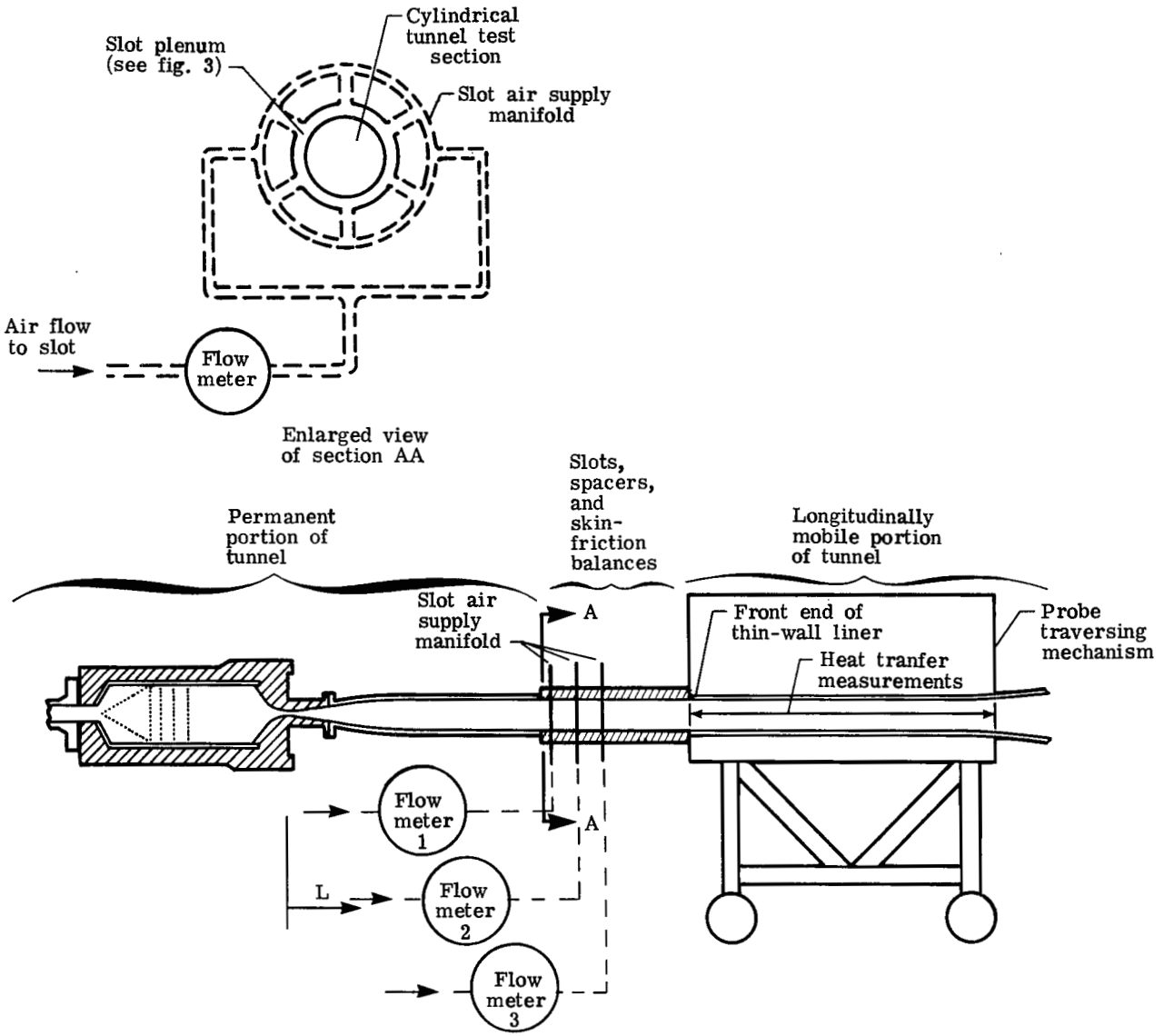

Figure 2.- Schematic diagram of typical test assembly for three slots.

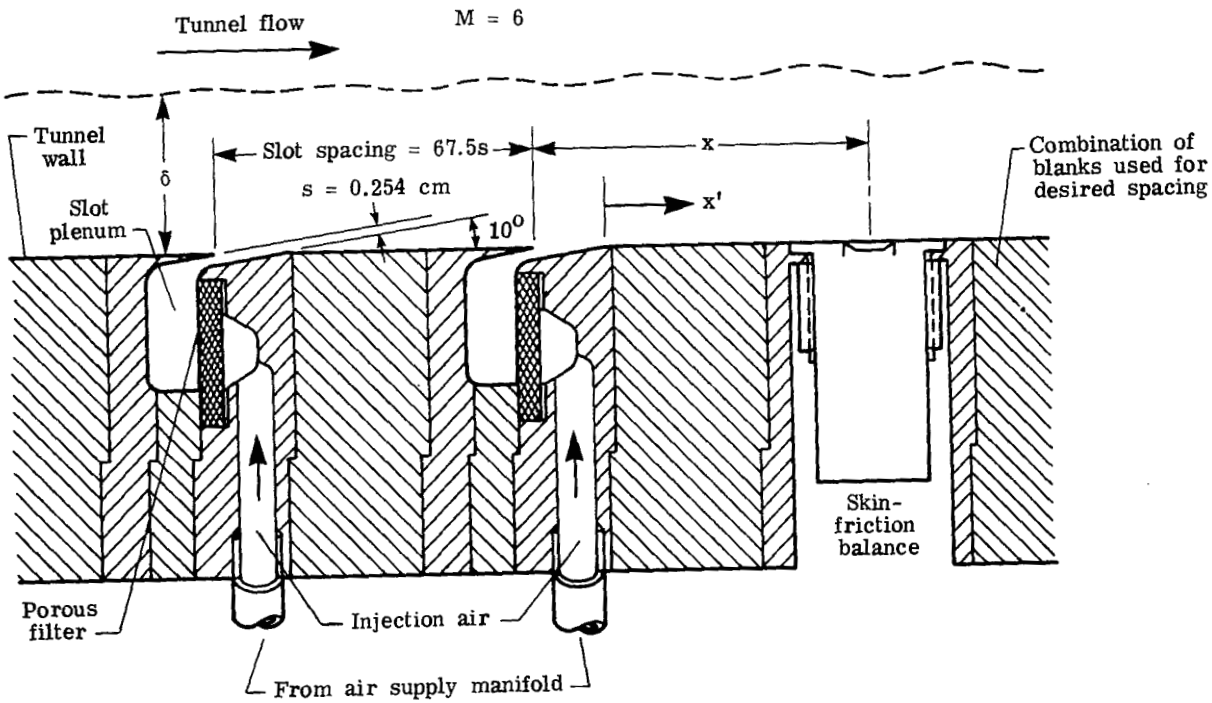

Figure 3.- Two-slot configuration with single skin-friction balance.

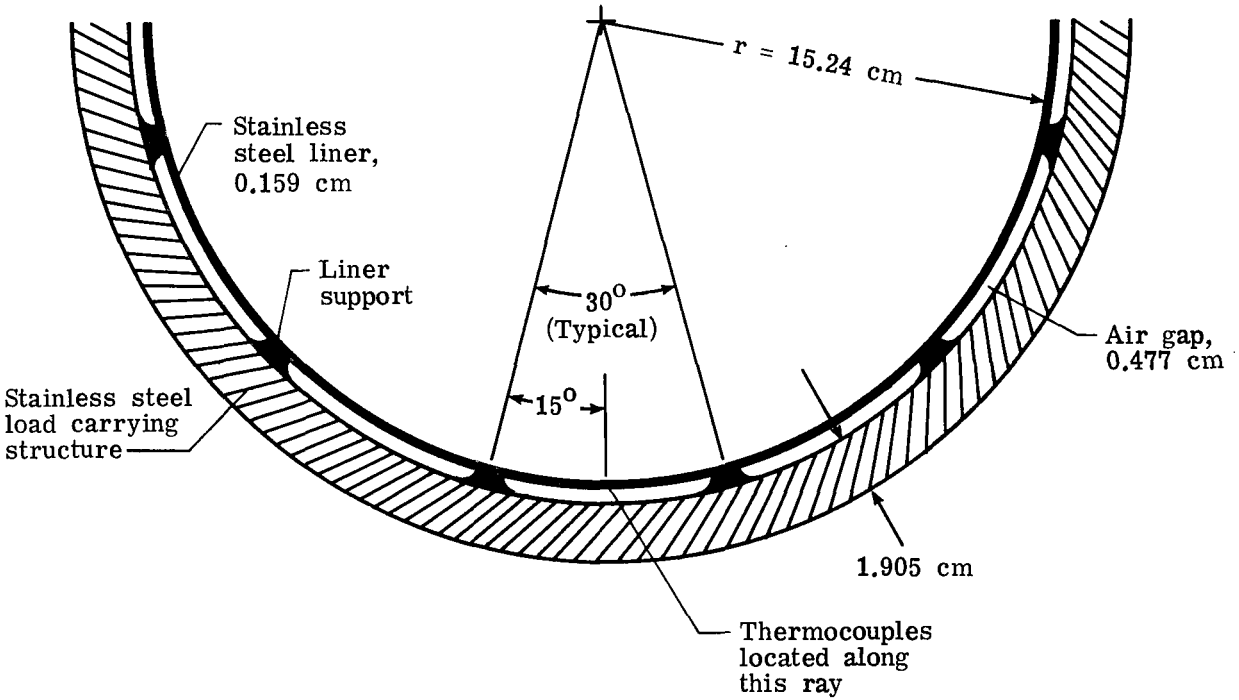

Figure 4.- Details of liner on which cooling effectiveness was measured.

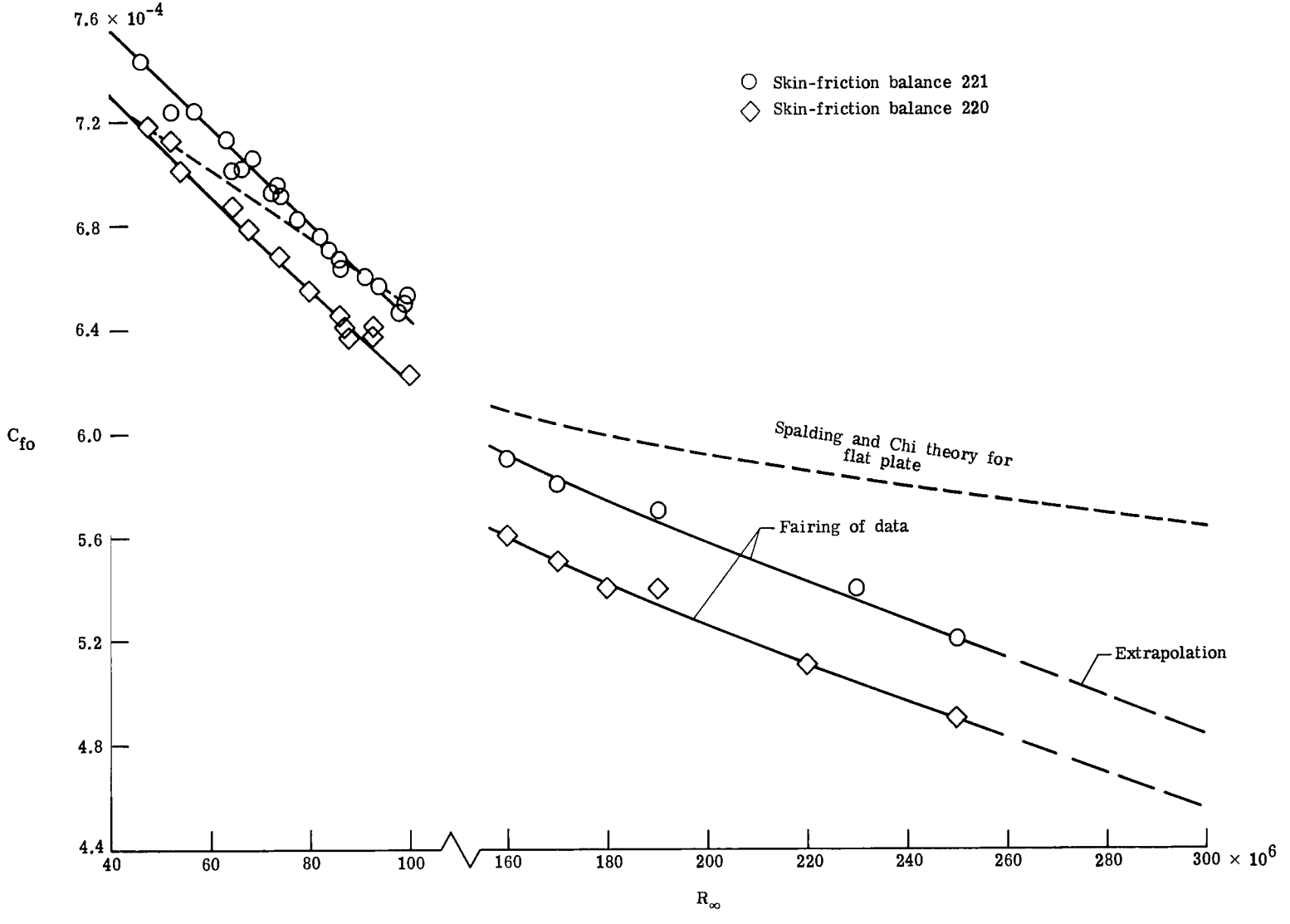

Figure 5.- Skin-friction coefficient without slot plotted against free-stream Reynolds number. (See table I.)

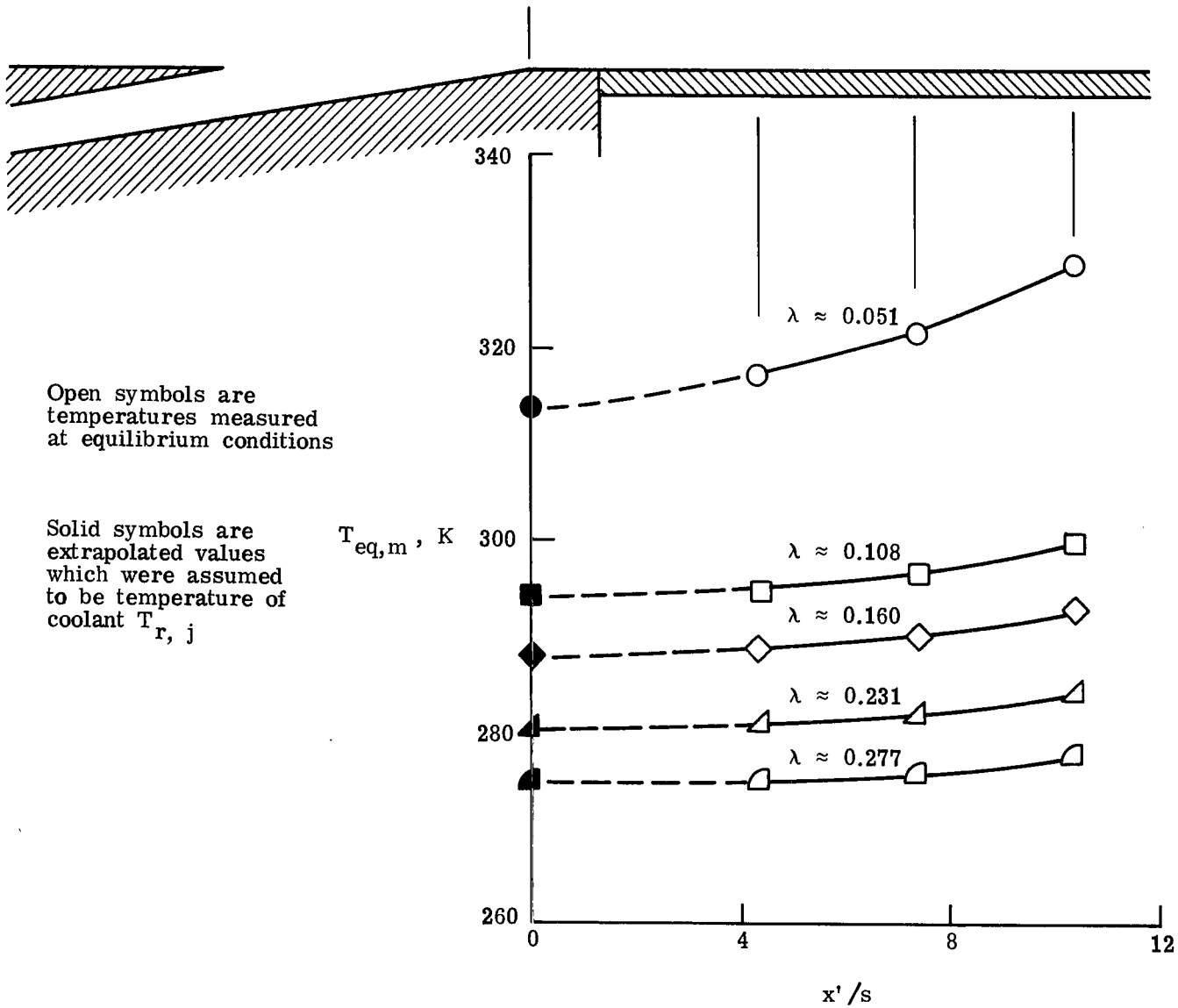

Figure 6.- Example of extrapolation of measured equilibrium wall temperatures $T_{eq,m}$ to $x'/s = 0.0$ for estimates of $T_{r,j}$. (N = 2, s = 0.254 cm.)

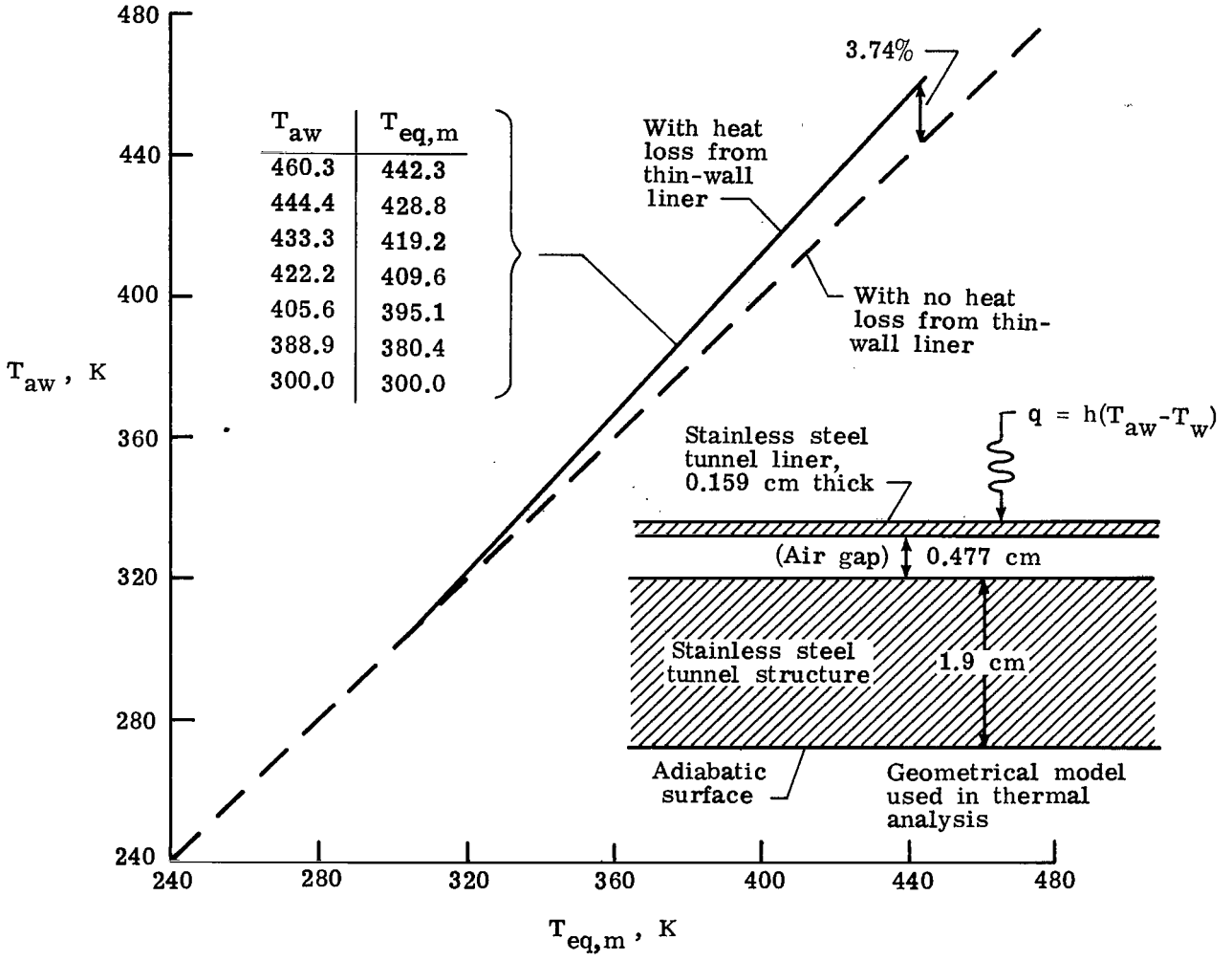

Figure 7.- Estimated effects of heat loss on adiabatic temperature T_{aw}.

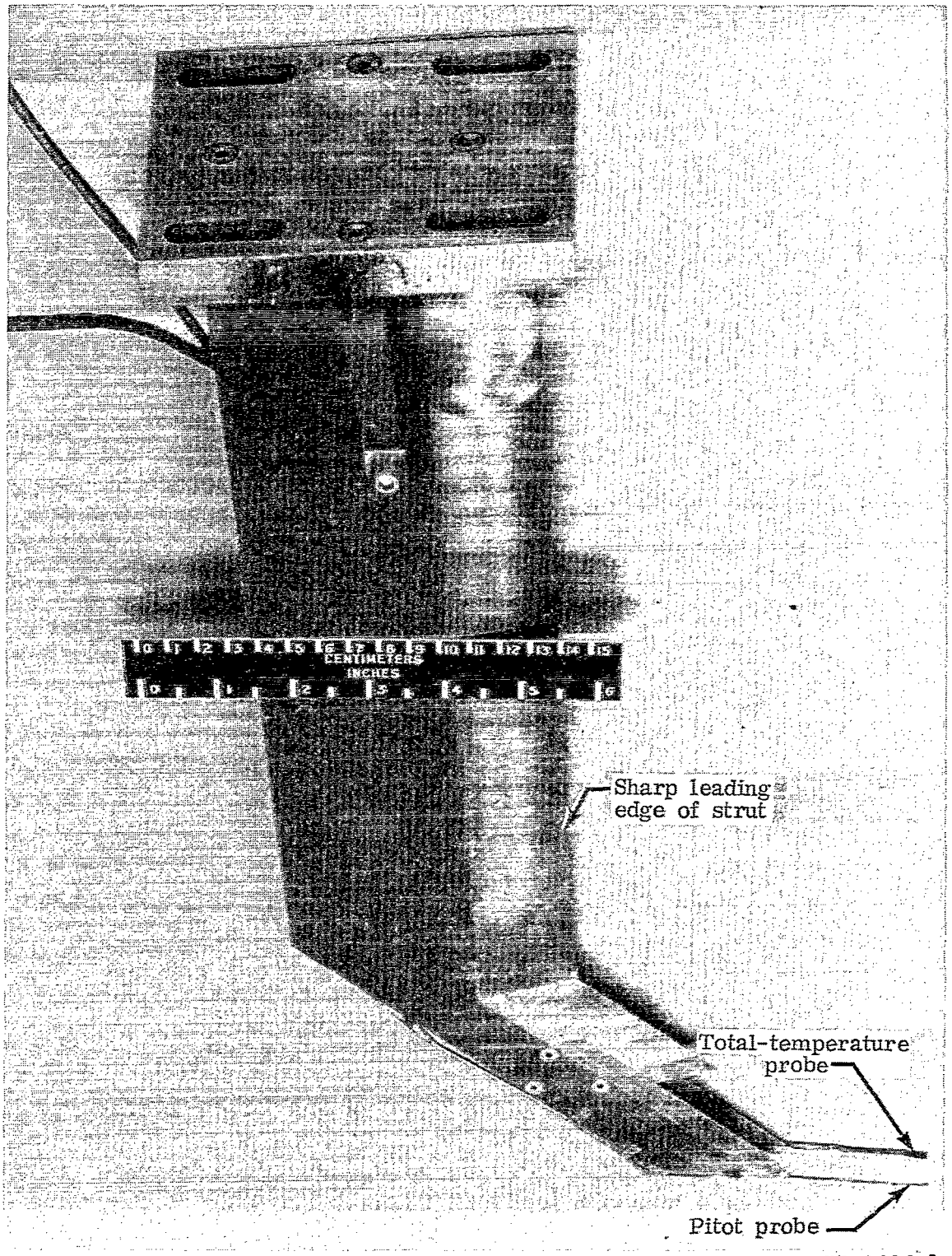

(a) Strut and probes.

Figure 8.- Pitot probe and total-temperature probe.

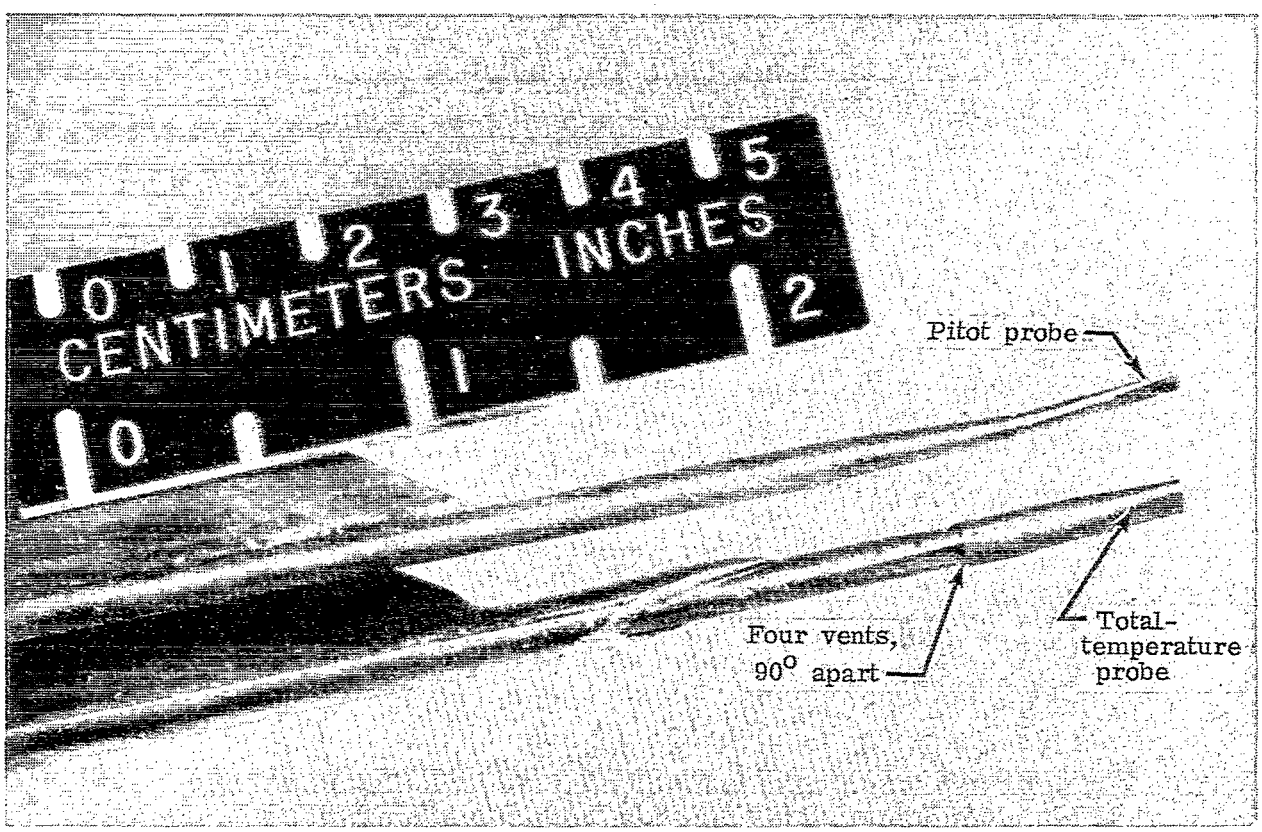

L-77-8424.1

(b) View showing bottom side of probes.

Figure 8.- Continued.

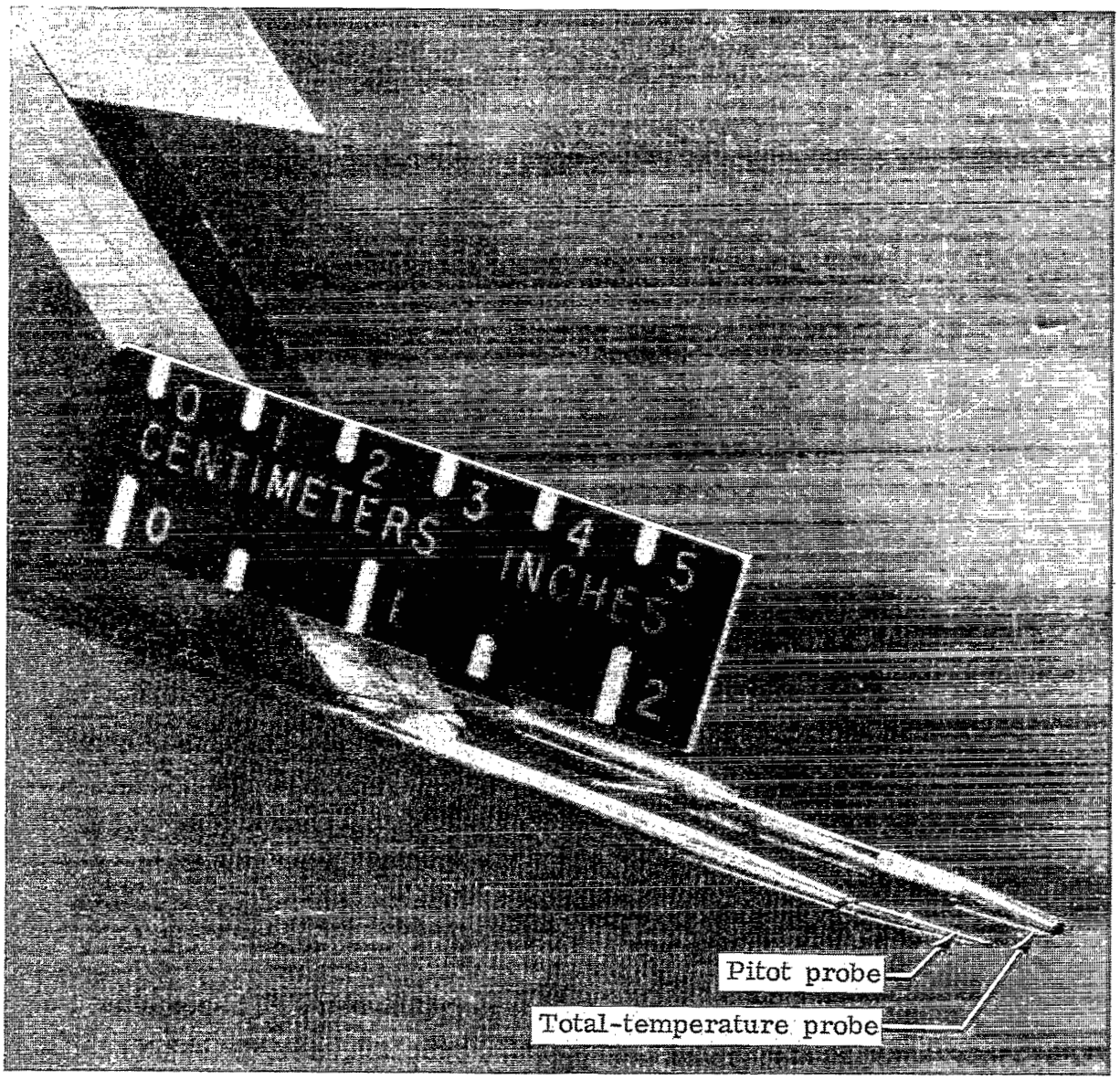

L-77-8425.1

(c) View showing opening of probes.

Figure 8.- Concluded.

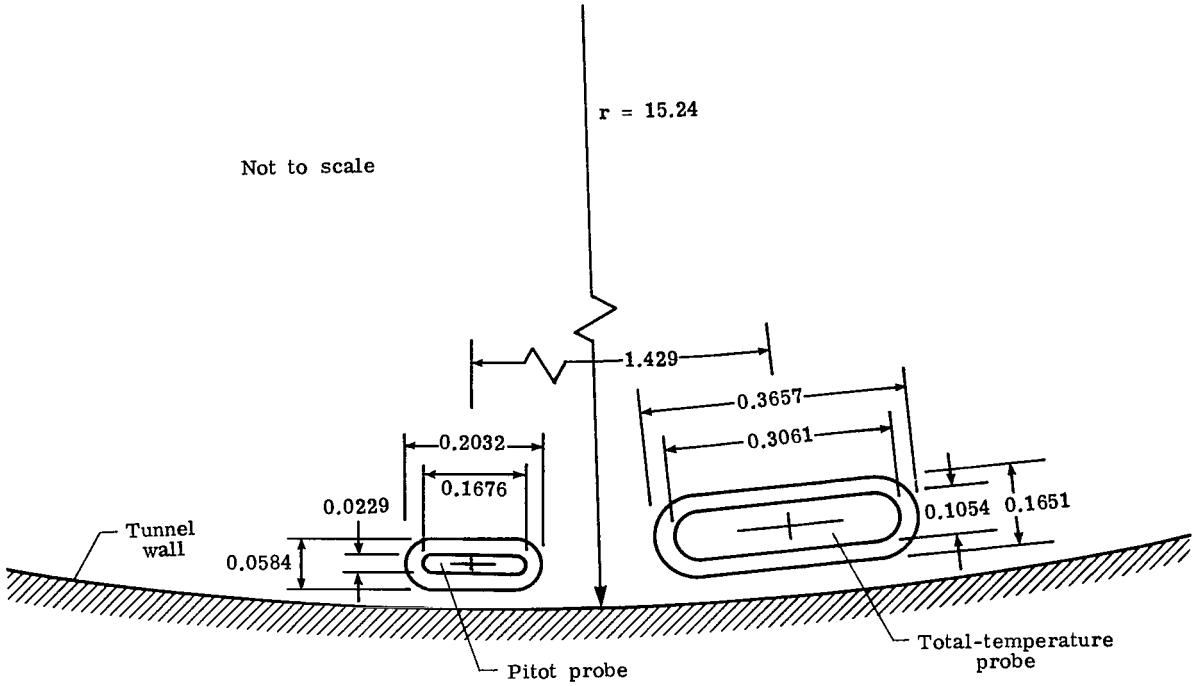

Figure 9.- Dimensions of pitot and total-temperature probe tips (nominal boundary-layer thickness, $\delta \approx 4.32$). All dimensions shown are in centimeters.

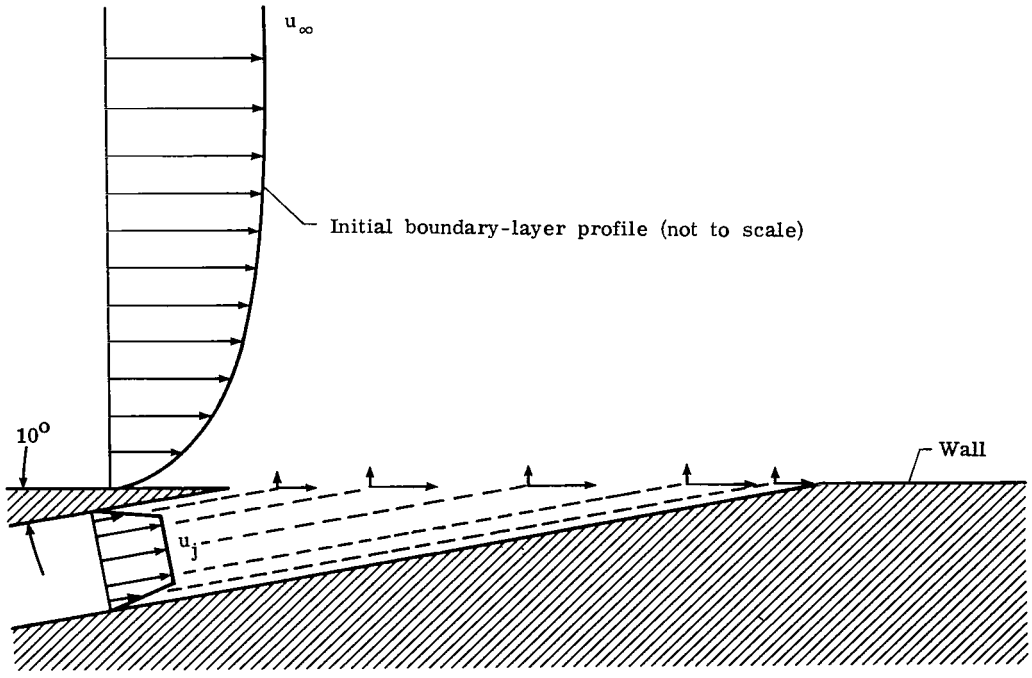

Figure 10.- Slot-flow representation for numerical finite-difference solution.

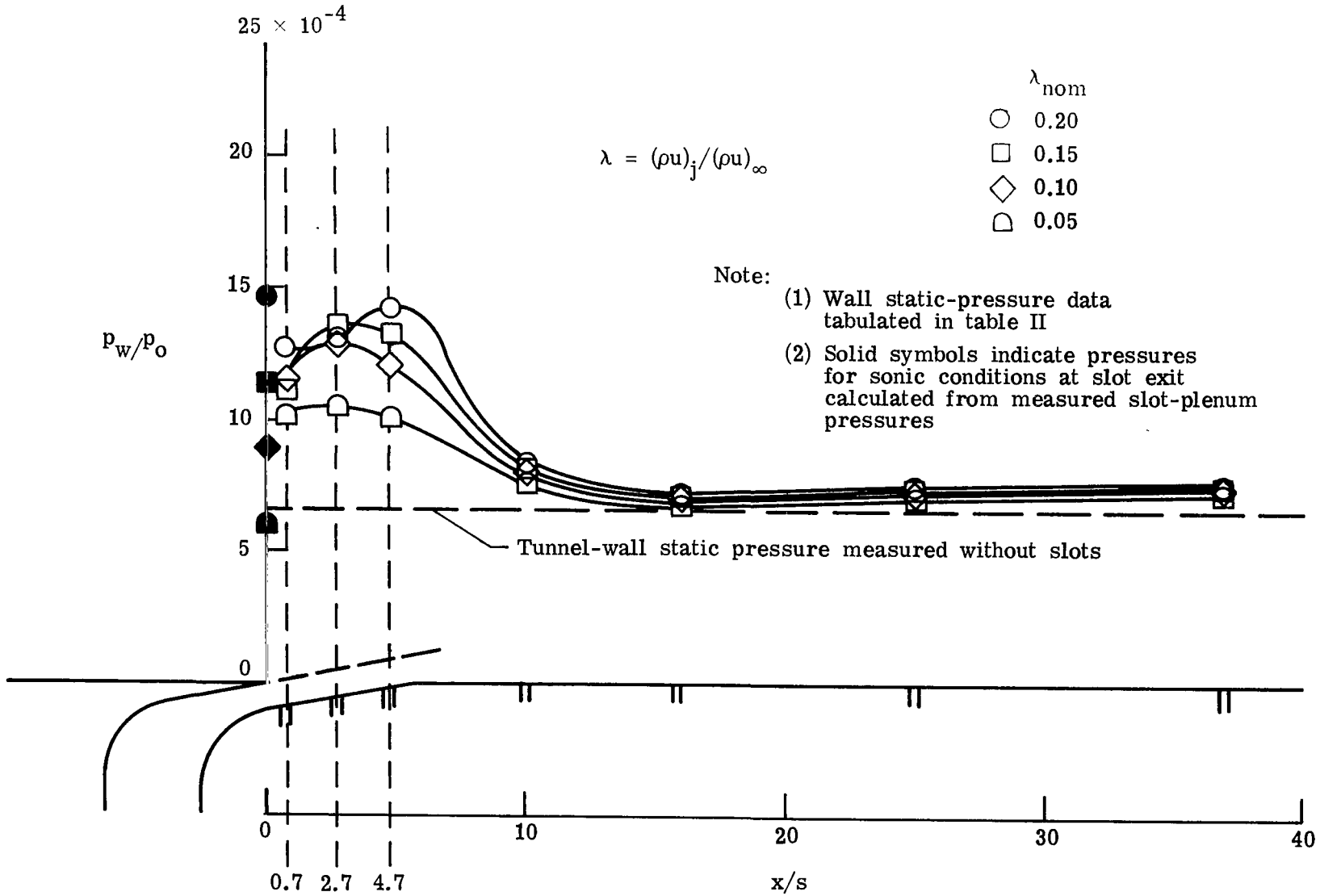

Figure 11.- Measured slot and downstream-wall static pressure (s = 0.254 cm).

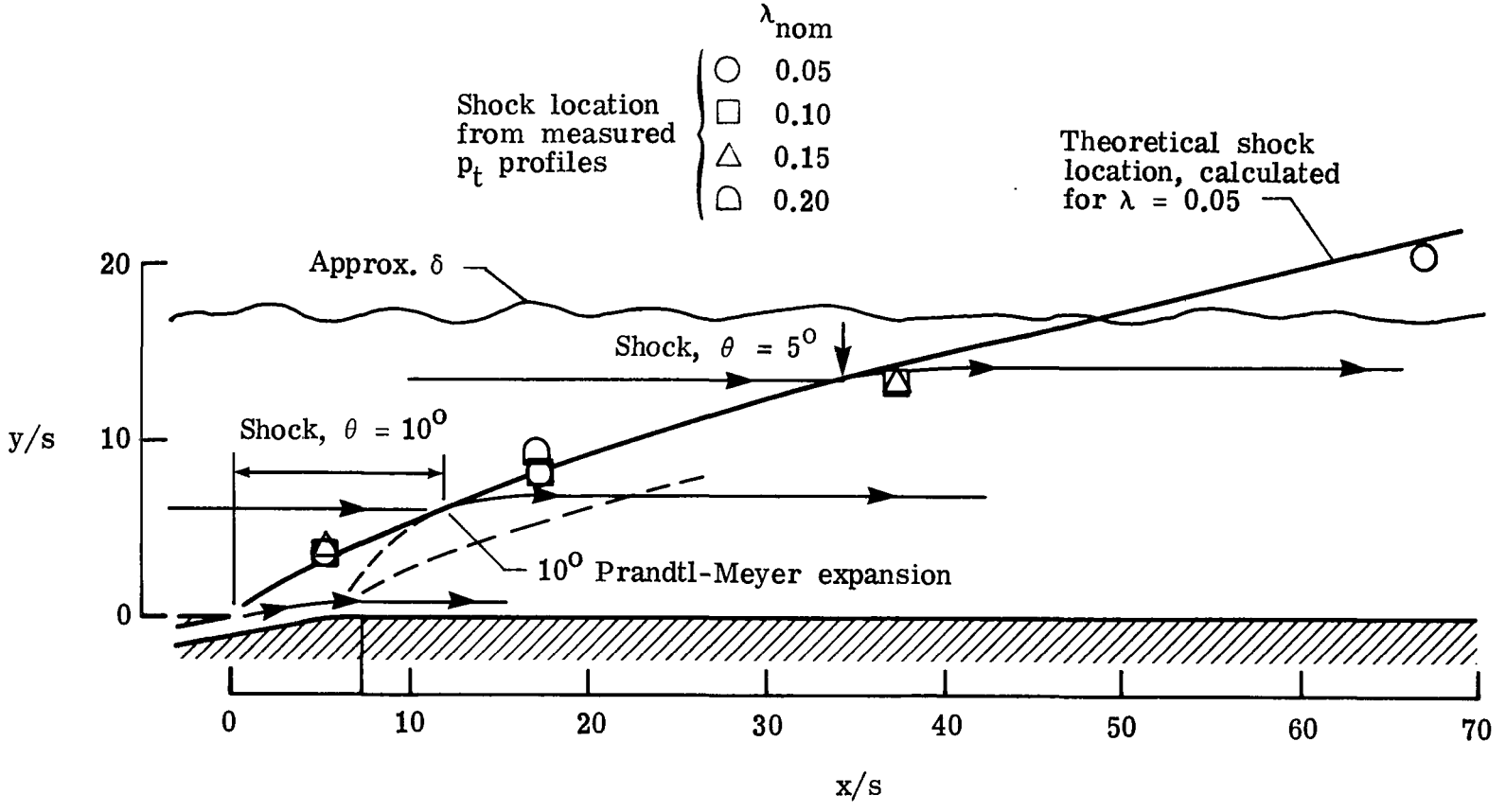

Figure 12.- Calculated and indicated shock locations at first slot (s = 0.254 cm).

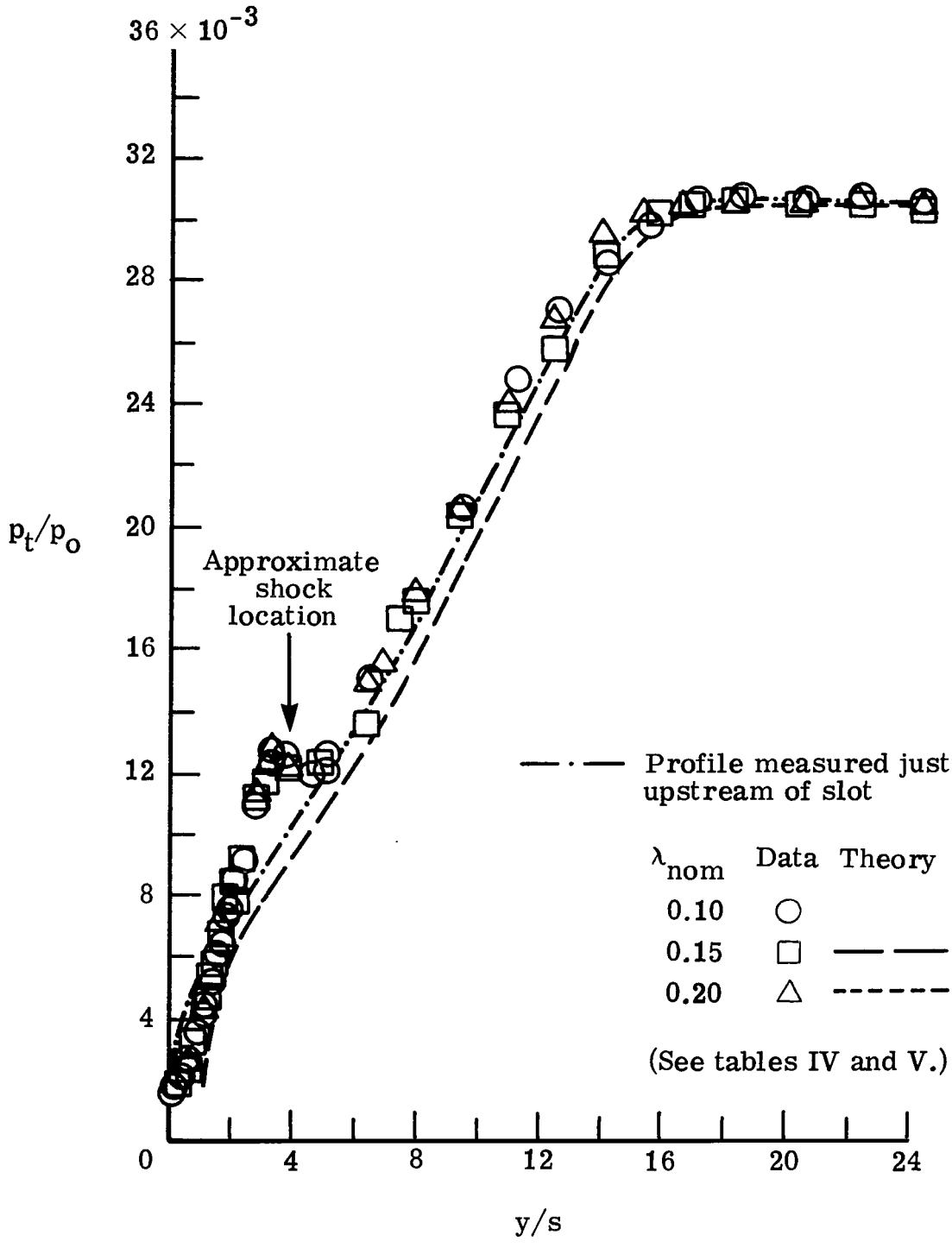

(a) x/s = 5.8.

Figure 13.- Pitot-pressure profiles measured downstream of single slot for λ_{nom} = 0.10, 0.15, and 0.20 (s = 0.254 cm).

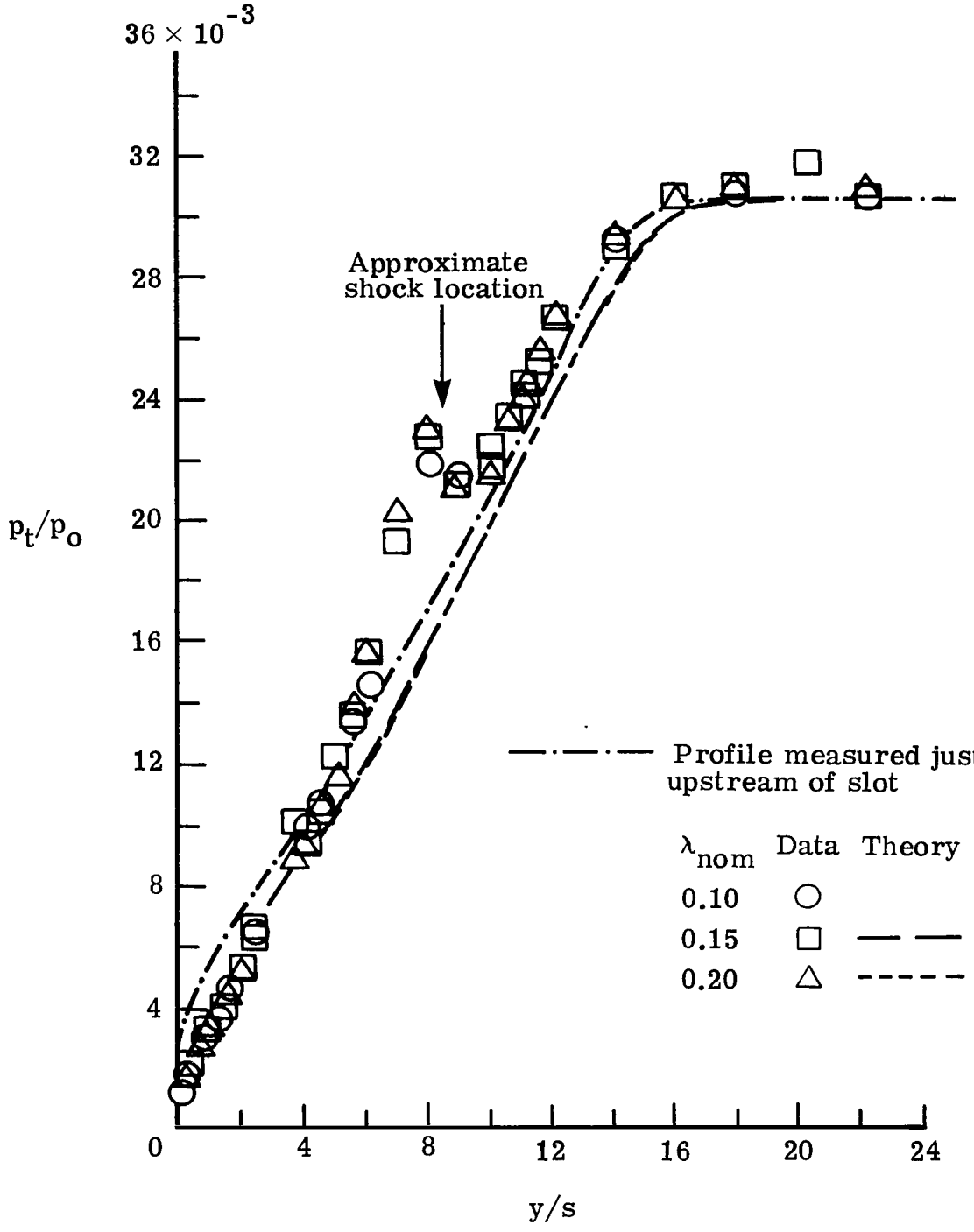

(b) x/s = 17.12.

Figure 13.- Continued.

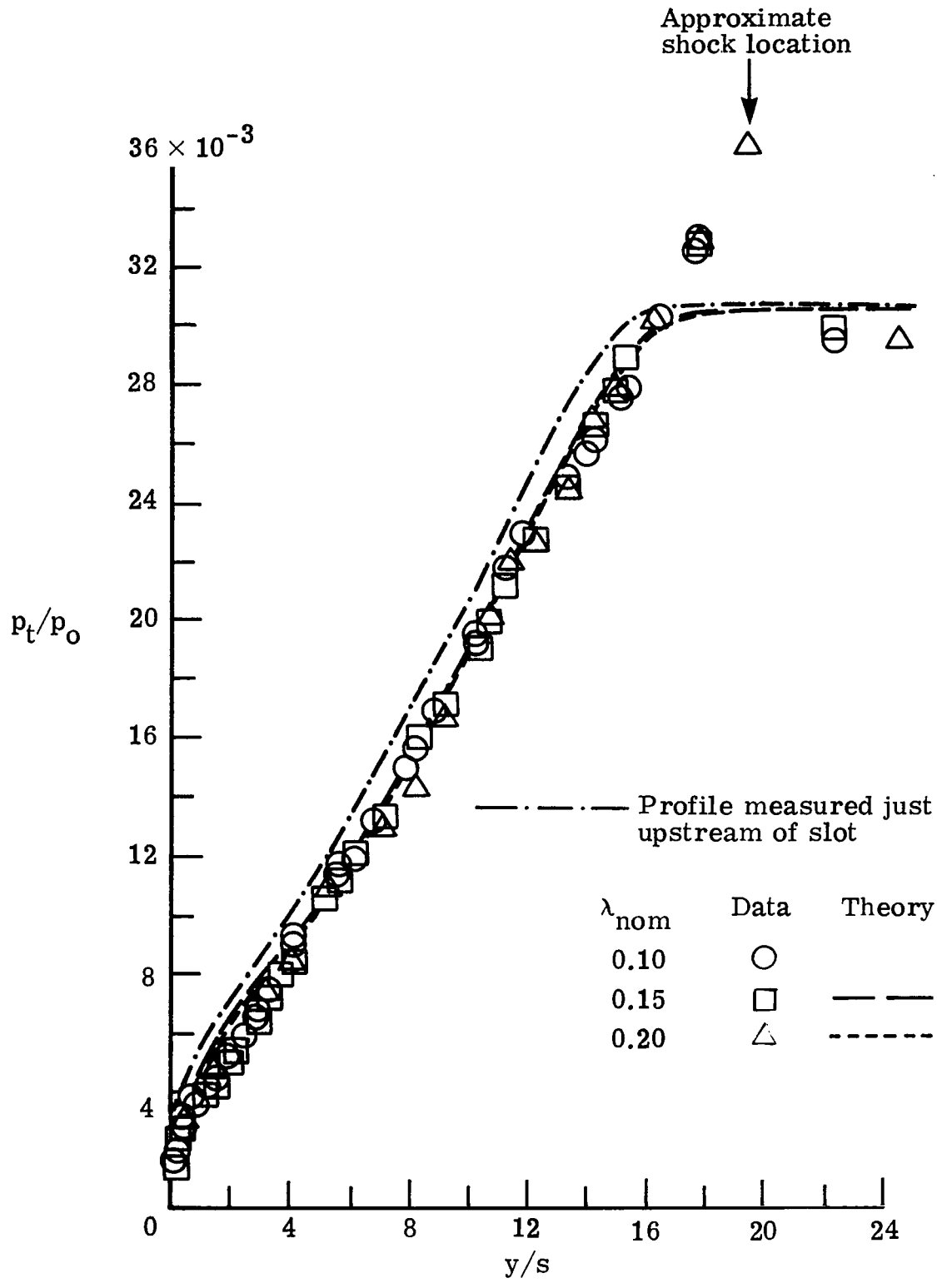

(c) x/s = 67.12.

Figure 13.- Concluded.

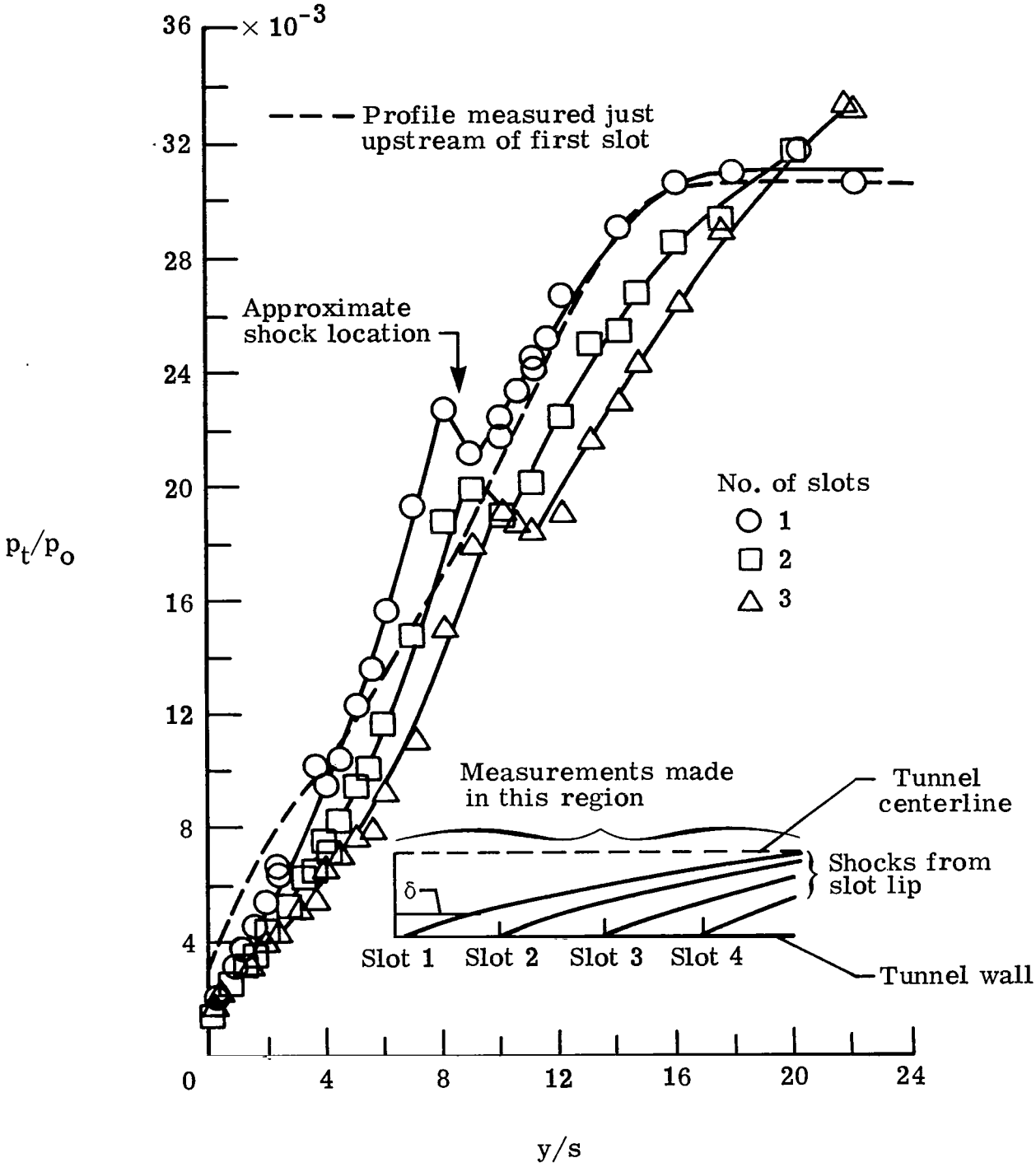

(a) x/s = 17.12.

Figure 14.- Comparison of pitot-pressure profiles measured for one, two, and three slots (λ_{nom} = 0.15; s = 0.254 cm).

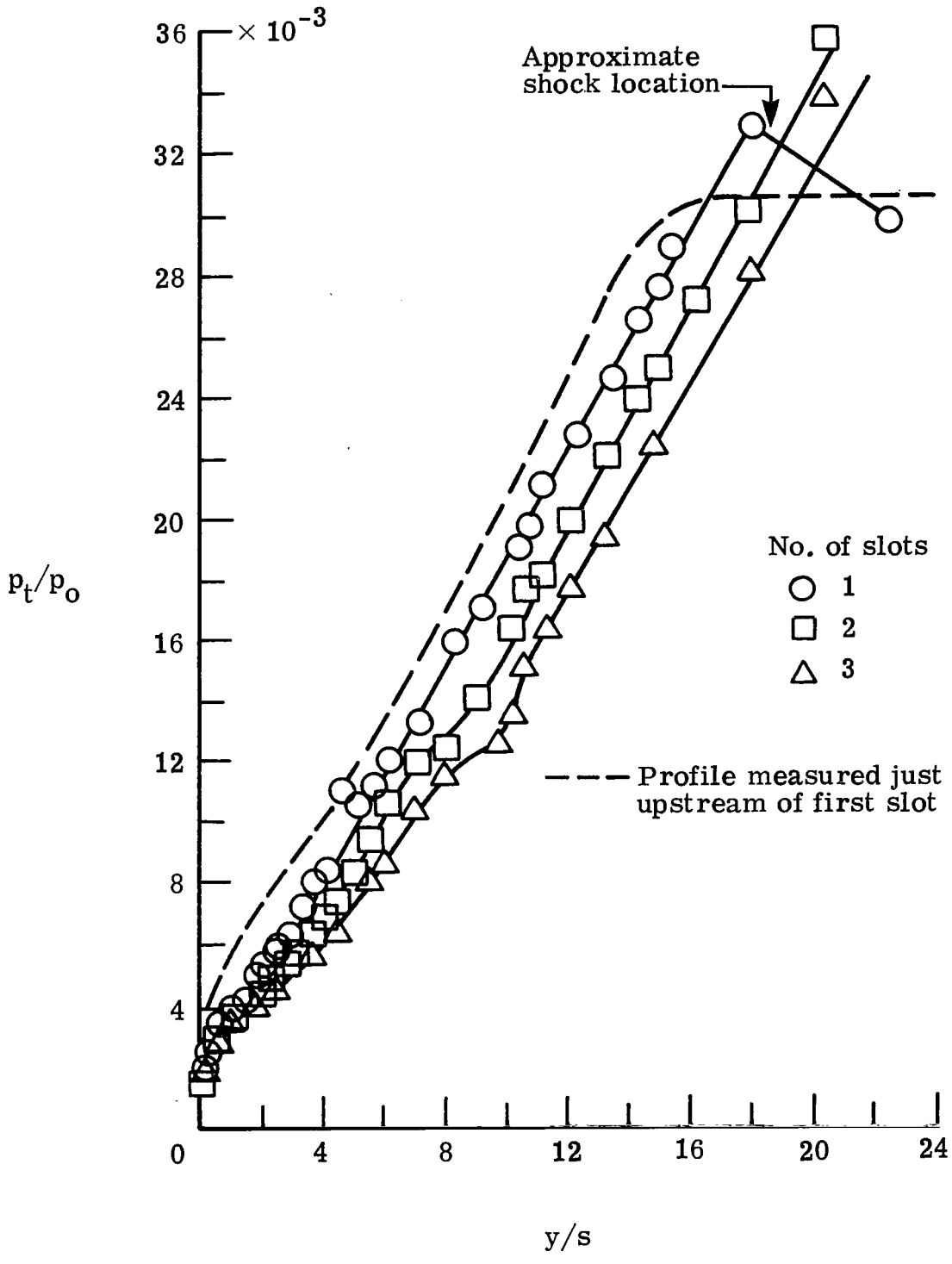

(b) x/s = 67.12.

Figure 14.- Concluded.

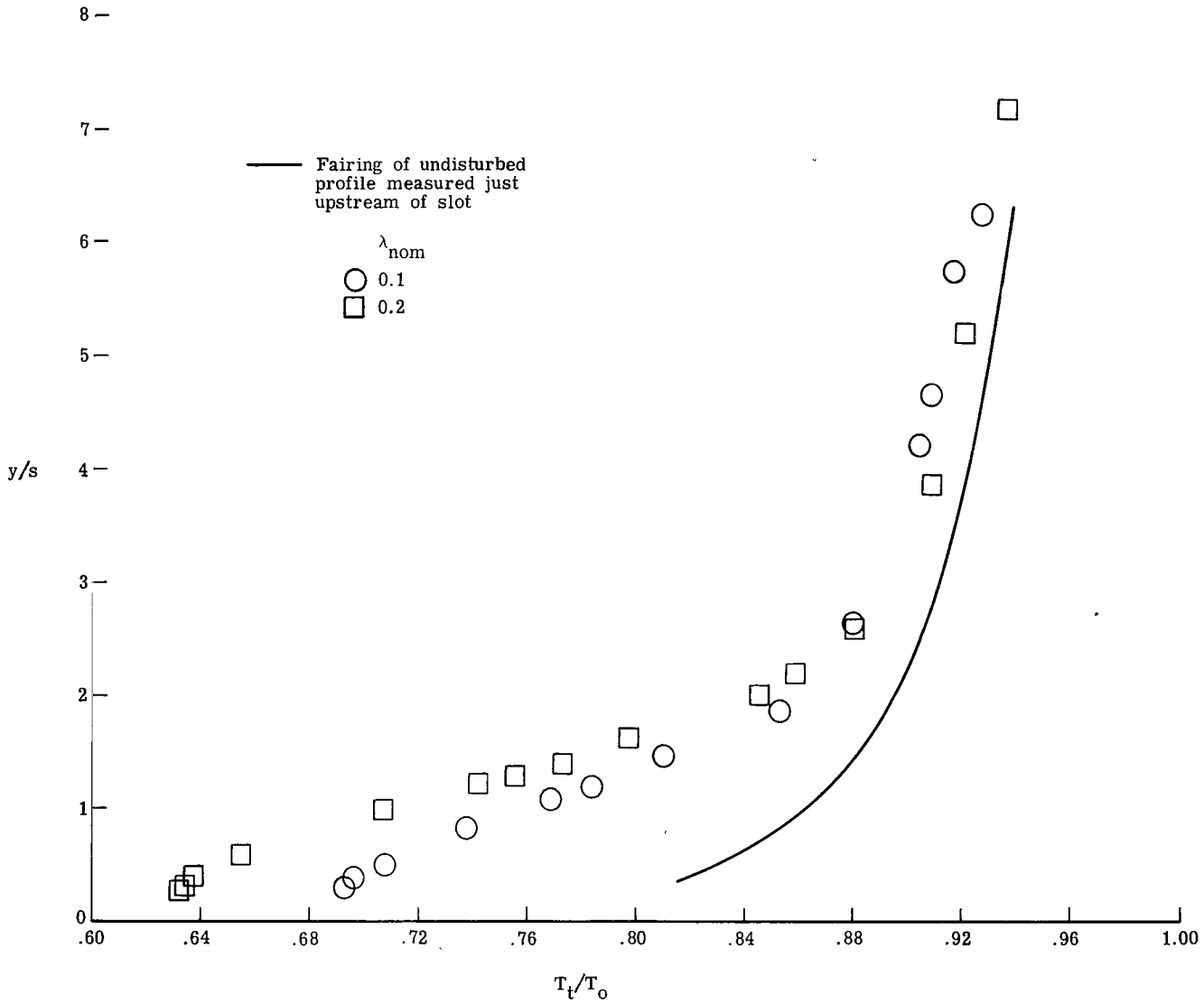

(a) x/s = 17.12.

Figure 15.- Profiles of experimental total temperature at four stations downstream of single slot (s = 0.254 cm).

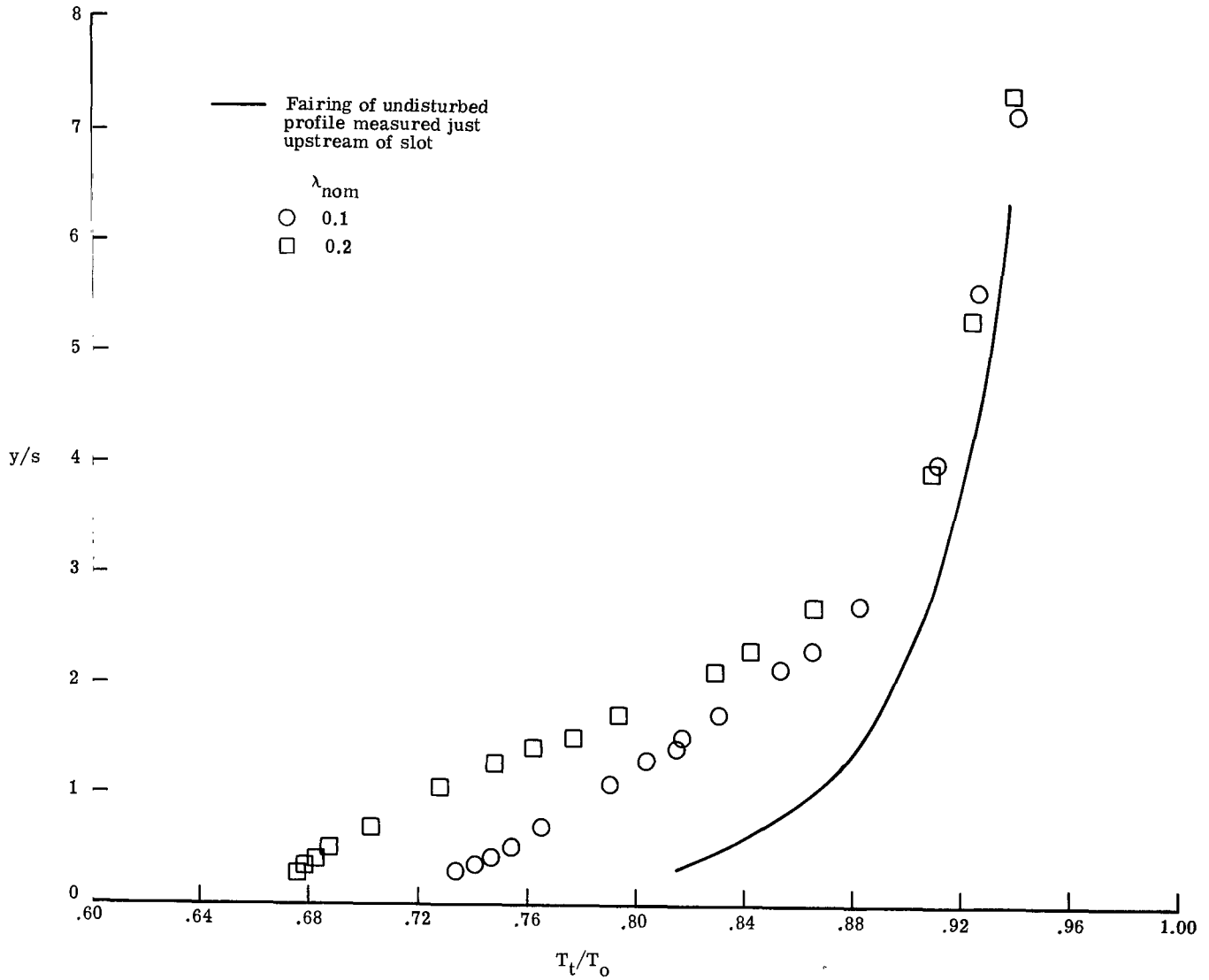

(b) x/s = 37.12.

Figure 15.- Continued.

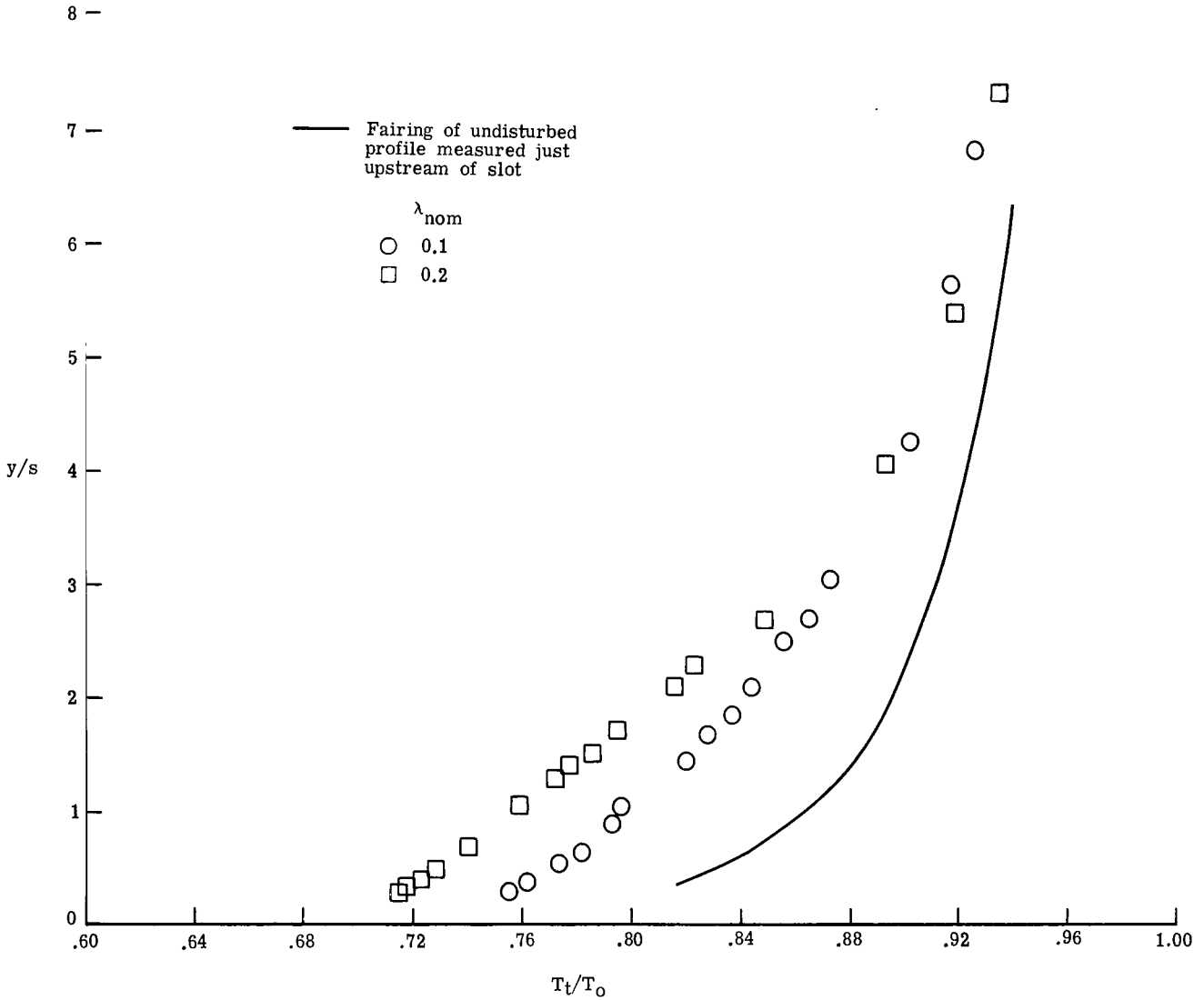

(c) x/s = 67.12.

Figure 15.- Continued.

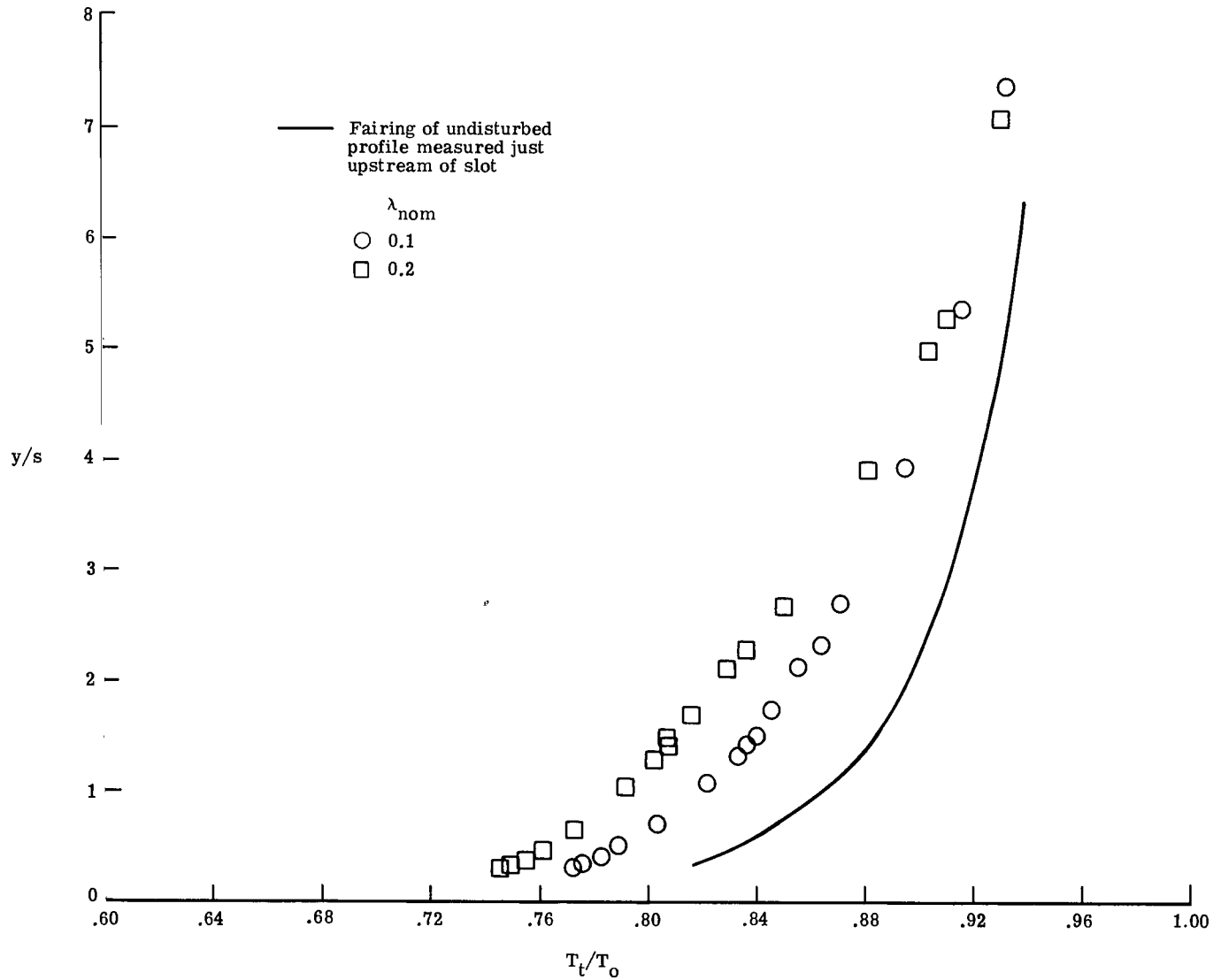

(d) x/s = 107.12.

Figure 15.- Concluded.

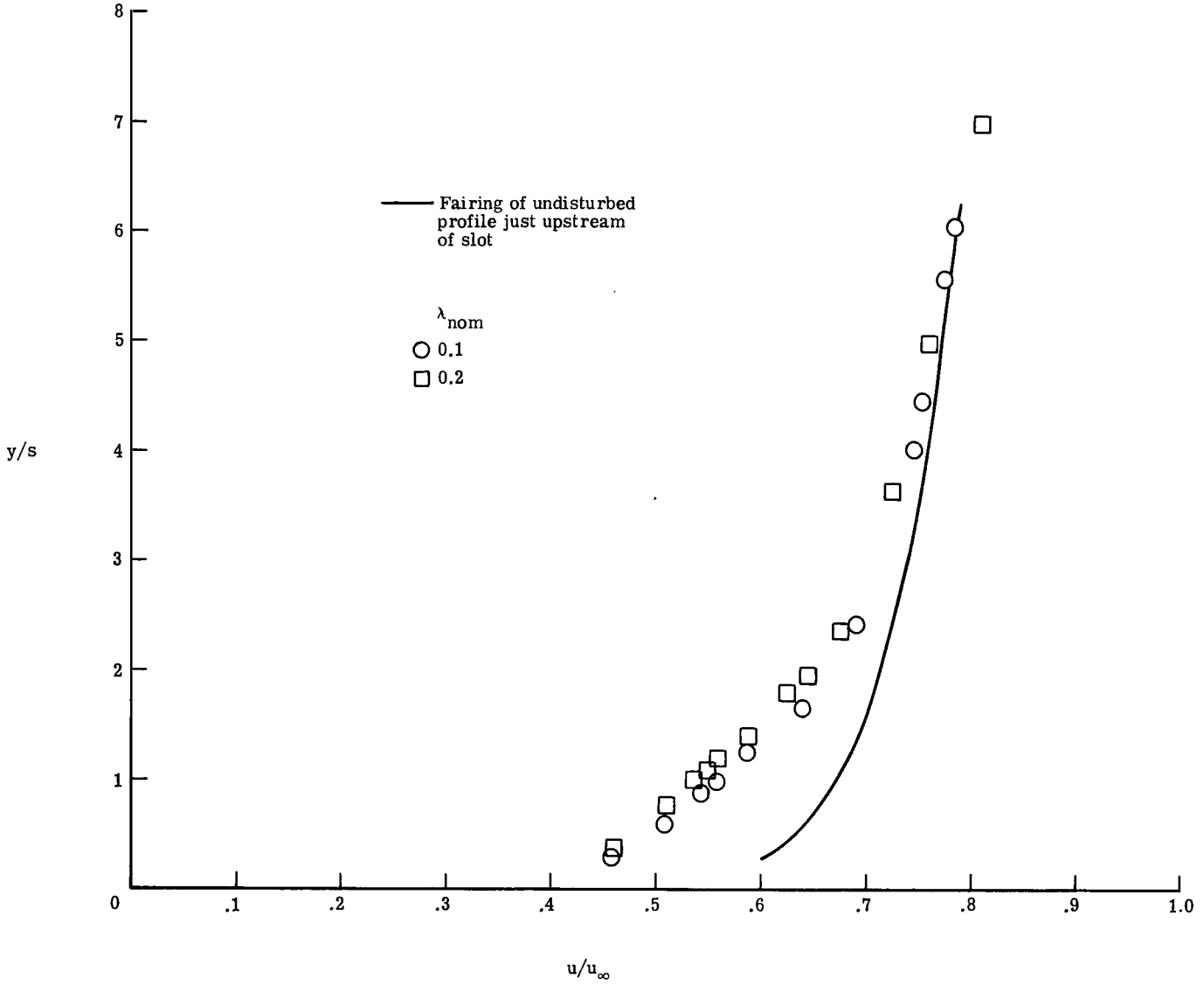

(a) x/s = 17.12.

Figure 16.- Experimentally derived velocity profiles at four stations downstream of single slot (s = 0.254 cm).

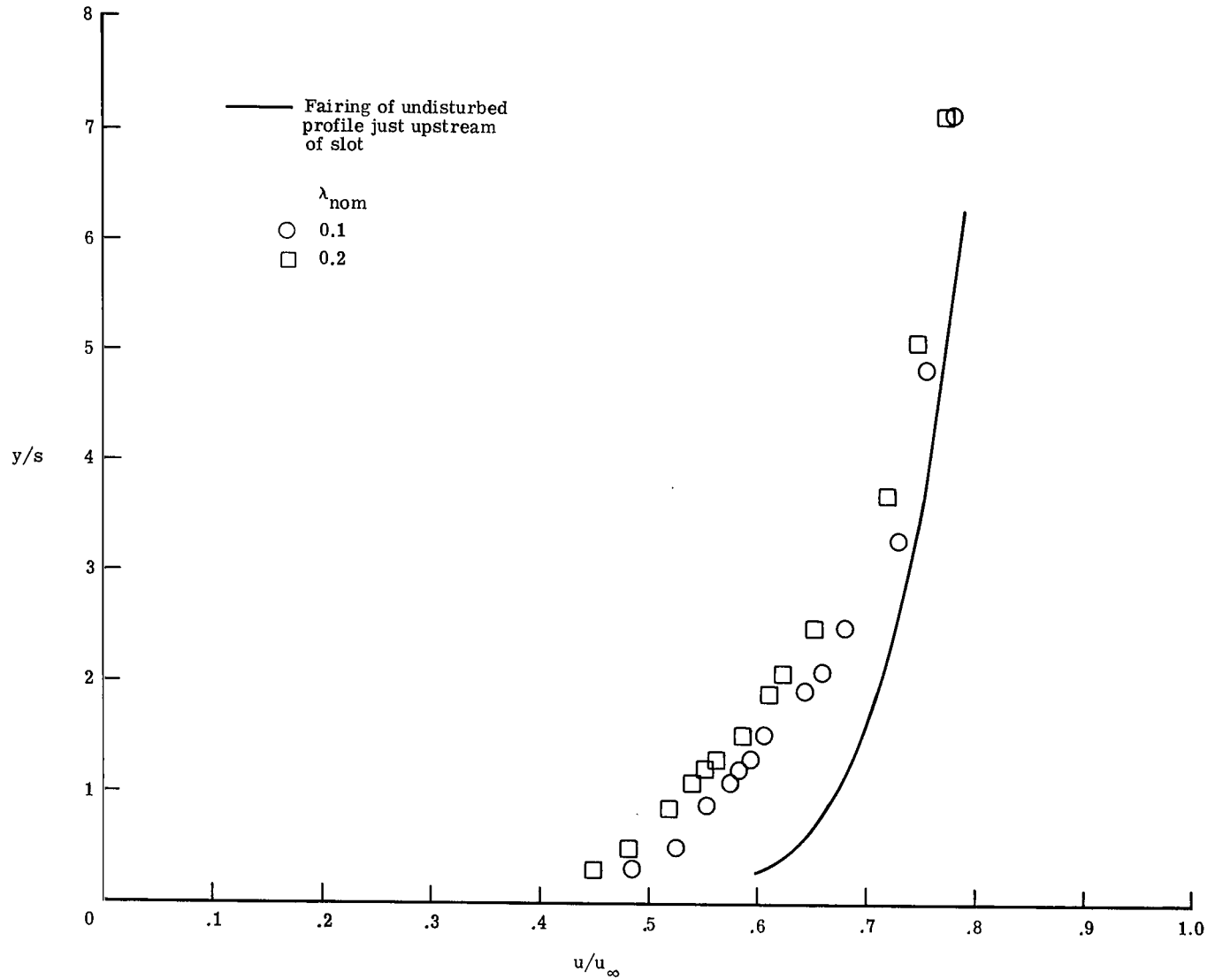

(b) x/s = 37.12.

Figure 16.- Continued.

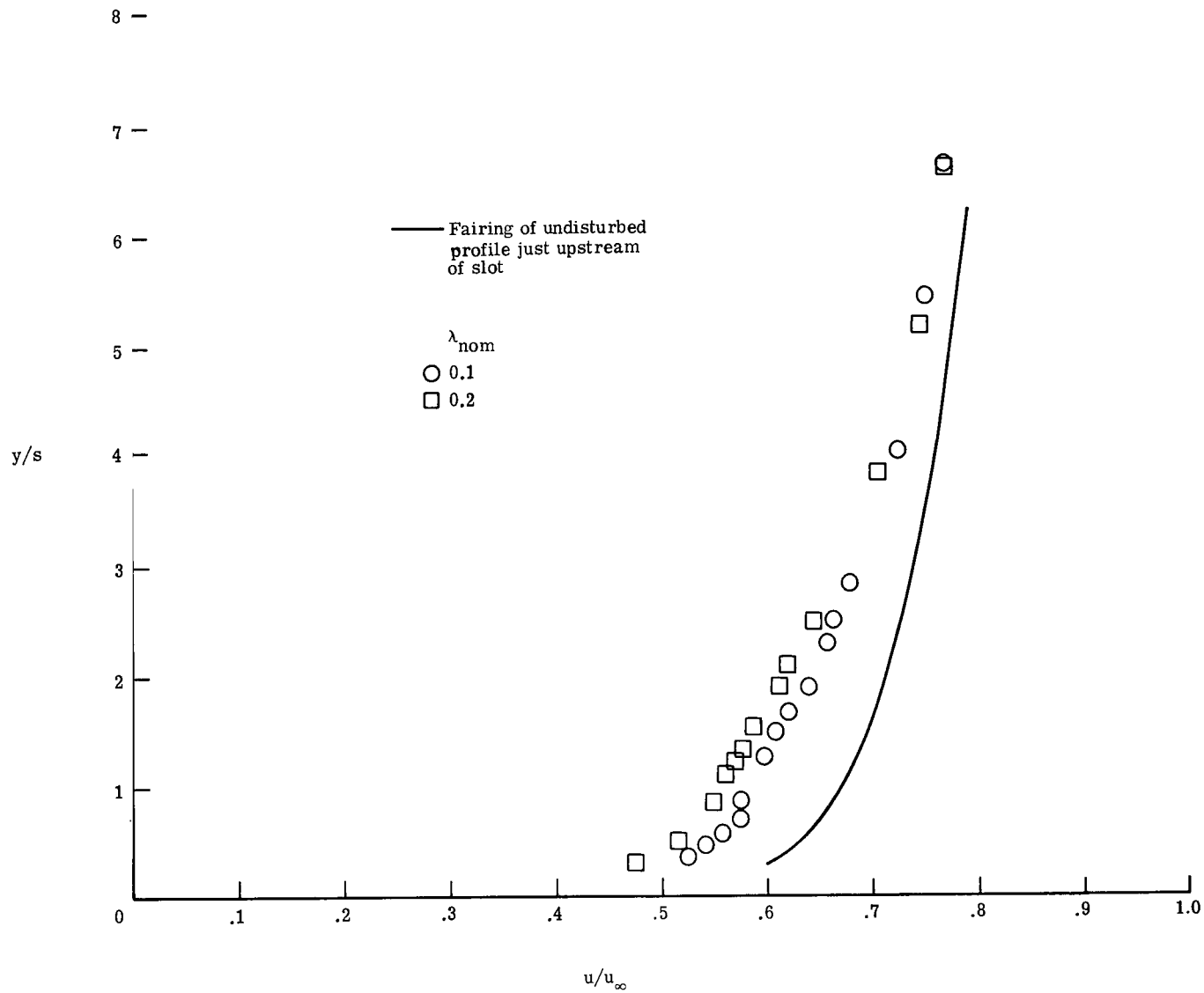

(c) x/s = 67.12.

Figure 16.- Continued.

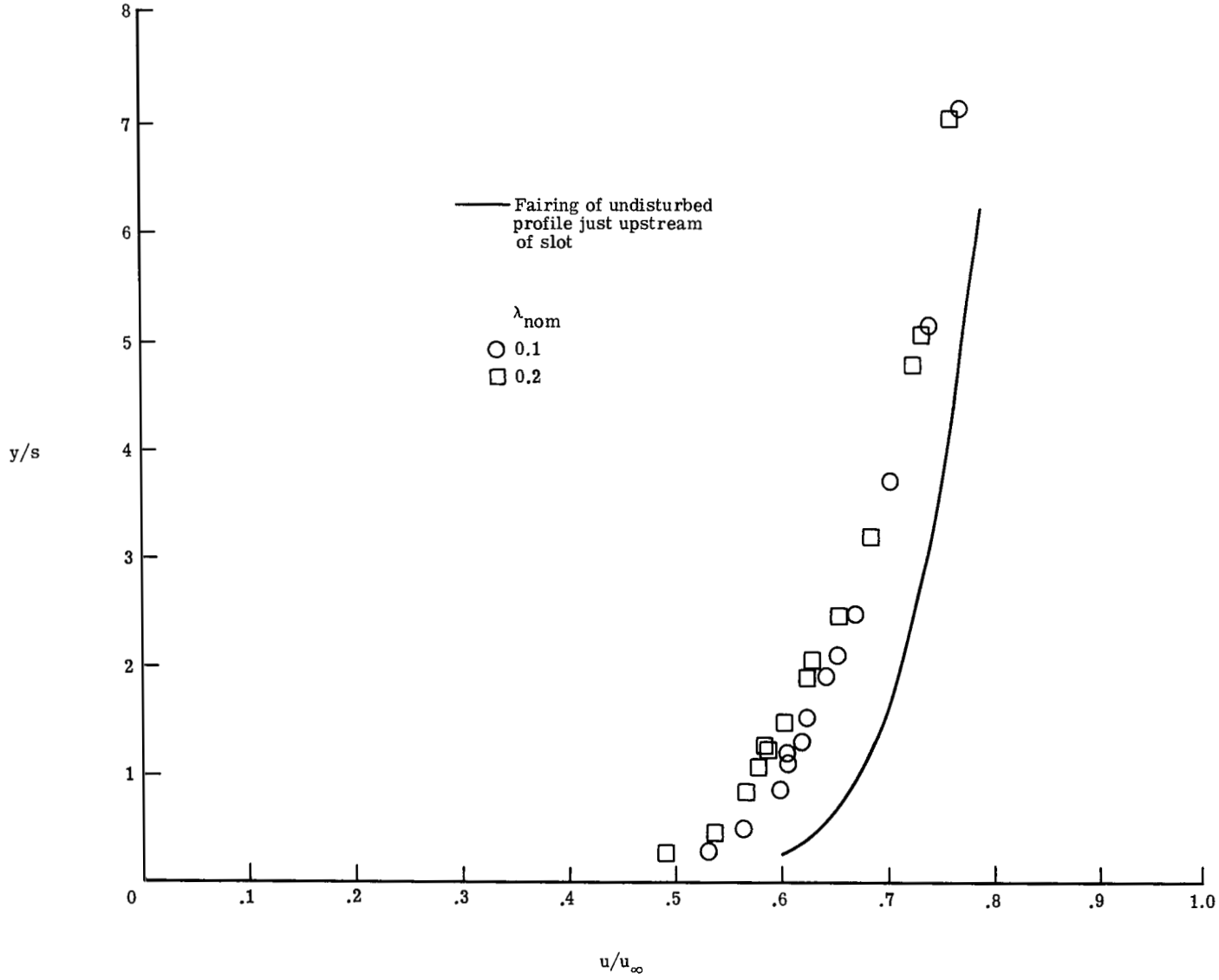

(d) x/s = 107.12.

Figure 16.- Concluded.

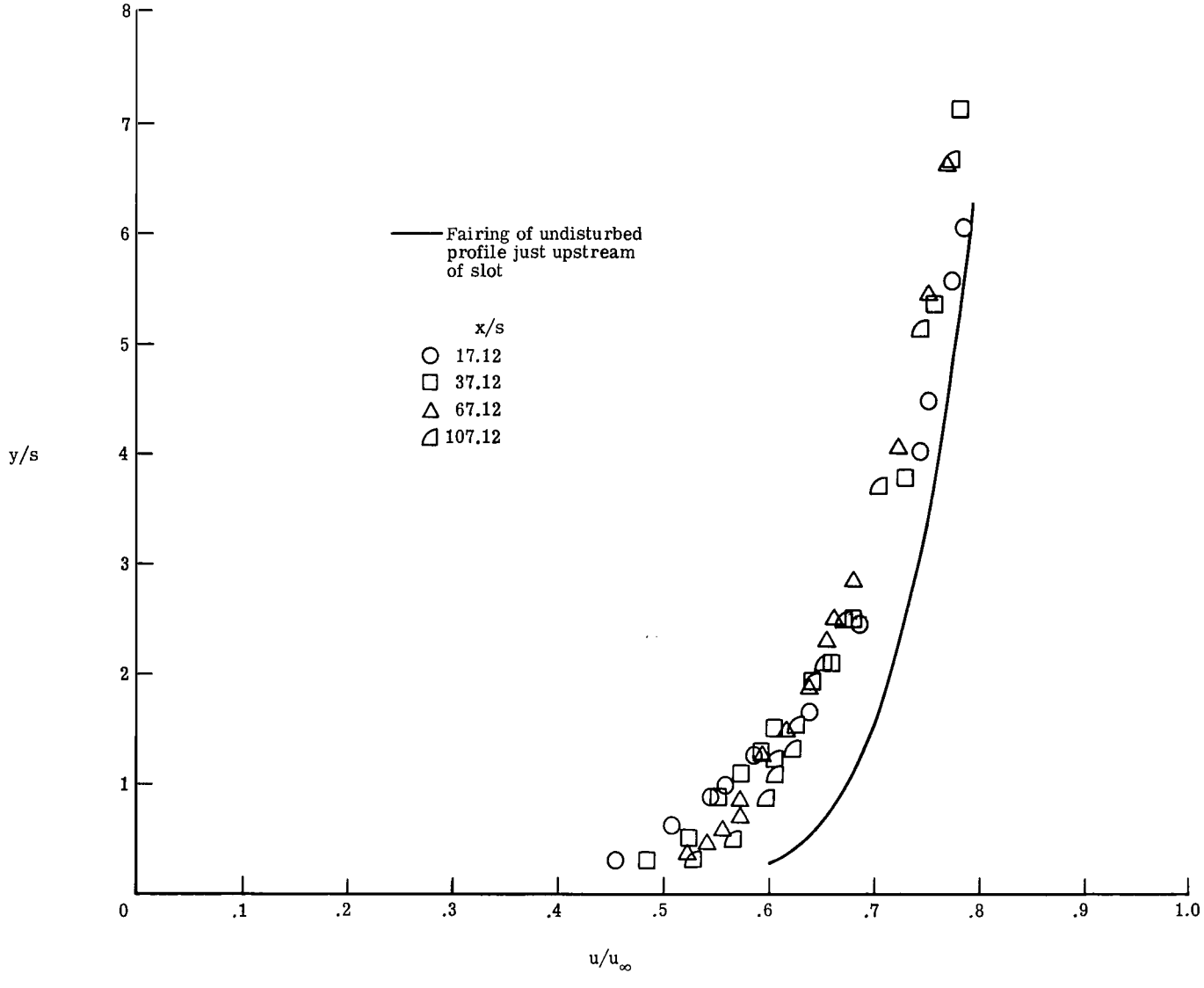

(a) $\lambda_{nom} = 0.10$.

Figure 17.- Comparison of velocity profiles at four stations downstream of single slot with undisturbed profile at slot location (s = 0.254 cm).

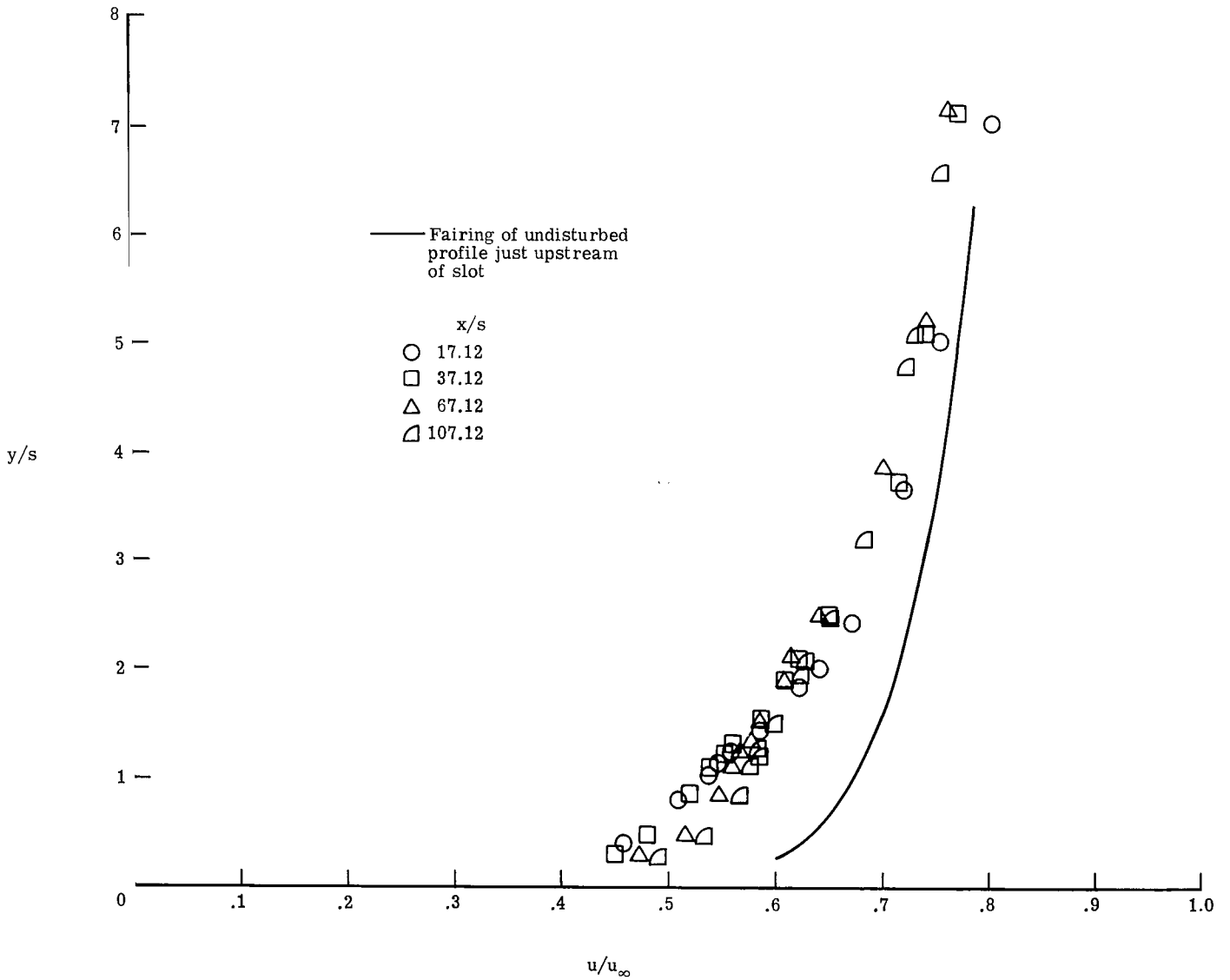

(b) $\lambda_{nom} = 0.20$.

Figure 17.- Concluded.

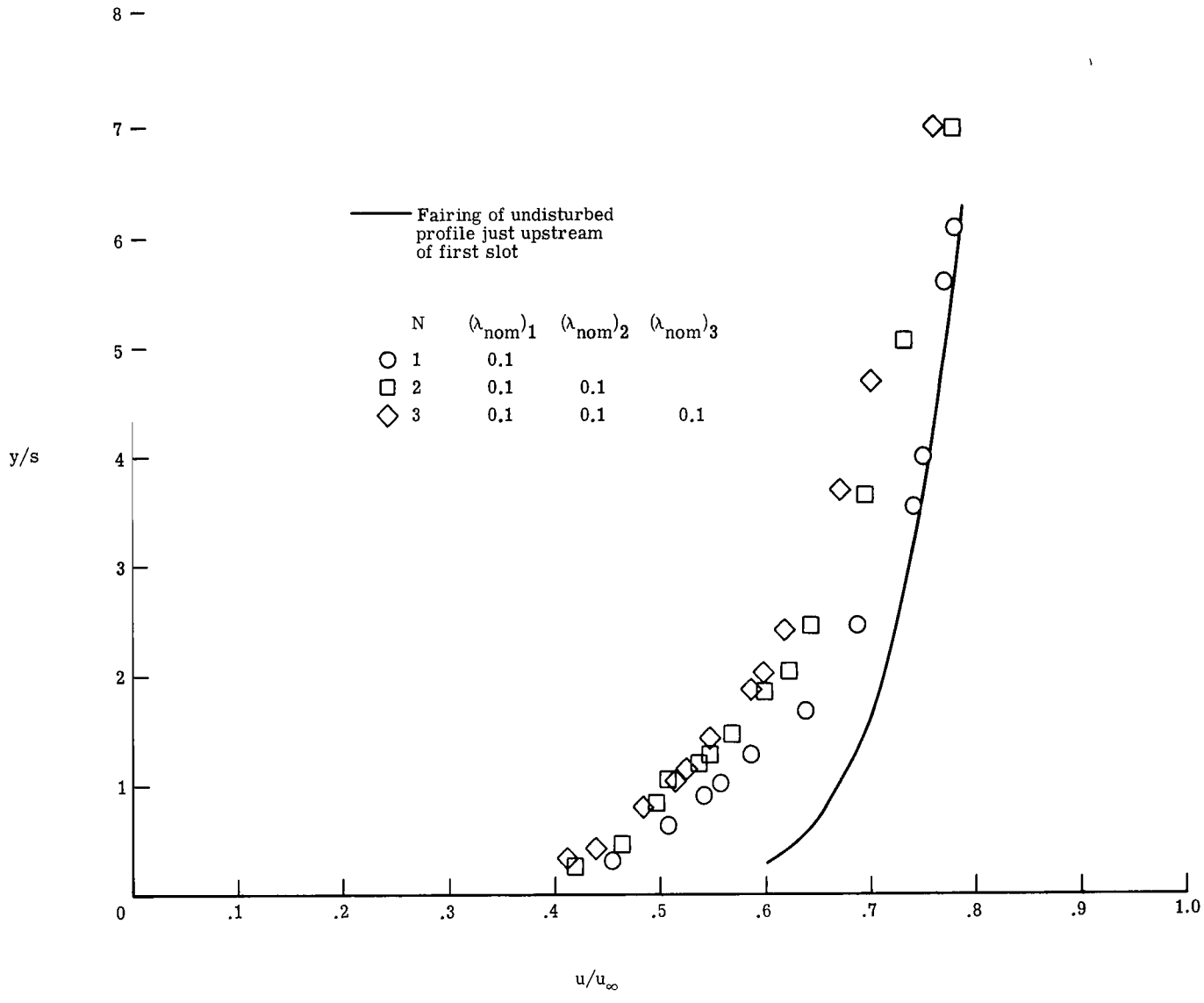

(a) x/s = 17.12.

Figure 18.- Effect of number of slots on velocity profiles downstream of last slot.

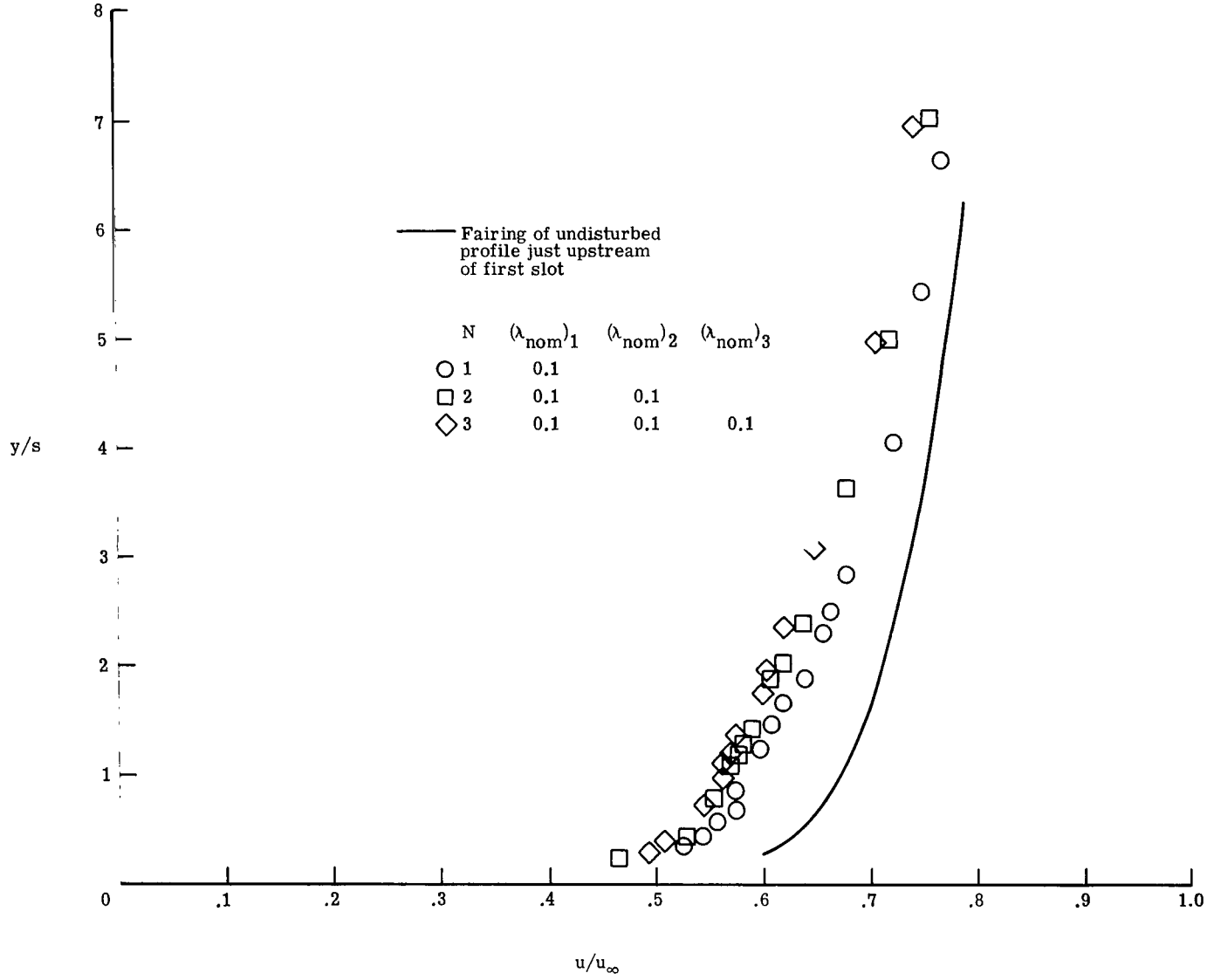

(b) x/s = 67.12.

Figure 18.- Concluded.

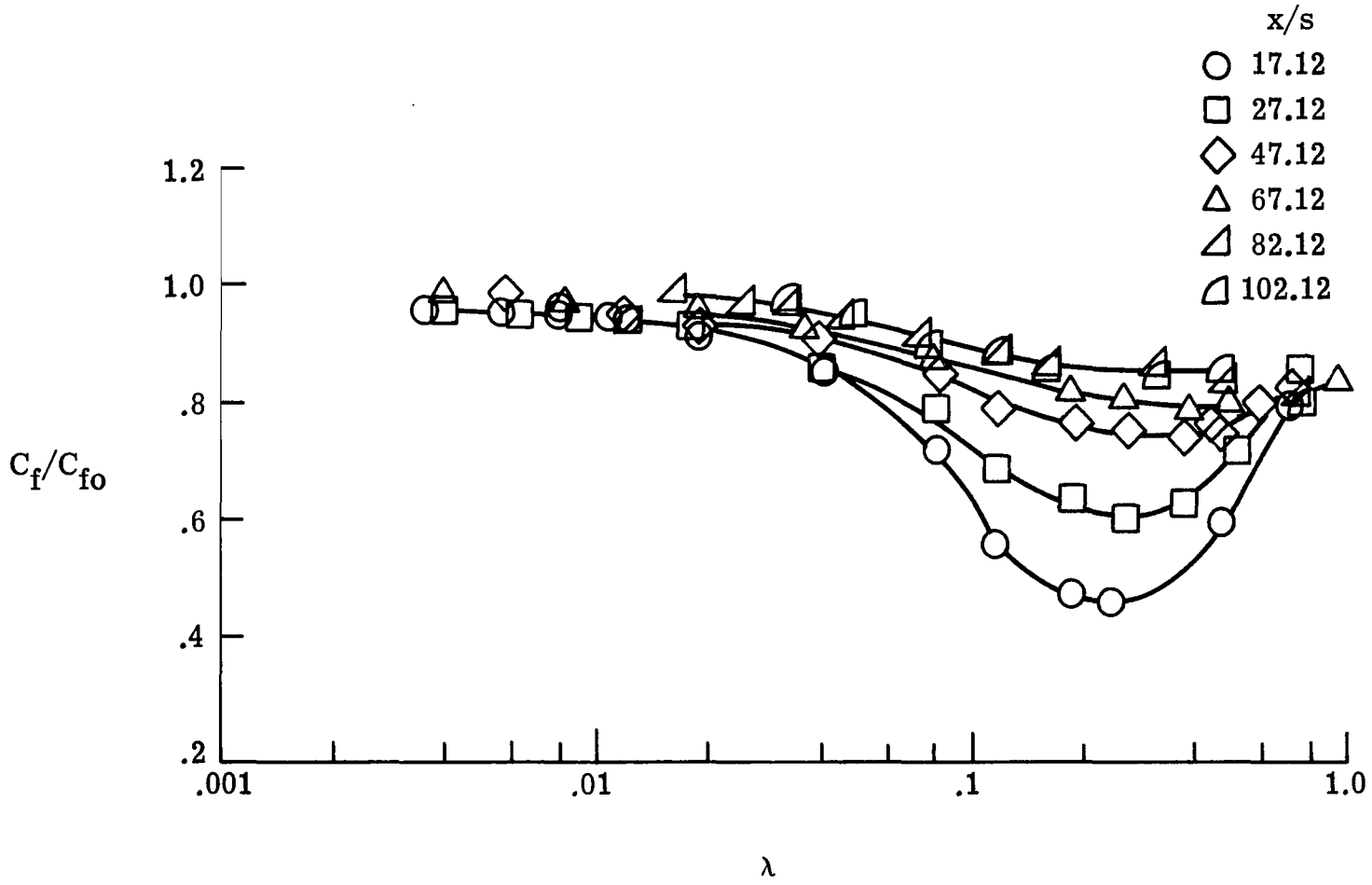

Figure 19.- C_f/C_{fo} as function of mass-flow parameter λ for one slot (s = 0.254 cm).

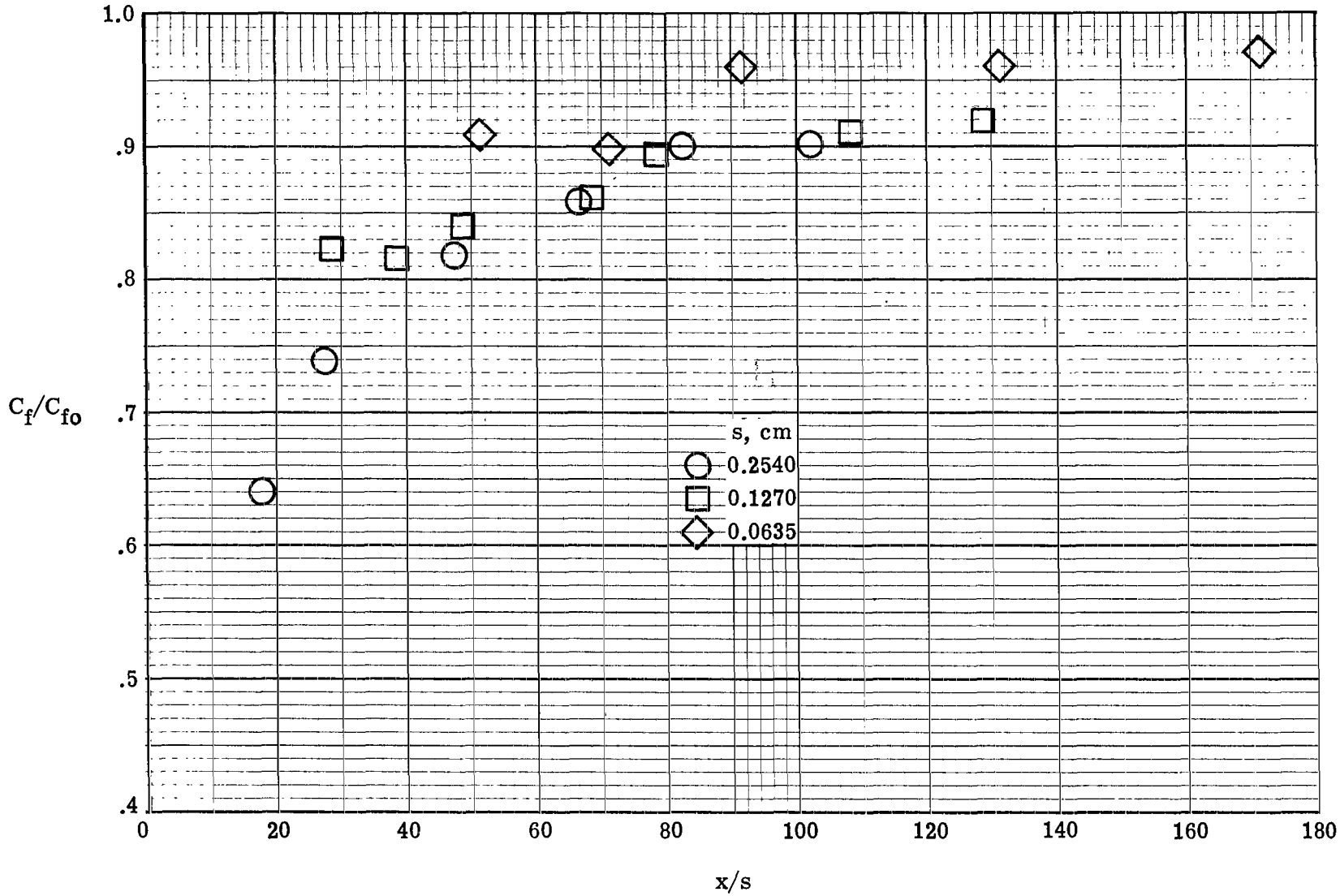

(a) $\lambda_{nom} = 0.10$.

Figure 20.- Effect of slot height s on skin friction downstream of single slot.

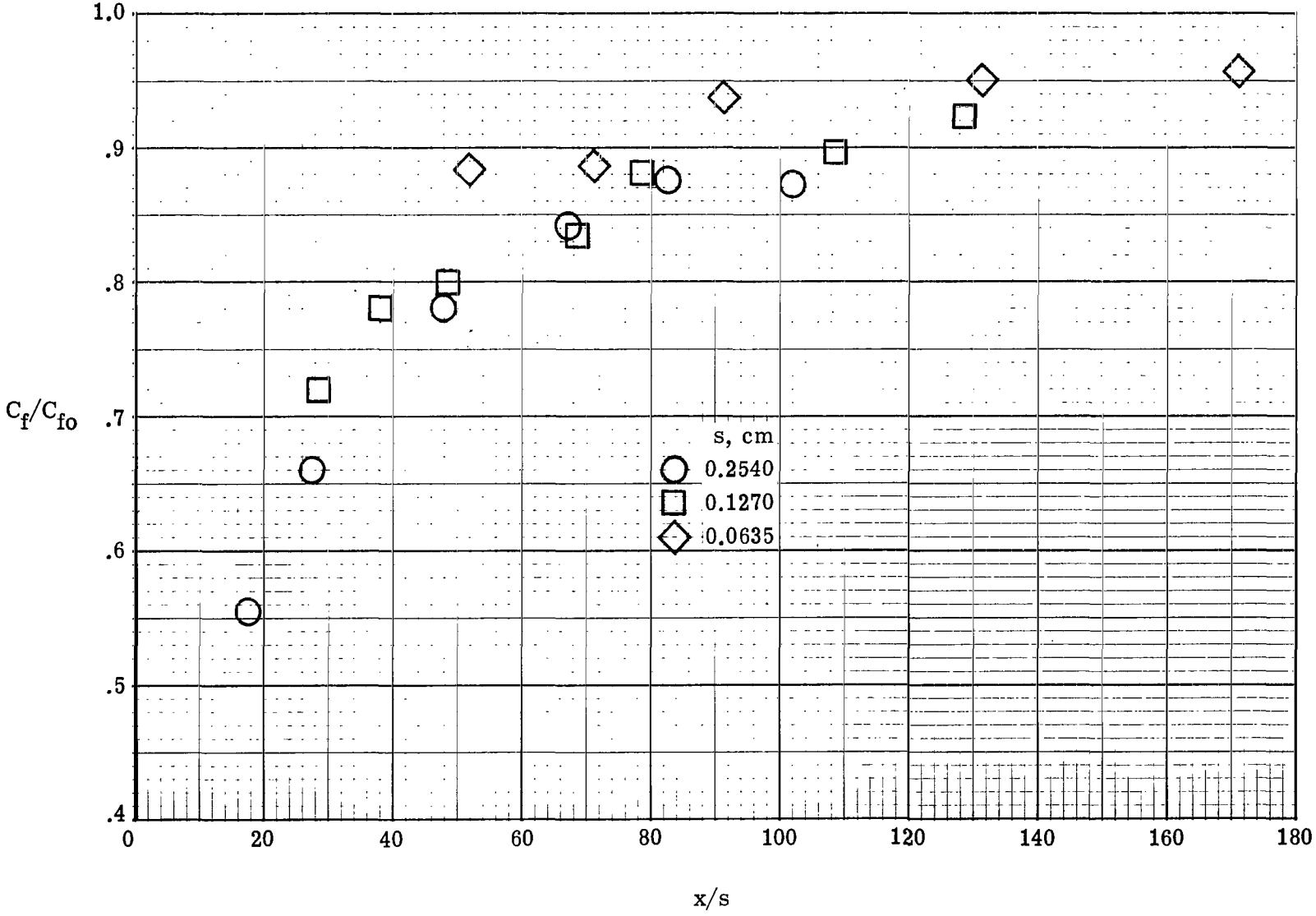

(b) $\lambda_{nom} = 0.15$.

Figure 20.- Continued.

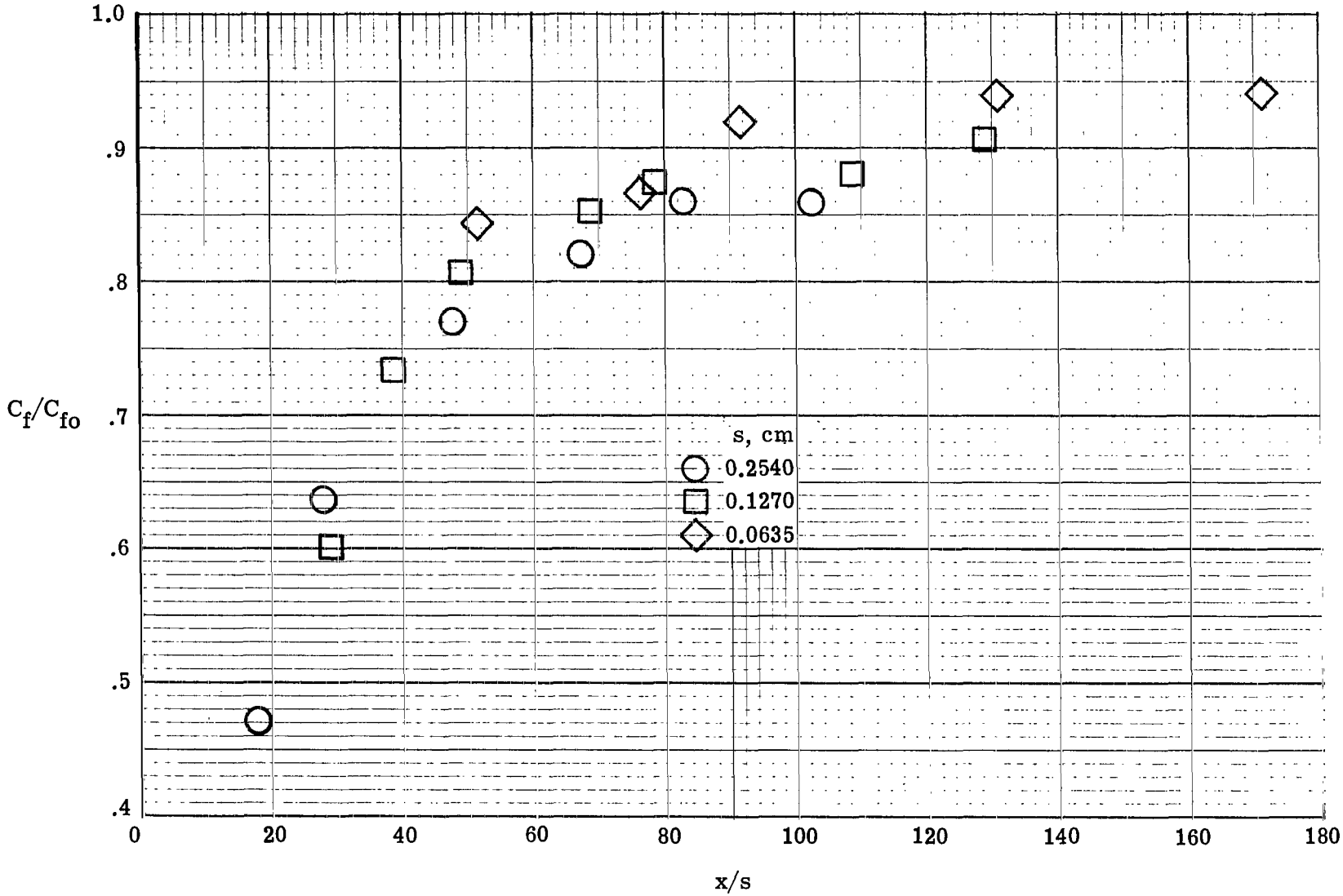

(c) $\lambda_{nom} = 0.20$.

Figure 20.- Concluded.

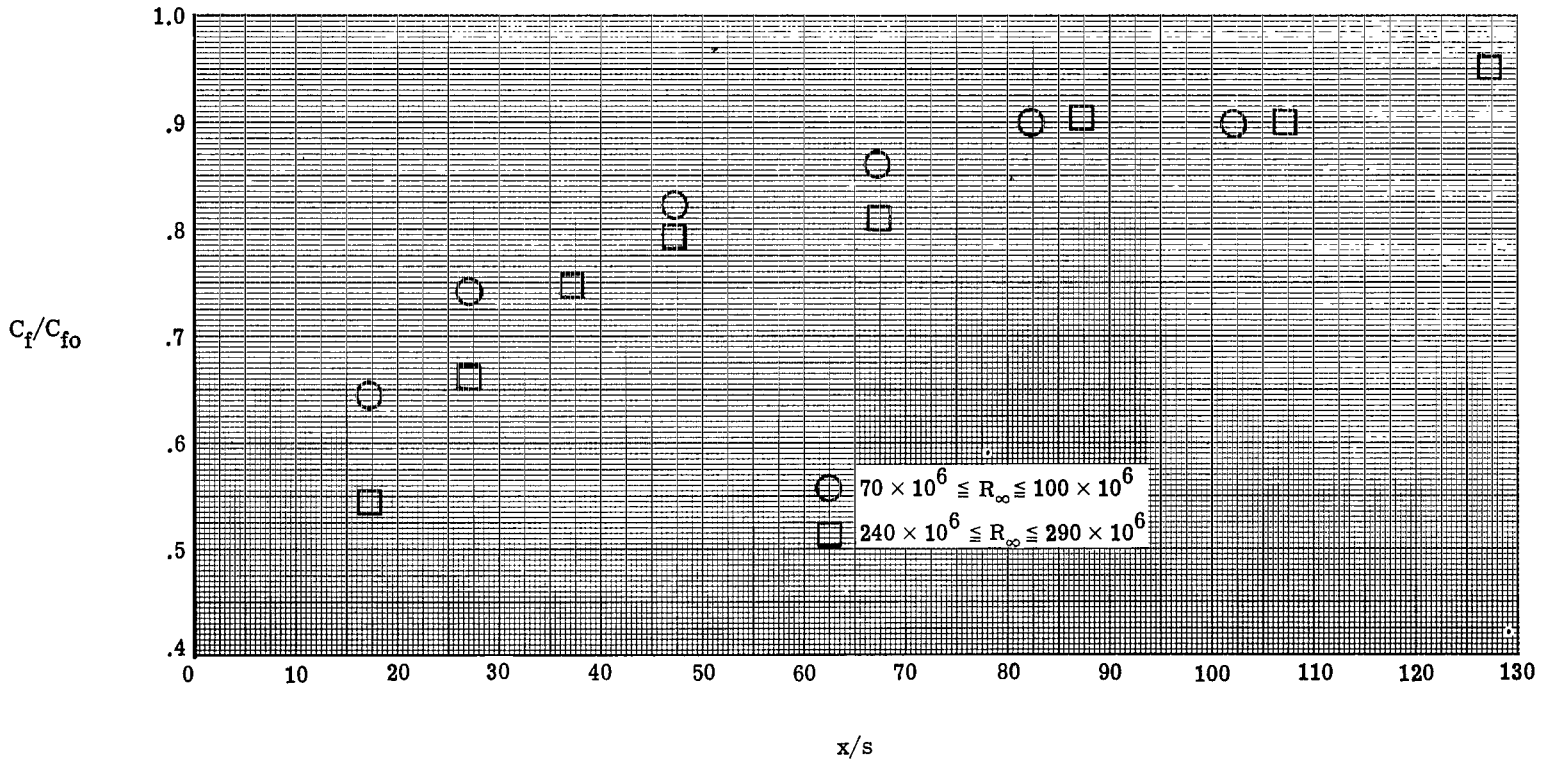

(a) $\lambda_{nom} = 0.10$.

Figure 21.- Effect of free-stream Reynolds number on skin friction downstream of single slot (s = 0.254 cm).

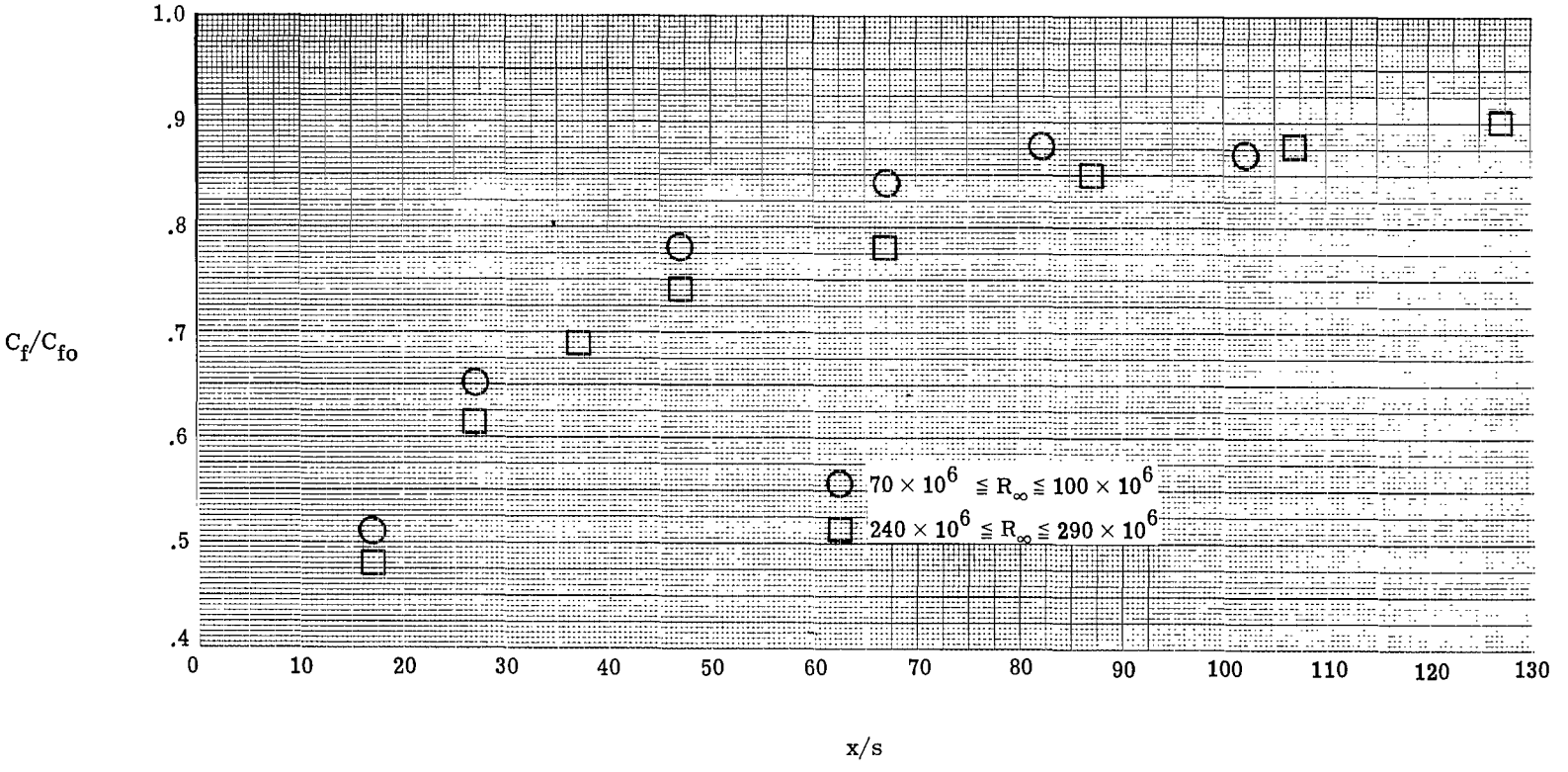

(b) $\lambda_{nom} = 0.15$.

Figure 21.- Continued.

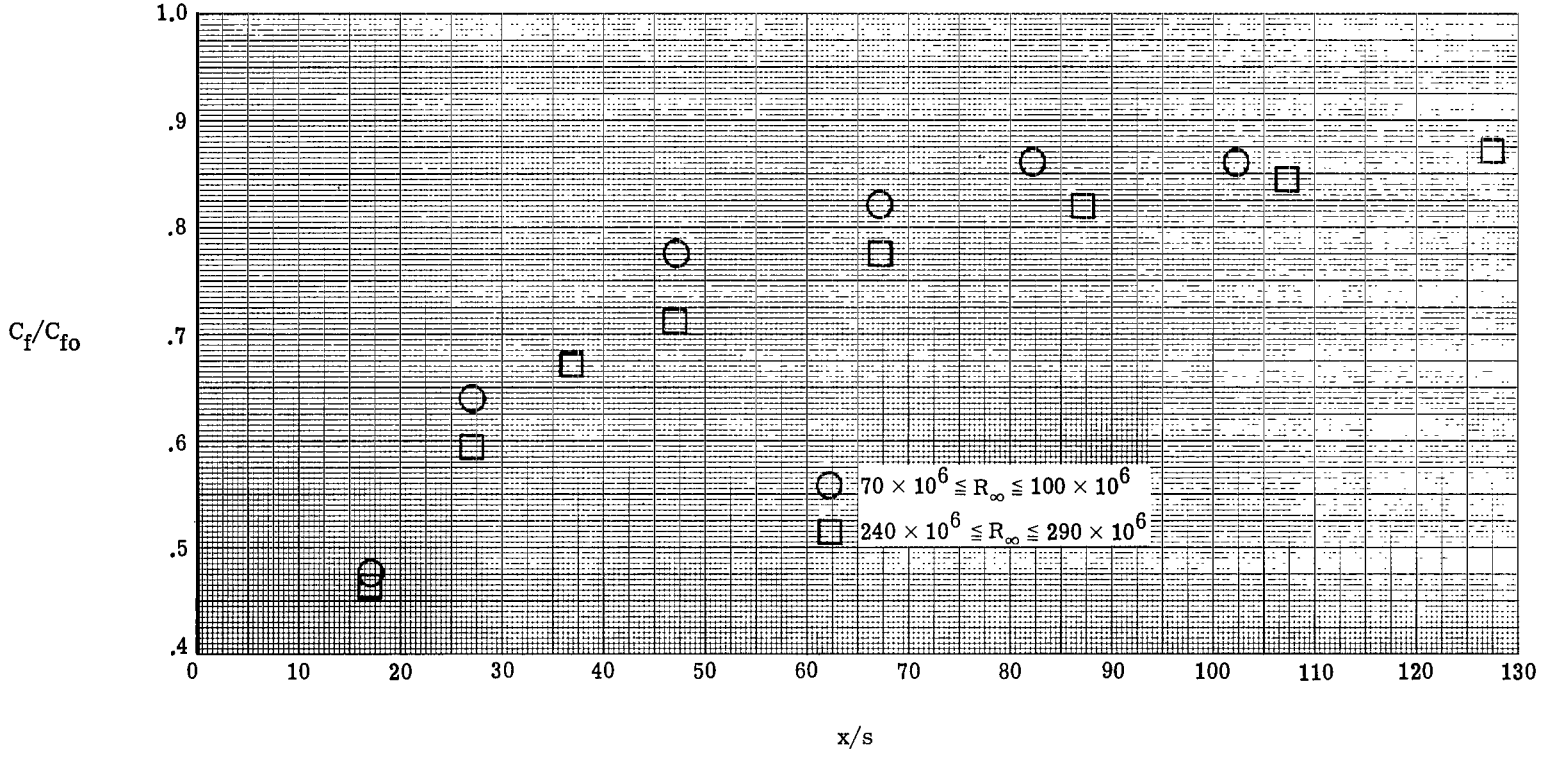

(c) $\lambda_{nom} = 0.20$.

Figure 21.- Concluded.

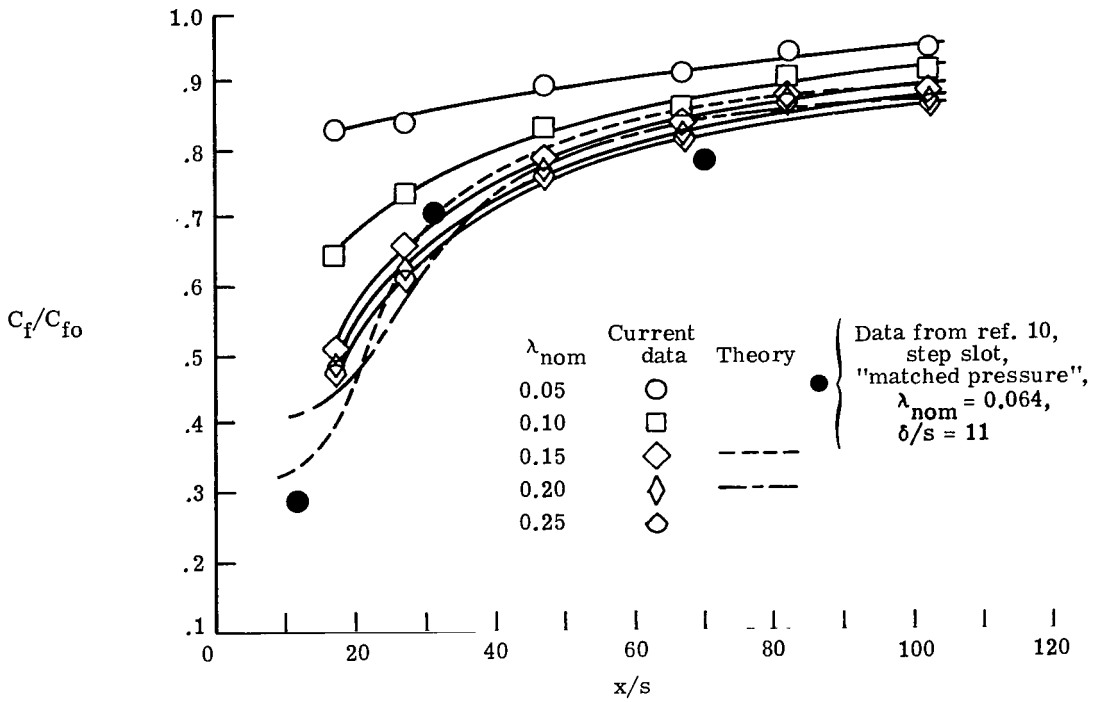

(a) One slot.

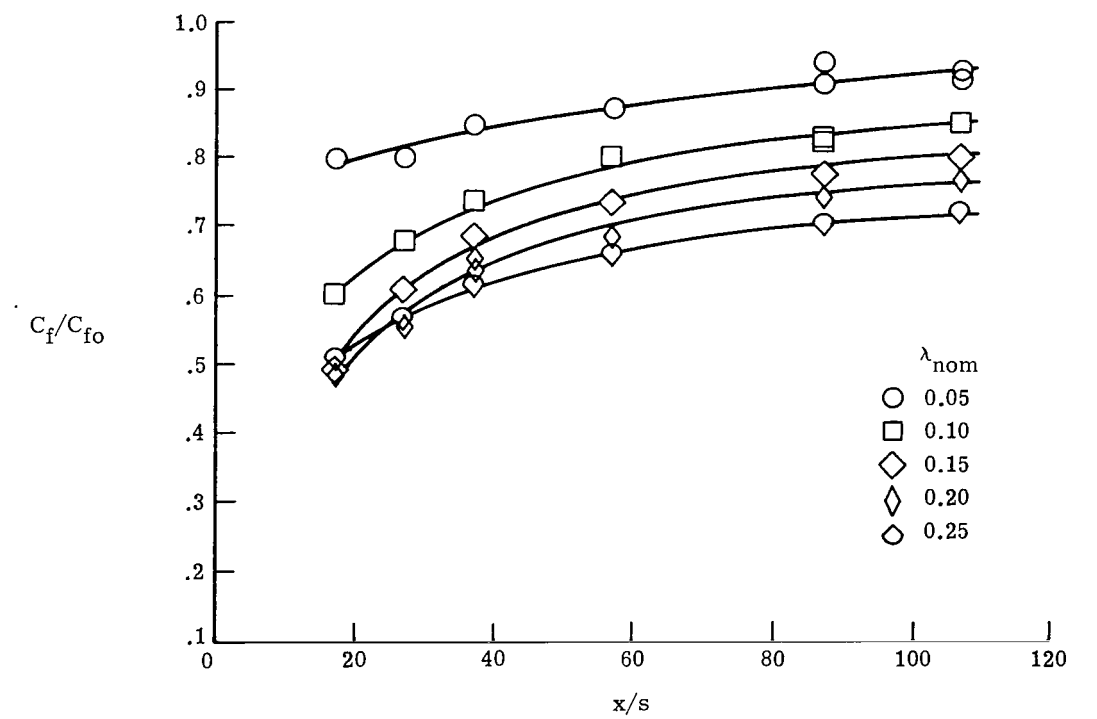

(b) Two slots.

Figure 22.- C_f/C_{fo} plotted against distance downstream of one to four slots at various values of mass flow λ (s = 0.254 cm).

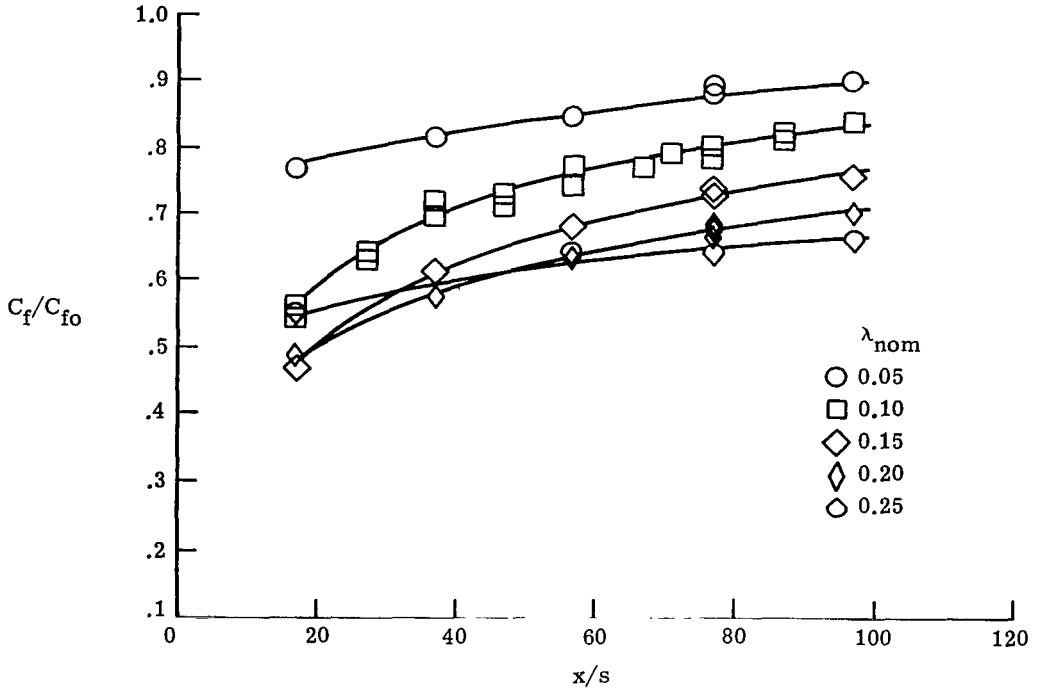

(c) Three slots.

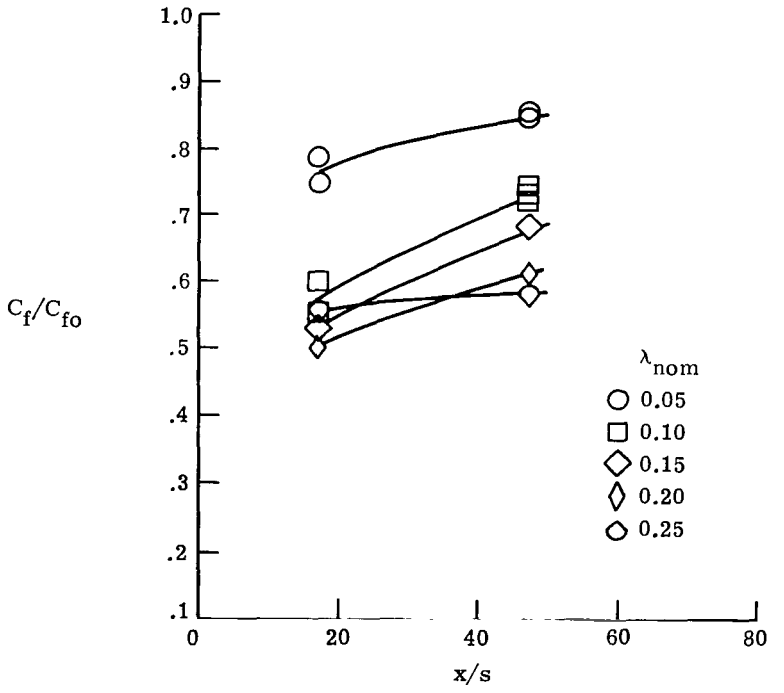

(d) Four slots.

Figure 22.- Concluded.

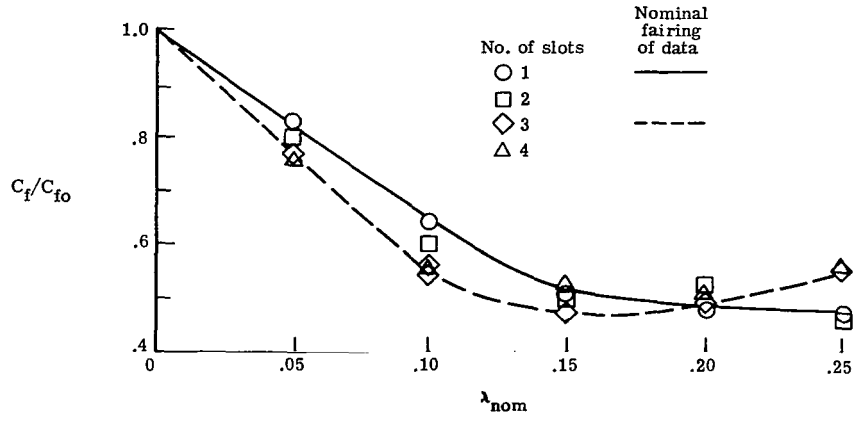

(a) x/s = 17.12.

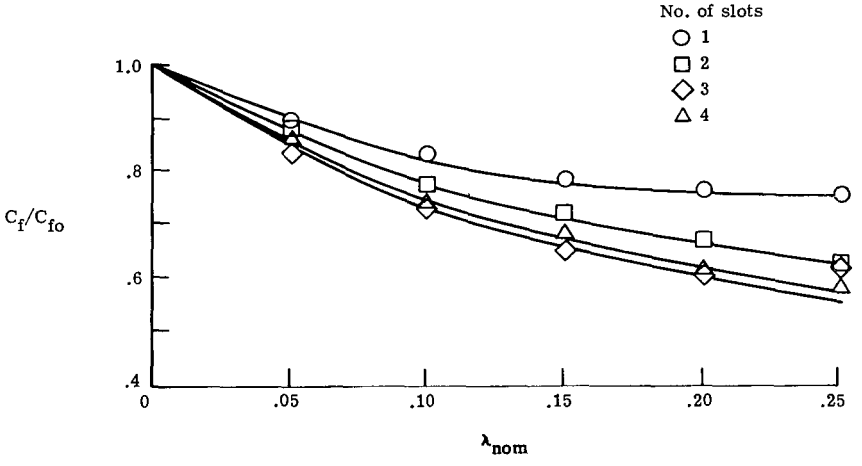

(b) x/s = 47.12.

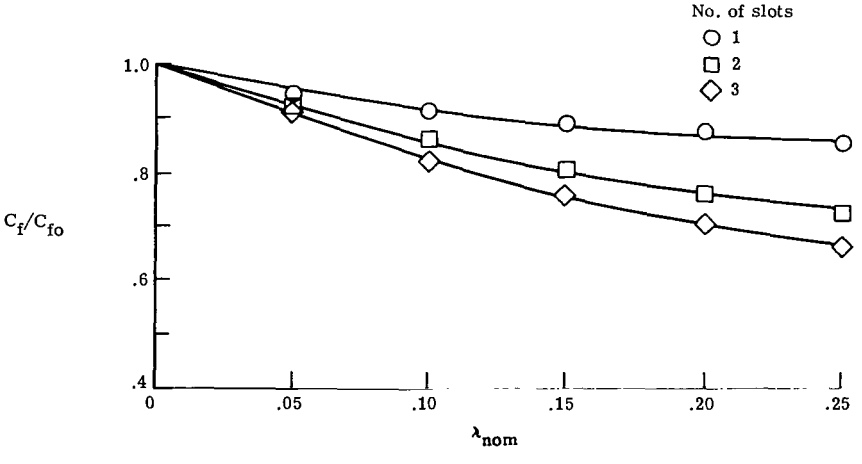

(c) x/s = 100.12.

Figure 23.- C_f/C_{fo} plotted against mass-flow parameter λ downstream of one to four slots (s = 0.254 cm).

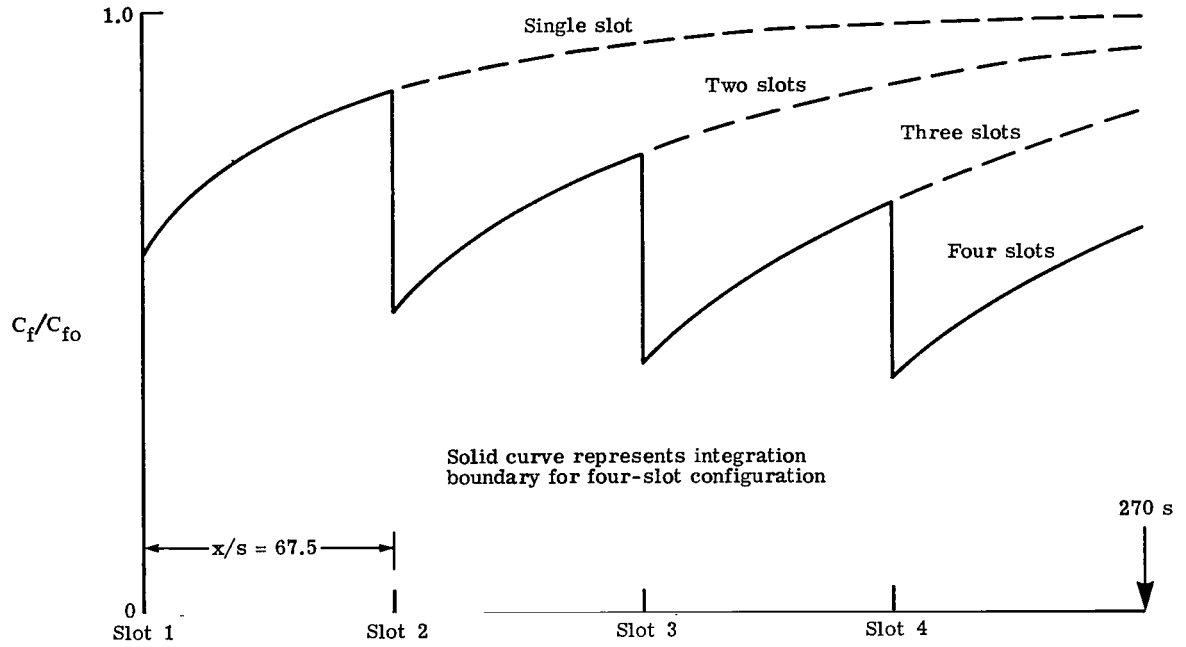

Figure 24.- Schematic illustration of curves under which skin friction was integrated over 270 slot heights.

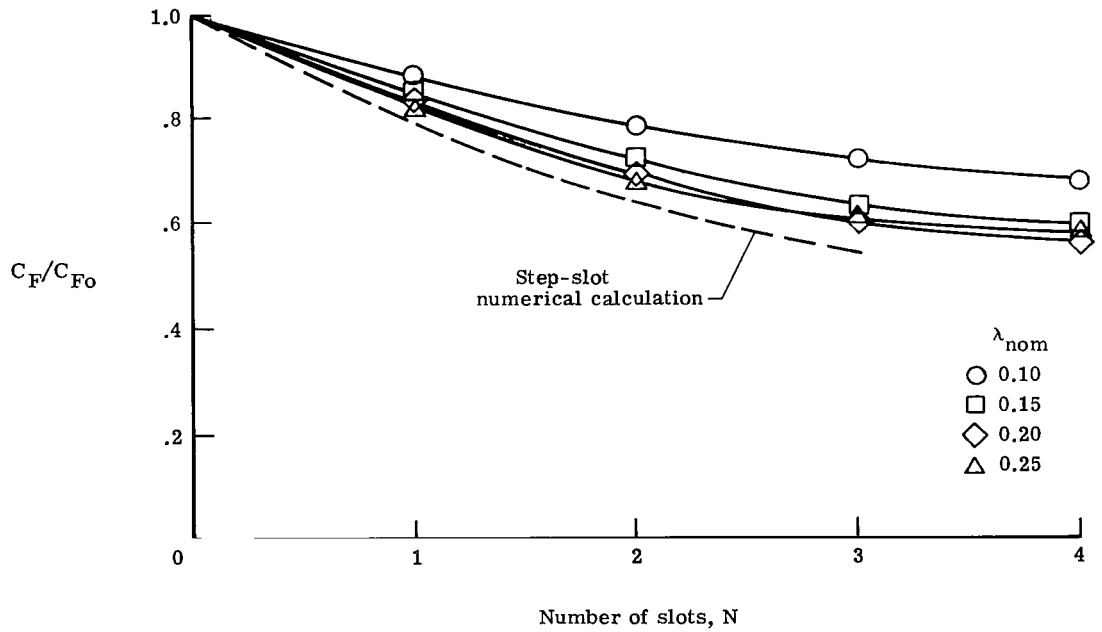

Figure 25.- Integrated skin friction as function of number of slots (s = 0.254 cm).

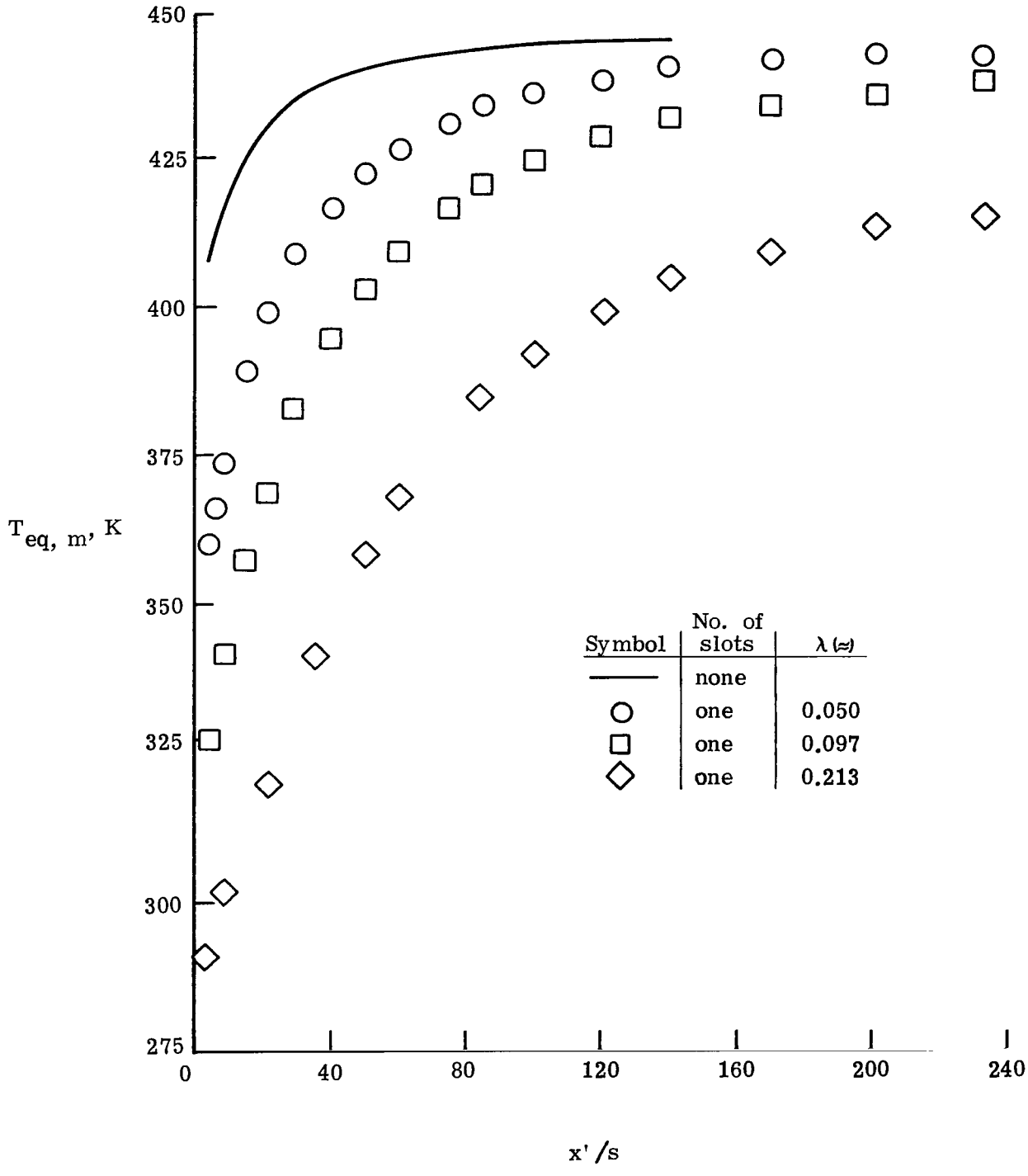

Figure 26.- Comparison of T_{eq} axial variation for single slot with that for no slot (s = 0.254 cm).

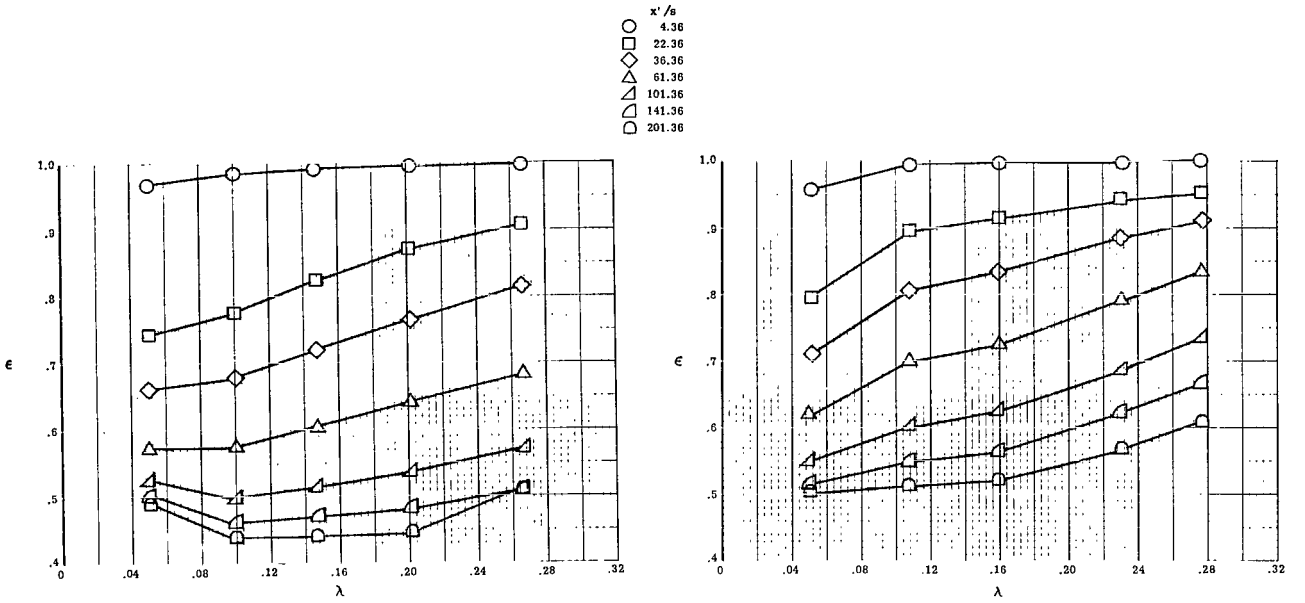

(a) Single slot.

(b) Two slots.

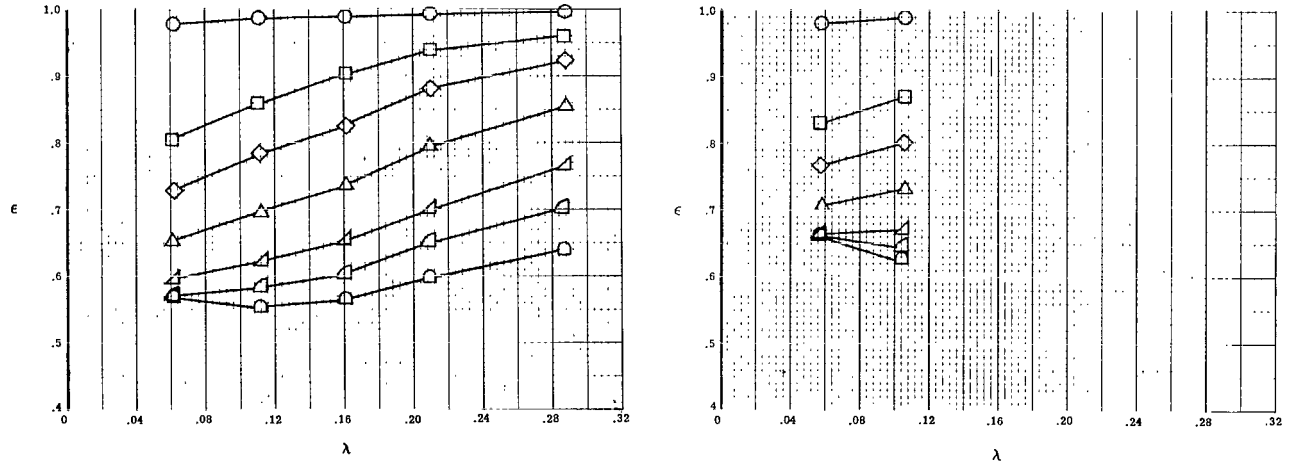

(c) Three slots.

(d) Four slots.

Figure 27.- Variation of cooling effectiveness with slot mass flow at several downstream stations (s = 0.254 cm).

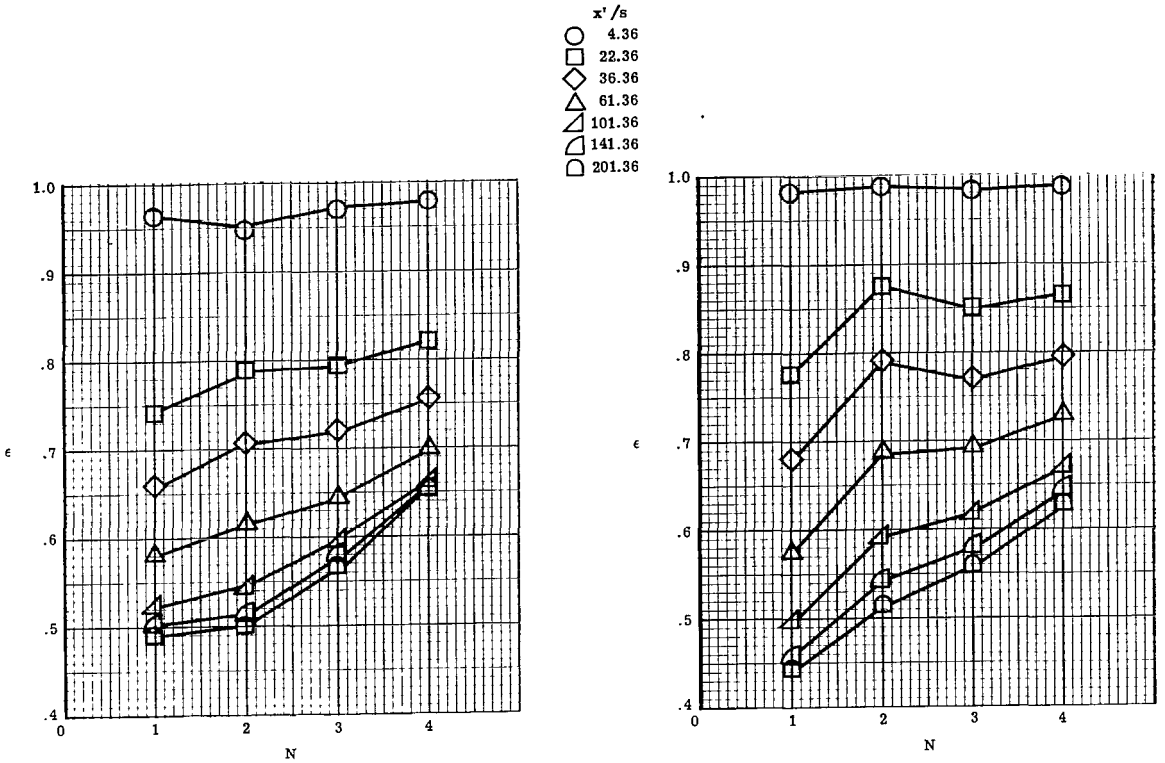

(a) λ_{nom} = 0.05. (b) λ_{nom} = 0.10.

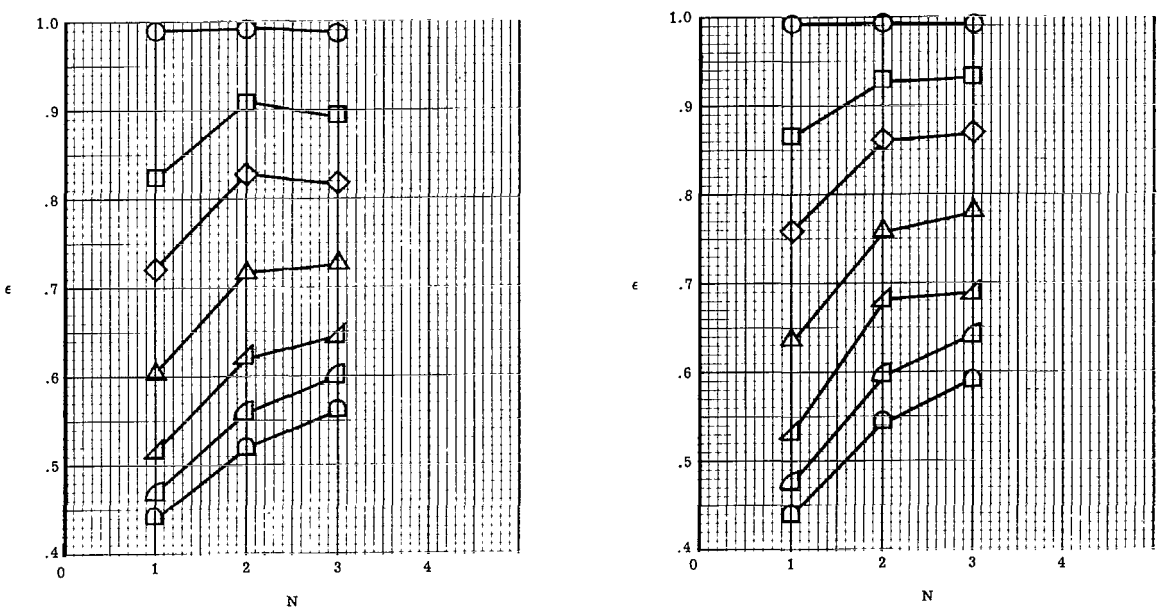

(c) λ_{nom} = 0.15. (d) λ_{nom} = 0.20.

Figure 28.- Variation of cooling effectiveness with number of slots N for several downstream stations (s = 0.254 cm).

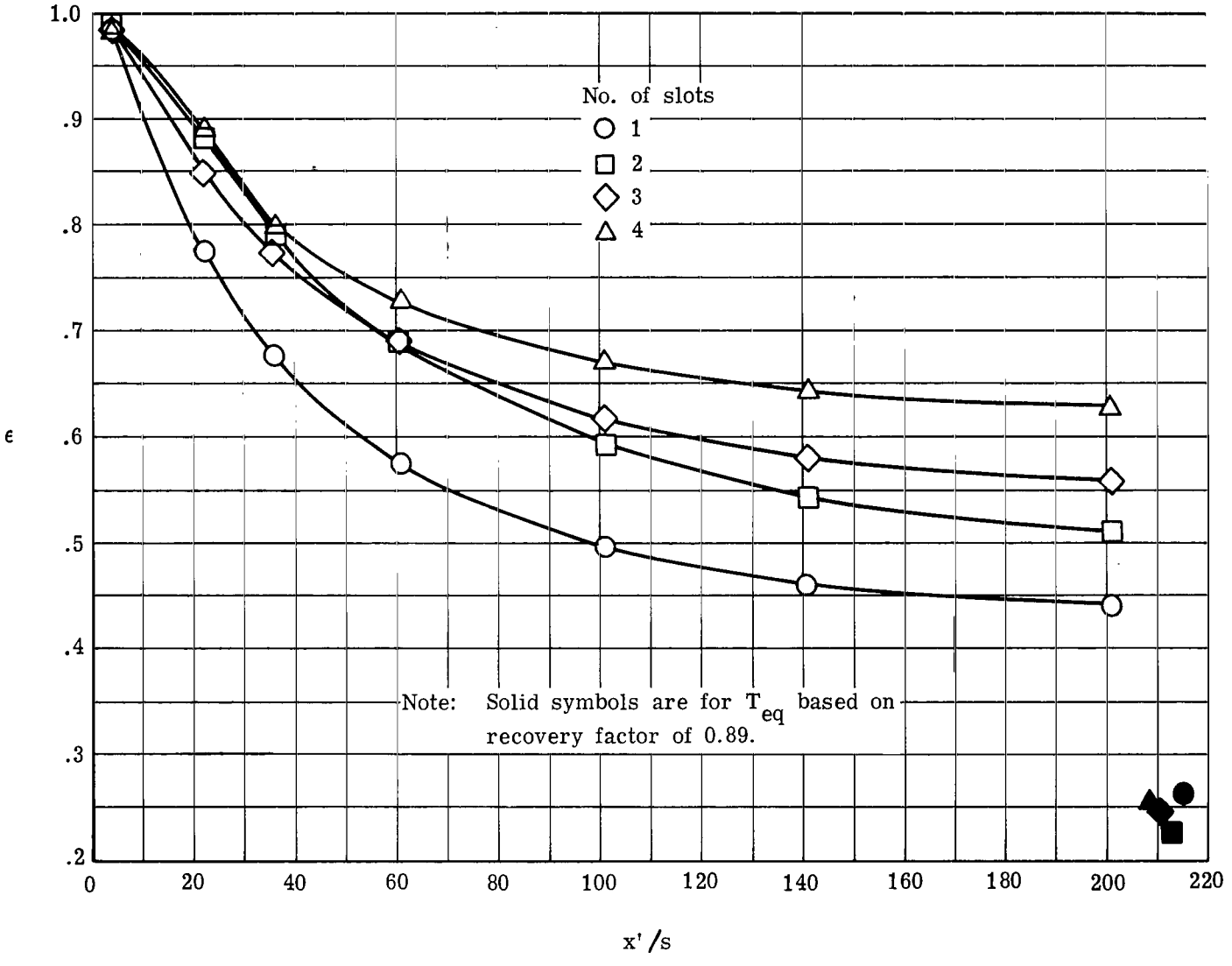

Figure 29.- Comparison of cooling effectiveness downstream of one, two, three, and four slots. λ_{nom} = 0.10 (s = 0.254 cm).

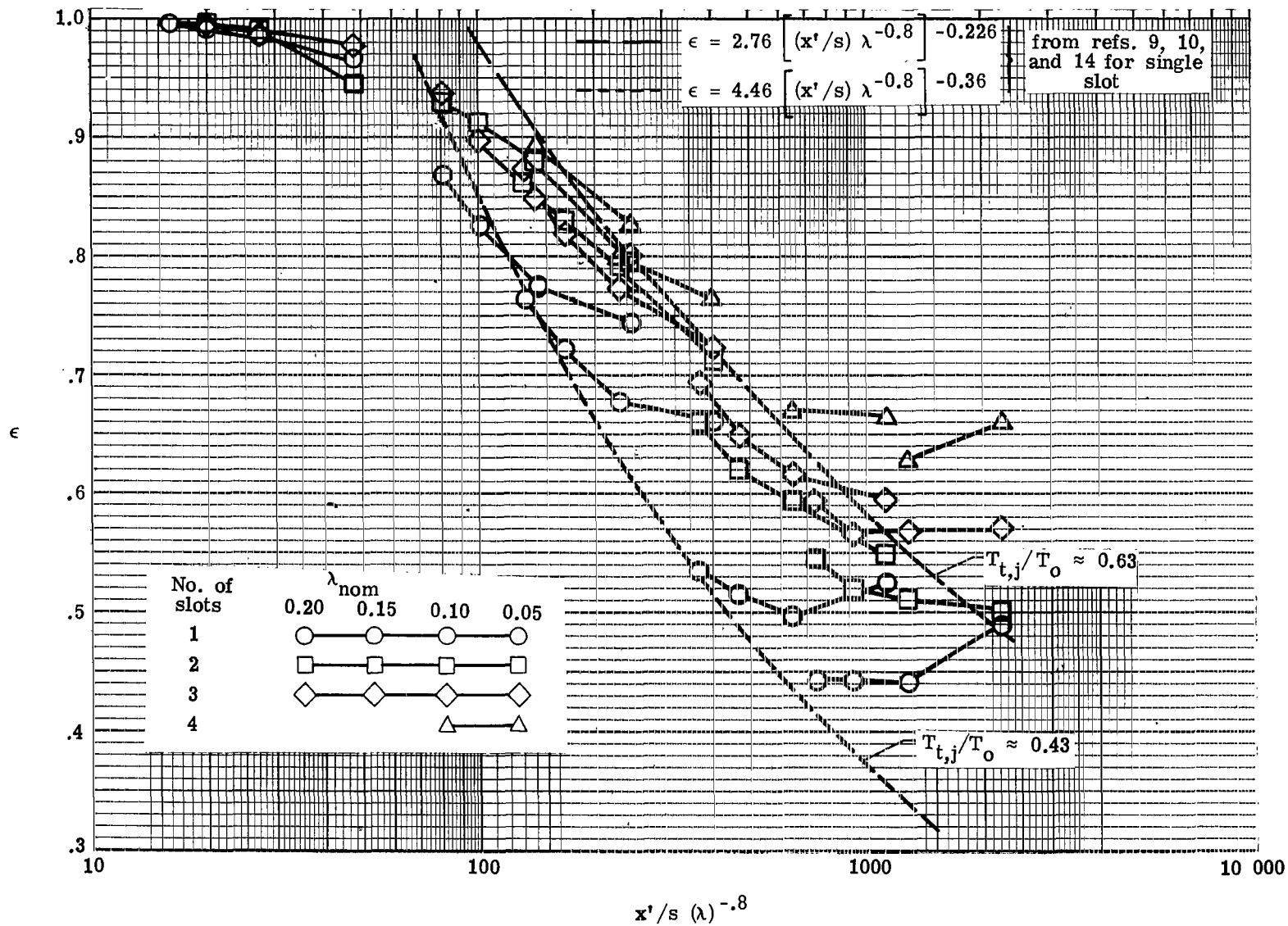

Figure 30.- Cooling effectiveness plotted against correlating parameter $(x'/s)\lambda^{-0.8}$ (s = 0.254 cm).

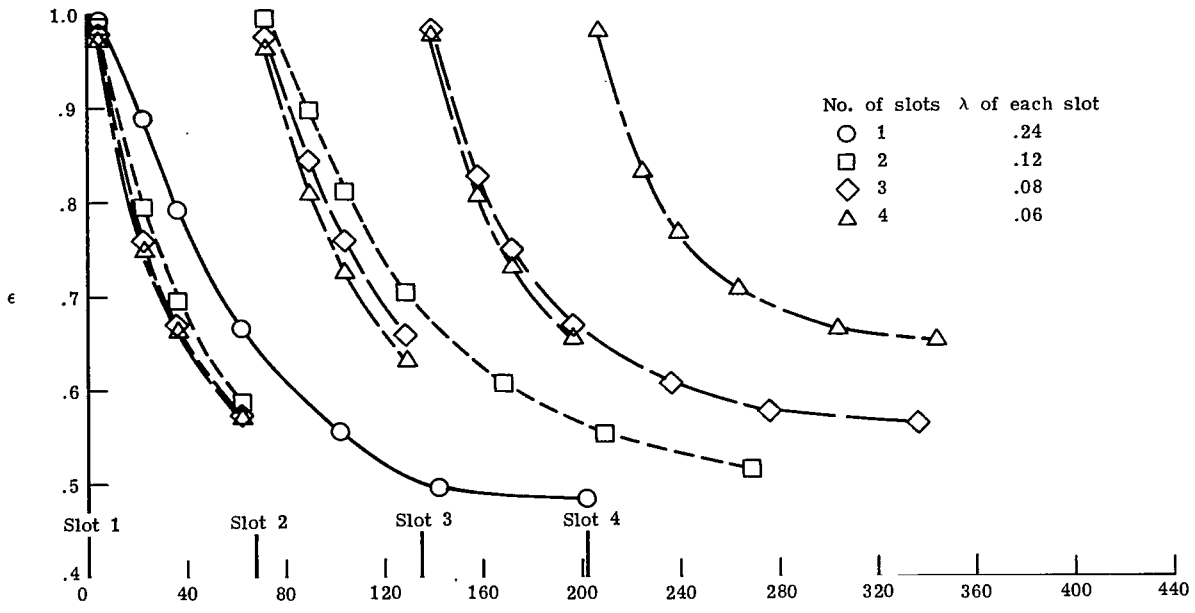

(a) $\lambda_{eff} = 0.24$.

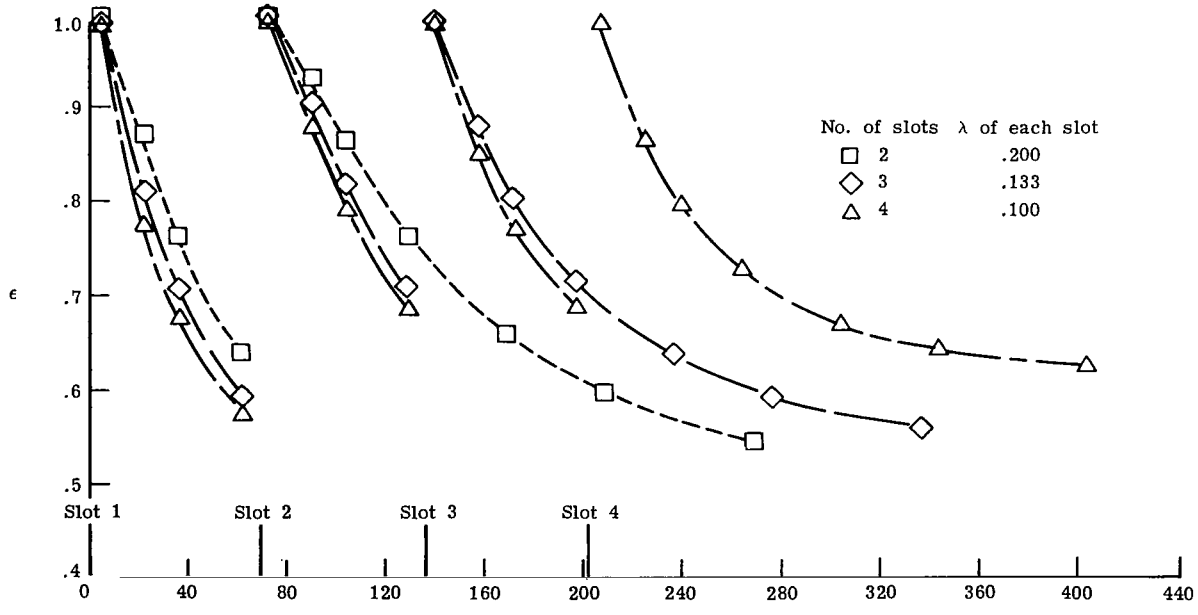

(b) $\lambda_{eff} = 0.40$.

Figure 31.- Cooling effectiveness ε for one, two, three, and four slots with same total mass injection (s = 0.254 cm, $T_j/T_t \approx 0.6$).

1. Report No.	2. Government Accession No.	3. Recipient's Catalog No.
NASA TP-1176		

4. Title and Subtitle

DIRECT MEASUREMENTS AND ANALYSIS OF SKIN FRICTION AND COOLING DOWNSTREAM OF MULTIPLE FLUSH-SLOT INJECTION INTO A TURBULENT MACH 6 BOUNDARY LAYER

5. Report Date: October 1978

6. Performing Organization Code:

7. Author(s)

Floyd G. Howard and Andrew J. Srokowski

8. Performing Organization Report No.: L-11950

10. Work Unit No.: 505-06-15-03

9. Performing Organization Name and Address

NASA Langley Research Center
Hampton, VA 23665

11. Contract or Grant No.:

13. Type of Report and Period Covered: Technical Paper

12. Sponsoring Agency Name and Address

National Aeronautics and Space Administration
Washington, DC 20546

14. Sponsoring Agency Code:

15. Supplementary Notes

16. Abstract

Experiments have been conducted to determine the reduction in surface skin friction and the effectiveness of surface cooling downstream of one to four successive flush slots injecting cold air at an angle of 10° into a turbulent Mach 6 boundary layer. Data were obtained by direct measurements of surface shear and equilibrium temperatures, respectively. Increasing the number of slots decreased the skin friction, but the incremental improvement in skin-friction reduction decreased as the number of slots was increased. Cooling effectiveness was found to improve, for a given total mass injection, as the number of slots was increased from one to four. Comparison with previously reported step-slot data, however, indicates that step slots with tangential injection are more effective for both reducing skin friction and cooling than the present flush-slot configuration. Finite-difference predictions are in reasonable agreement with skin-friction data and with boundary-layer profile data.

17. Key Words (Suggested by Author(s))

Slot injection
Slot cooling
Multiple flush slots
Skin-friction reduction
Boundary-layer profiles
Film cooling
Drag reduction

18. Distribution Statement

Unclassified - Unlimited

Subject Category 34

19. Security Classif. (of this report)	20. Security Classif. (of this page)	21. No. of Pages	22. Price*
Unclassified	Unclassified	109	$6.50

* For sale by the National Technical Information Service, Springfield, Virginia 22161

NASA-Langley, 1978

1. Report No.	2. Government Accession No.	3. Recipient's Catalog No.
NASA TP-1176		

4. Title and Subtitle

DIRECT MEASUREMENTS AND ANALYSIS OF SKIN FRICTION AND COOLING DOWNSTREAM OF MULTIPLE FLUSH-SLOT INJECTION INTO A TURBULENT MACH 6 BOUNDARY LAYER

5. Report Date: October 1978

6. Performing Organization Code:

7. Author(s)

Floyd G. Howard and Andrew J. Srokowski

8. Performing Organization Report No.: L-11950

9. Performing Organization Name and Address

NASA Langley Research Center
Hampton, VA 23665

10. Work Unit No.: 505-06-15-03

11. Contract or Grant No.:

12. Sponsoring Agency Name and Address

National Aeronautics and Space Administration
Washington, DC 20546

13. Type of Report and Period Covered: Technical Paper

14. Sponsoring Agency Code:

15. Supplementary Notes

16. Abstract

Experiments have been conducted to determine the reduction in surface skin friction and the effectiveness of surface cooling downstream of one to four successive flush slots injecting cold air at an angle of 10° into a turbulent Mach 6 boundary layer. Data were obtained by direct measurements of surface shear and equilibrium temperatures, respectively. Increasing the number of slots decreased the skin friction, but the incremental improvement in skin-friction reduction decreased as the number of slots was increased. Cooling effectiveness was found to improve, for a given total mass injection, as the number of slots was increased from one to four. Comparison with previously reported step-slot data, however, indicates that step slots with tangential injection are more effective for both reducing skin friction and cooling than the present flush-slot configuration. Finite-difference predictions are in reasonable agreement with skin-friction data and with boundary-layer profile data.

17. Key Words (Suggested by Author(s))

Slot injection
Slot cooling
Multiple flush slots
Skin-friction reduction
Boundary-layer profiles
Film cooling
Drag reduction

18. Distribution Statement

Unclassified - Unlimited

Subject Category 34

19. Security Classif. (of this report)	20. Security Classif. (of this page)	21. No. of Pages	22. Price*
Unclassified	Unclassified	109	$6.50

* For sale by the National Technical Information Service, Springfield, Virginia 22161

NASA-Langley, 1978

6 1 1U,D, 090878 S00903DS
DEPT OF THE AIR FORCE
AF WEAPONS LABORATORY
ATTN: TECHNICAL LIBRARY (SUL)
KIRTLAND AFB NM 87117